

# CHARACTERIZATION OF BRONZE CASTING IN INSULA 56, IN ROMAN AVENTICUM

by

JESSICA WHEAT COOK

(Under the Direction of Ervan Garrison)

## ABSTRACT

This study characterizes metallurgical wastes (slag) recovered from a bronze workshop during excavations in 1997-1998 at the Roman provincial city of Aventicum, located in western Switzerland, then Germania Superior. Previous research has identified the workshop as one devoted to the production of large leaded bronze statuary. The slag assemblage analyzed in this study is unusual due to the absence of ceramic crucible fragments normally associated with the production of copper alloys. Instead, this workshop is hypothesized to have used iron crucibles.

Electron Microprobe Analysis (EMPA) and X-Ray Diffraction (XRD) were used to analyze the chemical composition of the slags in contrast to previous bulk analysis studies. Modern metal casting methods were observed for analogues. The data show that the slag reached temperatures between 1350°-1400° C and chemical components indicated the use of sand and lime fluxes. Evidence of high temperatures is proposed as one chemical fingerprint that can be used to re-assess slag for the presence of iron crucibles in other Roman bronze workshops.

INDEX WORDS:     Aventicum, Classical Bronzes, EMPA, XRD, Roman Metallurgy

CHARACTERIZATION OF BRONZE CASTING IN INSULA 56, IN ROMAN AVENTICUM

by

JESSICA WHEAT COOK

AB History, Anthropology, The University of Georgia, 2003

A Thesis Submitted to the Graduate Faculty of The University of Georgia in Partial Fulfillment of the  
Requirements for the Degree

MASTER OF SCIENCE

ATHENS, GEORGIA

2008

© 2008

Jessica Wheat Cook

All Rights Reserved

CHARACTERIZATION OF BRONZE CASTING IN INSULA 56, IN ROMAN  
AVENTICUM

by

JESSICA WHEAT COOK

Major Professor:	Ervan Garrison
Committee:	Samuel Swanson Douglas Crowe

Electronic Version Approved:

Maureen Grasso  
Dean of the Graduate School  
The University of Georgia  
May 2008

## ACKNOWLEDGMENTS

The author wishes to thank Drs. Ervan Garrison, Douglas Crowe, and Samuel Swanson for their guidance and patience. It is not easy to make a scientist out of someone with a background in history and anthropology, no matter how eager the student. I also would like to thank Dr. Vincent Serneels of the University of Fribourg, Switzerland, for providing me with not only the materials for analysis but also a generous amount of good faith in an American graduate student. Professors RG Brown III and James “Jimbo” Buonaccorsi made it possible for me to actually engage in metal casting instead of merely studying from the relative safety of a laboratory. Finally, I would like to thank my friends and colleagues among the graduate students in the Geology Department at UGA. I am grateful beyond words for your support and encouragement during my time here.

This work is dedicated to the memory of my late father, Bobby Lee Cook, Jr., who first sparked my curiosity for the mysteries of history and pre-history. This work was driven not only by my own intellectual curiosity, but also by my dedication to my son Patrick Aidan Fell, whose eagerness to explore his world inspires my own. Finally, the completion of this manuscript would have been a far more miserable process without the help and support of my husband, Nathan.

## TABLE OF CONTENTS

	Page
ACKNOWLEDGEMENTS.....	iv
LIST OF TABLES.....	vii
LIST OF FIGURES .....	ix
INTRODUCTION .....	1
Previous Work.....	4
Current Hypothesis .....	6
Study Objectives .....	6
Copper Slag and Copper Alloys.....	7
Copper Alloys in Western Switzerland:	
From La Tene to the Gallo-Roman World .....	10
Copper Alloy Statuary in Aventicum .....	12
Techniques Used.....	14
METHODS.....	16
Electron Microprobe Analysis (EMPA).....	17
X-Ray Diffraction (XRD) .....	19
Modern Metal Casting Observations .....	20
RESULTS .....	21
Rough Sorting of Sample Types by Hand Sample .....	21
Images with EDS spectra.....	24
Electron Dispersive Spectrometry Data.....	39

Wavelength Dispersive Spectrometry Data .....	42
X-Ray Diffraction (XRD) .....	60
Modern Metal Casting Work .....	62
DISCUSSION.....	67
CONCLUSIONS .....	77
REFERENCES .....	79
APPENDICES.....	83
A: Stratigraphic profiles .....	83
B: Accession.....	86
C: Photographic and Image data.....	88
D: WDS data.....	97
E: Statistics .....	113

## LIST OF TABLES

	Page
Table 1: Oxide standards used for oxide analyses .....	18
Table 2: Element standards used in WDS analysis of metal.....	18
Table 3: Hand sample results and descriptions.....	22
Table 4: Phases suggested by EDS within the slag groundmass and ceramic.....	41
Table 5: Components detected in the metal inclusions within the samples .....	42
Table 6: Normalized data for ceramic, minus fayalite analysis.....	43
Table 7: Normalized data for metals .....	43
Table 8: WDS data for slag groundmass, normalized.....	47
Table 9: Correlation coefficients for WDS data, groundmass points only .....	59
Table 10: XRD results by d-spacing for AVS722, ceramic portion. ....	61
Table 11: XRD results by d-spacing for AVS722, vitrified portion. ....	61
Table 12: Average weight percentages, metals .....	67
Table 13: Normalized Element Weight Percent Alloy Components.....	69
Table 14: Oxide Standards.....	85
Table 15 : Element Standards.....	85
Table 16: Non-normalized data for ceramic portion of AVS722 .....	97
Table 17: Normalized data for ceramic portion of AVS722 .....	97
Table 18: Non-normalized data for metals .....	97
Table 19: Normalized data for metals.....	99
Table 20: Non-normalized data for groundmass .....	101
Table 21: Normalized data for slag minus null oxides .....	106



Table 22: Correlation results .....	113
-------------------------------------	-----

## LIST OF FIGURES

	Page
Figure 1: Aventicum, now known as Avenches, in Western Switzerland.....	1
Figure 2: Map of Aventicum showing the location of major structures. ....	2
Figure 3: Map of excavations from 1997-1998. ....	3
Figure 4: Stratigraphic profile of the transect excavated at Insula 56. 8.....	4
Figure 5: Reconstruction of the furnace at Insula 56.....	5
Figure 6: Ternary plot of copper alloy types .....	9
Figure 7: Portrait statue of a boy. ....	13
Figure 8: AVS722 zircon .....	24
Figure 9: AVS 722 fayalite.....	25
Figure 10: AVS905 biotites .....	25
Figure 11: ABR028 rutile.....	26
Figure 12: AVS722 zircon.....	27
Figure 13: AVS905 biotite.....	28
Figure 14: Cu prills in ABR002.....	29
Figure 15: Cu-Sn alloy prills.....	30
Figure 16: ABR025 leaded bronze silicate .....	30
Figure 17: AVS901 silicate groundmass enriched in leaded bronze .....	31
Figure 18: ABR006 fractured quartz grain.....	33
Figure 19: ABR019 Feldspar .....	33
Figure 20: ABR006 zircon.....	34

Figure 21: ABR009 SnO <sub>2</sub> dendrites in PbO rich groundmass.....	34
Figure 22: ABR009 SnO <sub>2</sub> dendrites in FeO rich groundmass .....	35
Figure 23: ABR004 fayalite with SnO <sub>2</sub> and CuO.....	35
Figure 24: ABR008 FeO rim around vesicles .....	36
Figure 25: ABR004 FeO prills within flowbanding .....	36
Figure 26: ABR019 possible pyrite.....	37
Figure 27: ABR029 Cu-Fe-S inclusion .....	37
Figure 28: ABR024 chrome spinel .....	38
Figure 29: ABR014 Chrome spinel – like area.....	38
Figure 30: ABR009 SnO <sub>2</sub> in FeO enriched groundmass .....	39
Figure 31: Cu Distribution, all metal samples .....	45
Figure 32: Sn distribution, all metal areas.....	46
Figure 33: Pb in the metal portions of the samples .....	46
Figure 34: Fe distribution, all metals .....	47
Figure 35: SiO <sub>2</sub> -FeO-CaO ternary system .....	55
Figure 36: SiO <sub>2</sub> -FeO-Al <sub>2</sub> O <sub>3</sub> ternary system .....	56
Figure 37: SiO <sub>2</sub> -FeO binary plot. $R^2 = 0.337956$ .....	57
Figure 38: FeO-CaO binary plot. $R^2 = 0.249305$ .....	57
Figure 39: SiO <sub>2</sub> -CaO binary plot. $R^2 = 0.211299$ .....	58
Figure 40: Cluster analysis: “Elbow” Method.....	60
Figure 41: Molds during an iron pour showing pour cups and risers.....	63
Figure 42: Pouring into the molds.....	65
Figure 43: Cu-Pb-Sn ternary plot, metal components .....	70
Figure 44: CaO-SiO <sub>2</sub> -Al <sub>2</sub> O <sub>3</sub> system .....	71

Figure 45: $\text{CaO-SiO}_2\text{-Al}_2\text{O}_3$ system.....	72
Figure 46: Cu-Fe binary phase diagram.....	73
Figure 47: Fe-Sn binary plot.....	74
Figure 48: Modern Poling Slag, 2/2008, and ABR020 from Insula 56.....	76
Figure 49: ABR001, ABR002, ABR003 .....	88
Figure 50: ABR004.....	88
Figure 51:ABR005 .....	88
Figure 52: ABR006.....	88
Figure 53:ABR007 .....	88
Figure 54:ABR008 .....	88
Figure 55:ABR009 .....	89
Figure 56:ABR010 .....	89
Figure 57:ABR011 .....	89
Figure 58:ABR012 .....	89
Figure 59:ABR013 .....	89
Figure 60:ABR014 .....	89
Figure 61:ABR016 .....	90
Figure 62:ABR017 .....	90
Figure 63:ABR018 .....	90
Figure 64:ABR019 .....	90
Figure 65:ABR020 .....	90
Figure 66:ABR021 .....	90
Figure 67:ABR022 .....	91
Figure 68:ABR023 .....	91

Figure 69:ABR024 .....	91
Figure 70:ABR025 .....	91
Figure 71:ABR027 .....	91
Figure 72:ABR028 .....	91
Figure 73:ABR029 .....	92
Figure 74:AVS901.....	92
Figure 75:AVS902.....	92
Figure 76:AVS903.....	92
Figure 77:AVS905.....	92
Figure 78:AVS722.....	92
Figure 79: ABR019 Feldspar .....	93
Figure 80: ABR006 fractured quartz grain.....	93
Figure 81: ABR006 zircon.....	93
Figure 82: ABR009 SnO <sub>2</sub> dendrites in PbO rich groundmass.....	93
Figure 83: ABR009 SnO <sub>2</sub> dendrites in SiO <sub>2</sub> -FeO-SnO <sub>2</sub> groundmass.....	93
Figure 84: ABR012 SnO <sub>2</sub> in PbO groundmass with Cu prills (round) .....	93
Figure 85: ABR012 SnO <sub>2</sub> -PbO enriched groundmass .....	94
Figure 86: ABR004 fayalite within SnO <sub>2</sub> , PbO silicate groundmass.....	94
Figure 87: ABR008 FeO rim around vesicles .....	94
Figure 88: ABR008 FeO prills.....	94
Figure 89: ABR019 possible pyrite.....	94
Figure 90: ABR029 pyrite.....	94
Figure 91: ABR029 Cu-Fe-S inclusion .....	95
Figure 92: ABR029 chalcopyrite.....	95

Figure 93: ABR024 chrome spinel .....	95
Figure 94: ABR024 chrome spinel .....	95
Figure 95: ABR014 Chrome spinel – like area .....	95
Figure 96: ABR014 Cr phase with anomalous nucleation .....	95
Figure 97: Cu prills in ABR002 .....	96
Figure 98: ABR025 leaded bronze silicate .....	96
Figure 99: Criterion values in cluster analysis plotted against potential number of clusters ....	113
Figure 100: Cluster analysis dendrogram of all WDS analyses of the groundmass .....	114

## INTRODUCTION

This study examines a suite of metallurgical waste in order to characterize it and to determine what technological operations created it. The sample suite is of debris from some form of copper alloy working and consists of approximately 30 samples from Aventicum, now Avenches, located western Switzerland (Figure 1). It was recovered from a portion of the site known as *Insula 56* located in the southern portion of the city adjacent to the theater (Figure 2, Figure 3) The hypothesis to be tested is that this sample suite was created during the casting of large bronze statues, during which non-ceramic crucibles, specifically iron crucibles, appear to have been used (Serneels and Wolf, 1999).



Figure 1: Aventicum, now known as Avenches, in Western Switzerland. From Google Maps.

<http://maps.google.com/>

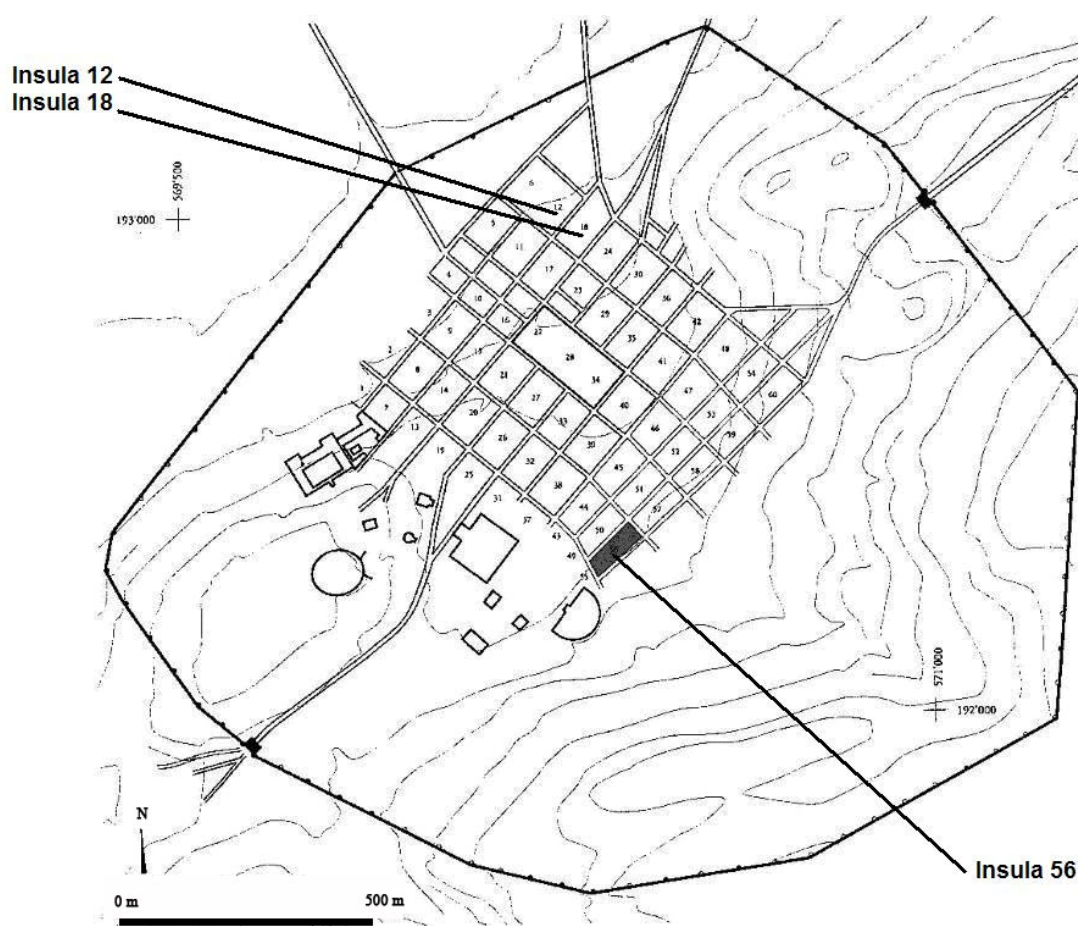


Figure 2: Map of Aventicum showing the location of major structures. Insula 56 is the shaded block Map from Blanc, 1999a. (Blanc, et al., 1999a)



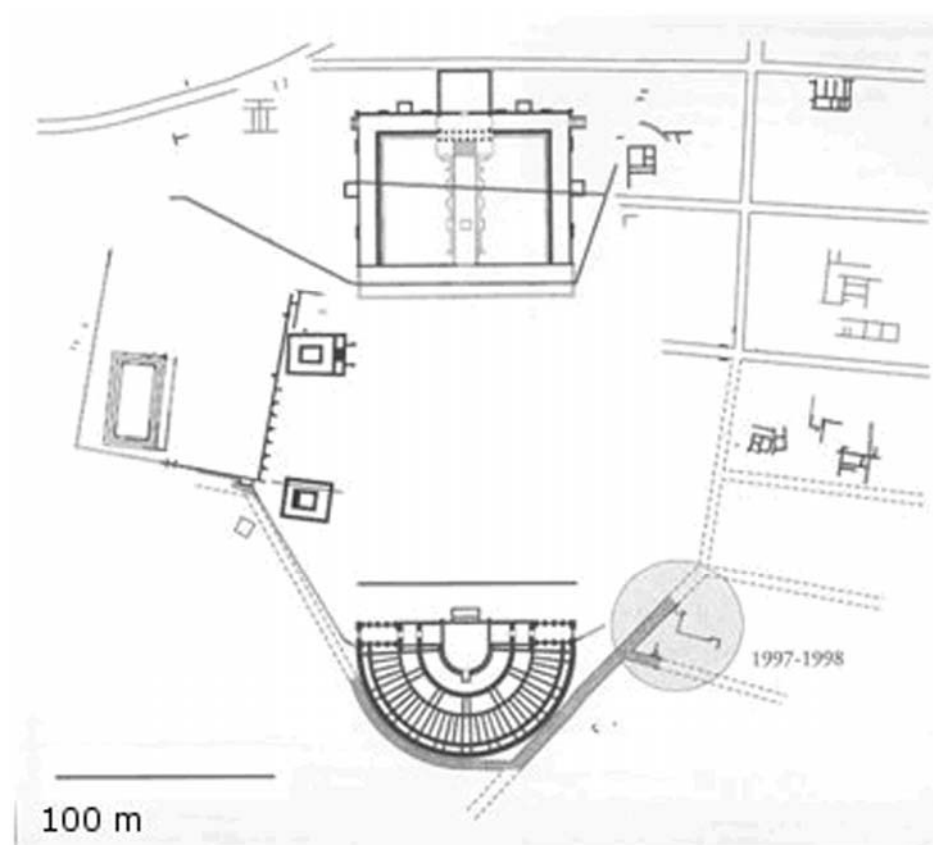


Figure 3: Map of excavations from 1997-1998. The area under excavation at Insula 56 is circled in gray. Map from Blanc, 1999b (Blanc, et al., 1999b)

## Previous Work

The samples were found in an archaeological level dated to the second half of the 2nd century AD (Figure 4). Associated debris from the same level was examined by Vincent Serneels and Sophie Wolf of the University of Fribourg using bulk composition analysis techniques and optical microscopy (Serneels and Wolf, 1999). Serneels and Wolf determined that this debris was composed of slag, ceramic fragments from the furnace, and metal prills of copper alloy that included tin and lead. The assemblage is noteworthy for the absence of baked clay crucibles; instead, there is evidence for the use of non-ceramic crucibles, most likely iron (Serneels and Wolf, 1999). Instead of ceramic crucibles, the ceramic portion of the assemblage appears to be fragments from both the furnace and an external crucible liner (“*cuve*” Fr.) that was presumably placed inside the furnace to hold the iron crucible during alloying (Figure 5). The use of an iron crucible in tandem with this external ceramic liner is an unusual case in the Gallo-Roman world of metallurgy.

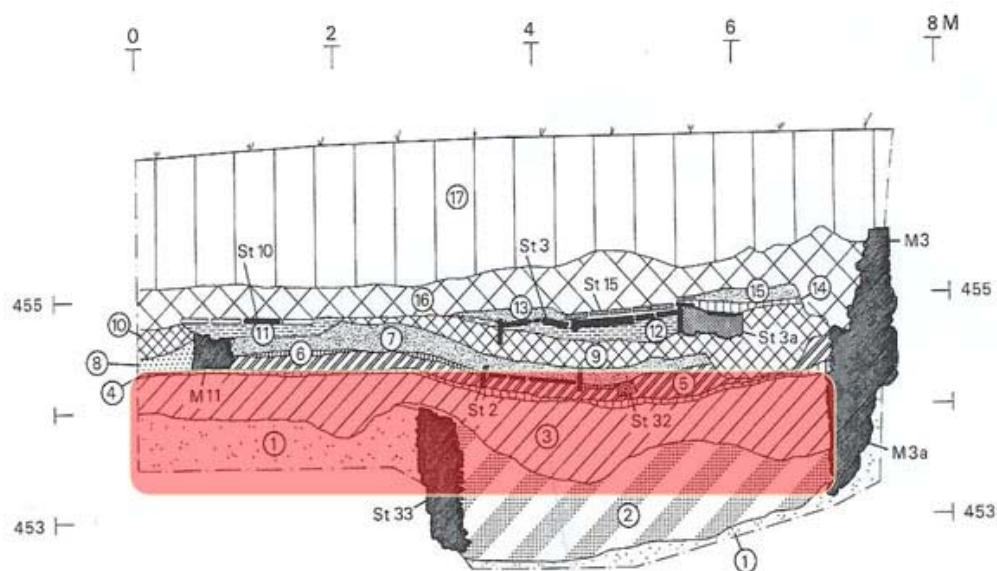


Figure 4: Stratigraphic profile of the transect excavated at Insula 56. The sample suite was recovered from level 3, which is associated with occupation from the second to the third century AD. Profile from Blanc 1999b (Blanc, et al., 1999b) See Appendix A for full key, translated from the French by Cook Hale, 2008.

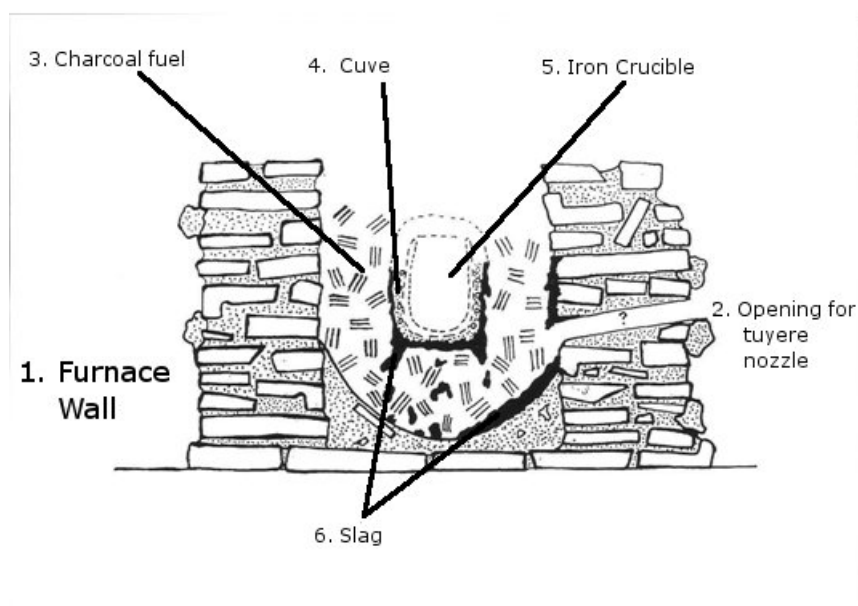


Figure 5: Reconstruction of the furnace at Insula 56. From Serneels and Wolf, 1999, with labels added by Cook Hale, 2008.

Typically, Roman copper alloy workers employed ceramic, not iron, crucibles made of local clay. These were usually tempered with refractory materials such as quartz sand. There is no evidence that they were fired, though some seem to have been heated in order to dry them (Hein, et al., 2007). Their most prominent quality seems to have been their disposability. Four questions are raised by this unique technology: 1) An iron crucible would have taken more effort and money to make, so what were the benefits to these artisans in expending more resources to employ them? 2) Also, what sort of effect would the use of the iron crucible have had on the residual waste materials left behind? 3) What purpose may have been served by the “cuve”? 4) Finally, once these remains have been characterized, what are some unique aspects of this assemblage that can be potentially used to identify the use of non-ceramic crucibles in the rest of the Gallo-Roman world?

## Current Hypothesis

The current hypothesis is that this debris was created during the casting of large Classical bronze statues typical of Roman statuary styles of the 2nd century AD (Serneels and Wolf, 1999). This hypothesis is shaped by the location of the site in an urban context as well as the presence of copper, tin, and lead in the slag samples previously analyzed by bulk analysis (Serneels and Wolf, 1999). If so, then the copper alloy present within this suite should also contain Cu-Sn-Pb, and the slag groundmass should not show widely different chemical groups if one type of technology created it (Dillman, 2007).

## Study Objectives

1) First to determine what specific metallurgical process(es) created this assemblage 2) Second, to look for what, if any, mineralogical or chemical aspects of this assemblage can be tied to the hypothetical use of an iron crucible and *cune*. 3) Third, to compare these characteristics with modern metal casting techniques to draw parallels that can elucidate the technology used at Insula 56, and provide direction for further studies into iron crucible and “*cune*” usage in the Gallo-Roman world.

If the slag was created using a distinct technology such as an iron crucible and a *cune*, then the resulting slag and metal components of alloy within the slag can reflect this technology (Pryce, et al, 2007; Zaghis, et al., 2005, Rehren and Pernicka, 2008). Conversely, if the sample suite consists of materials created by more than one type of technology, such as both iron crucible usage and ceramic crucible usage for different types of castings at different times, then this can leave behind different types of waste materials that reflect these different technologies. In other words, each technology can leave its own “fingerprint”, chemically speaking. In the absence of the metal artifacts themselves, slag and other waste materials from metallurgical contexts can be used as proxies for the manufacturing techniques employed (Hein et al., 2007; Lyle, 2002; Paynter, 2006; Serneels and Wolf, 1999; Tumati, et al., 2005; Zivkovic, et al., 2004; Rehren and Pernicka, 2008). As Rehren and Pernicka have noted not only is slag often the most recoverable material related to metallurgical activities, it is also retains the

most distinct traces of the technology that produced it (Rehren and Pernicka, 2008). In the case of this assemblage, the chemical reactions between the metal components, the gangue materials, and the iron crucible should leave behind chemical and mineralogical traces that will be discernibly different from reactions between metal components, gangue materials, and a ceramic crucible. Alloy type should also be clear, based on the presence or absence of metal components within the assemblage, suggesting possible artifact type(s) created by the technology in use at Insula 56 (Craddock; 1977; Goodway, 1989).

### **Copper Slag and Copper Alloys**

Copper or copper alloy slag results from two types of operations: smelting or melting. Slag is produced during smelting when the gangue materials of an ore are separated from the copper metal. The initial smelting of the ore often resulted in an impure copper due to incomplete reactions within the furnace (Tumiati et al., 2005). The resulting slag is typically composed of gangue (usually silicates), charcoal, and melted portions of the furnace. Copper ore is relatively common throughout Europe in places such as the Pyrite Belt of Spain, the Northern Italian Alps, et al., though the 1999 study by Serneels and Wolf noted that there is no evidence for where and how copper was obtained within Aventicum itself (Serneels and Wolf, 1999). Roman smelting operations were highly industrialized throughout the Empire (Holland, 2003; Ponting, 2002a; Weisgerber, 2003), leaving behind immense quantities of slag and tailings. No such remains have been recorded at Aventicum, and it seems unlikely that such an industrial process would have taken place within a city, especially one that was not in direct proximity to ore sources (Blanc, et al., 1999a; Blanc et al., 1999b).

Melting or casting slag is created when metal is melted in order to cast it. The source for melting slag is created from the metal components, reactions that occur along the side of the crucible where the melted metal components come into contact with it, and from any additional materials added as fluxes to remove residual impurities left over from smelting. Common fluxes include quartz

and lime and crucibles were usually ceramic, as noted above (Craddock et al, 2003; Datta et al., 2007; Rehren, 2003). The melting slag was removed before the molten alloy was poured.

Melting slag could have run off through prepared channels or it could have been removed in a process now called “poling” in modern metal casting. The casting of metals, or more commonly alloys composed of multiple metal components, could be performed in small workshops within a more urban environment, whereas smelting sites were far more industrial and located outside of cities or towns. It is by far most likely that the assemblage from Insula 56 is melting slag, and not smelting slag.

Copper alloys are classified according to their components and can consist of copper plus one, or more, additional metal components. The most common alloys are tin bronze (copper plus tin), leaded bronze (copper, tin and lead), brass (copper plus zinc), and gunmetal (copper, tin, and zinc Fig. 6). The empirical nature of ancient metallurgy appears to have given rise to alloys with some variation in the percentages of their respective components (Ponting, et al., 1998). However, different proportions of the metal components within a given copper alloy create variation in the viscosity of the molten alloy, in differences in the final appearance, and tensile strength of the piece (Craddock, 1977; Goodway, 1989).

Tin bronze contains from 5% (low tin bronze) to 20% tin (high tin bronze). Low tin bronze consists of only an  $\alpha$  phase while high tin bronze consists of both an  $\alpha$  and a  $\delta$  phase. The  $\alpha$  phase consists of a simple substitution of Sn atoms in the Cu crystal lattice, but the lattice remains face-centered cubic, with atoms of the metal placed at all eight corners and on the faces of the cubic crystal lattice (Sidot, et al., 2005). The  $\delta$  phase exsolves within the alloy when tin constitutes more than 11%. A  $\delta$  phase is also face-centered cubic, but the greater amount of Sn within the crystal lattice distorts it more; Both of the exsolution of the  $\delta$  phase and the crystal lattice distortion created by the higher number of Sn within the lattice structure lower the final tensile strength in the high tin alloy (<11% Sn by weight percent).

Leaded tin bronze typically consists of about 80 – 85 % copper, <10% tin, and 5-10% lead. This ratio of components reduces the alloy's tensile strength, but conversely it improves the viscosity of the melt allowing for an easier pour. When a leaded bronze is cast, the  $\alpha$  phase of the copper-tin alloy segregates from the lead during cooling, making leaded bronze suitable only for casting; cold and hot working are both precluded by the segregation of the lead after solidification, as any hammering would have fractured the casting. The addition of the lead also changes the final color of the cast item, which can appeal to aesthetics (Craddock, 1977; Goodway, 1989).

Brass usually consists of up to 30% zinc in the ancient world and had to be alloyed by a different process known as cementation. Zinc vaporizes below the temperature needed to melt the copper component, and will escape an open crucible (Rehren, 1999, 2003). Recycled brass is subject to the same problem, and every recycling event will reduce the amount of zinc present in brass (Ponting, 2002; Ponting, et al., 1998).

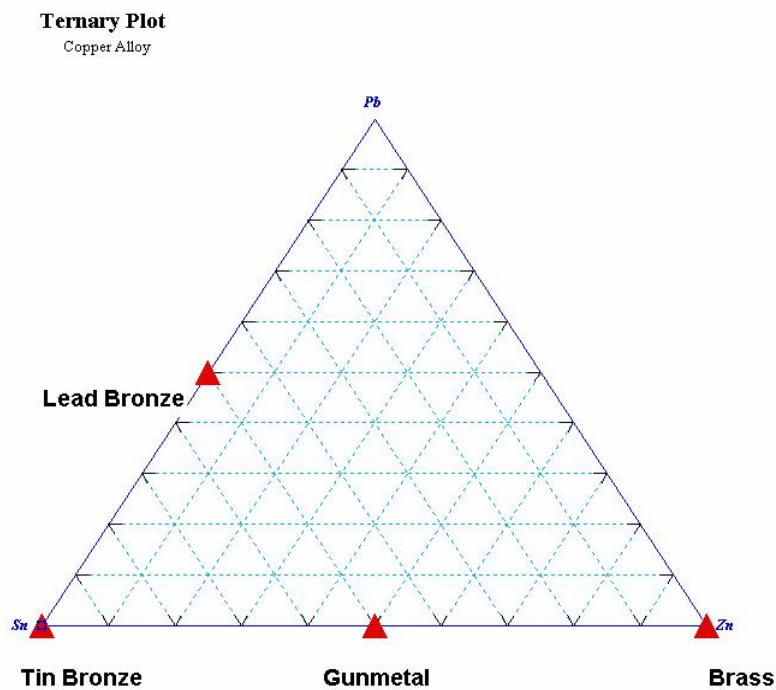


Figure 6: Ternary plot of copper alloy types

## Copper Alloys in Western Switzerland: from La Tène to the Gallo-Roman World

From the Bronze Age onward, the great skill of the metal workers within the Swiss Plateau is well known (Sauter, 1976). Some of the earliest usage of copper and its alloys are found within this area (Ottaway et al., 1975; Rychner 1988; Rychner et al, 1995). The Iron Age in this area spans from 850 B.C. to 51 B.C., and the second half of this period is known as La Tène; La Tène begins at 450 B.C. This period, known as the Second Iron Age, is known for its sophisticated metallurgy, both ferrous and non-ferrous (James, 1993).

Late La Tène copper alloy workers employed crucibles that were small (*forme de bateau* Fr. “boat-shaped”) and formed out of available ceramic sources around the charge itself. There is no evidence that they were fired, though they were often kiln dried (Fr. *terre cuite*, “baked earth”). The crucible was placed in the small furnace (less than 1.5 meters wide and about 1 meter high, fed by two to three tuyeres<sup>1</sup>) and heated to above 1100 C (Serneels and Wolf, 1999; Mauvilly, et al, 2001). The bronze was then poured off into the mold, which could be made from a number of materials (Mauvilly, et. al., 2001). Prior to the Roman conquest (hereafter, “the conquest”), there was variety in alloy recipes that appear to correlate with political boundaries, but lead and zinc were both used in copper alloy statuary; the Swiss Plateau was within an area known for statuary particularly rich in zinc (Hamilton, 1996).

In contrast to late La Tène copper alloy casting, Roman bronze casting employed larger scale crucibles; Roman crucibles capable of holding as much as 1kg of bronze are known by the 1st century AD. Molds were made of a variety of materials, with ceramic, stone, and sand being among them (Bayley, et al., 2001; Guillaumet, 2003; Hamilton, 1996; Mattusch, 1977, 1995). Roman copper alloys

---

<sup>1</sup> Tuyeres : nozzles that forced air into the furnace, raising the temperature high enough to melt the metal components. See Figure 5



for cast statuary did not employ zinc, with the notable exception of the Alexandrian style of small figurines. Lead was used instead (Hamilton, 1996).

The composition of the alloy used for casting was controlled as much by the engineering properties of the alloy in question as by any attendant cultural preferences (Dungworth, 1997). This parallels changes in copper alloy recipes in other areas of the Empire, particularly Judaea (Ponting, 2002a, 2002b). After the conquest, technical knowledge traveled even if the actual artisans did not, creating an “overprint” of Roman copper alloy recipes in addition to local ones (Hamilton, 1996; Ponting, 2002a, 2002b).

In terms of actual stylistic choices available, there are also differences between La Tène statuary and Roman statuary. Though smaller copper alloy statuary is known during the La Tène period that preceded the Roman conquest of Gaul in 51 B.C., large bronze statues are a strictly Classical style of sculpture; there is no evidence for the introduction of this Classical sculpture style into Gaul prior to Roman rule. Typically, large Celtic statuary was made of stone and far more stylized than their classical analogues (Kleiner, 1973).

### **Copper Alloy Statuary in Aventicum**

Large (e.g., life sized or larger) leaded bronze statues were a high status item purchased by the Roman, or Romanized, elites for both public and private aggrandizement of civic accomplishment and typically portrayed an individual (Pliny the Elder, 75 A.D.). These statues were crafted by casting the smaller individual portions of the Figure and then riveting or soldering these pieces together to form the complete form. The casting processes involved multiple pours of leaded bronze of the same proportions of copper, tin, and lead (Giulia-Mair, 2005; Gostencnik, 2002; Mattusch, 1977; Mattusch, 1995). A singular artifact type such as this ought to have a consistent alloy composition for both engineering and aesthetic reasons. Waste products left behind by the manufacture of these statues ought to have a relatively homogenous chemical composition as well.

Pliny the Elder says this about the high cost of these statues, using the wealth of the sculptor who cast them as a measure for the value of the statues:

*“...for Lysippus alone is said to have executed no less than fifteen hundred works of art, all of which were of such excellence that any one of them might have immortalized him. The number was ascertained by his heir, upon opening his coffers after his death, it having been his practice to lay up one golden denarius out of the sum which he had received as the price of each statue.”*

-Pliny the Elder, The Natural History, Book XXXIV, Chapter Seventeen

Such expensive items would not have been cast or purchased on a daily basis. The artisans who crafted them were clearly thought of as fine artists and masters of their craft, and were well remunerated for their works (Gostencnik, 2002; Mattusch, 1995). Figure 7, below, amply illustrates the fine detail of these works; it is thought to represent a member of the Julio-Claudian family (The Metropolitan Museum of Art, 2000).



Figure 7: Portrait statue of a boy. New York: The Metropolitan Museum of Art, from [http://www.metmuseum.org/toah/ho/05/eusb/ho\\_14.130.1.htm](http://www.metmuseum.org/toah/ho/05/eusb/ho_14.130.1.htm). The portrait is approximately life-sized.

Excavations at Aventicum revealed several sites throughout the city with evidence for copper alloy working: Insula 12, Insula 18, and Insula 56 (Figure 3).<sup>2</sup> Absent actual metal artifacts, metallurgy is inferred based on remains of crucibles, defective metal items, prills broken from the edges of the molds, and the molds themselves. Insulae 12 and 18 were located in the northern section of the city, and Insula 56 was located in the southern section of Aventicum (see Figure 2). Evidence for local bronze production is found at Insula 18 in a level dating from the 3rd century AD, and in Insula 56 in

---

<sup>2</sup>*Insulae* (sing., *insula*) were city blocks typical of Roman urban centers and usually contained commercial establishments on the ground floor and private apartment-style residences above.

a structure that was occupied from the second century through the 4th century AD (Fellman, 1988, 1992). At Insula 12, a piece of a mold used for casting a section of a large bronze statue was found; the mold was originally emplaced in a ditch, suggesting a workshop that was producing large bronze statues (Morel, 2001). As noted above, the sample suite under scrutiny in this study was found in Insula 56 within the level dated to the 2nd Century A.D (Blanc, et al., 1999a, Blanc, et al., 1999b) (See Figure 3). Bronze, lead, and iron were all used by artisans in Aventicum for items ranging from the mundane to the most luxurious (Blanc, et al., 1999a, Blanc, et al., 1999b).

### **Techniques used for this study**

This study employs two different techniques in order to expand on the previous findings by Serneels and Wolf: electron microprobe analysis (EMPA) and X-ray diffraction (XRD). EMPA can explore these samples on a level of detail that is impossible to attain using bulk analysis only. While bulk analysis has an averaging effect, EMPA can explore individual phases within the slag, both quantitatively and qualitatively. Of all the current methods available at the present, point analysis such as that which is offered by EMPA is considered the most effective means with which to explore complex materials such as metallurgical debris (Rehren and Pernicka, 2008). XRD is being used here as an additional bulk technique in order to assess the samples for semi-quantitative internal changes in individual mineral phases within the samples. Finally, the author participated in the Spring of 2008 in three metal casting events, as well as studying the work of sculpture students at the University of Georgia, in order to obtain a more thorough understanding of the specific steps involved in casting large metal sculptures, particularly those activities that influence technological choices but which do not leave direct traces in the archaeological record.

Two types of data are sought in this study: 1) Qualitative identifications and semi-quantitative analysis of hand samples, and microscopic phases and inclusions not revealed in bulk analysis; and 2) Quantitative chemical composition of the slag groundmass. The quantitative analyses of the chemical

composition of the slag groundmass will be assessed for evidence of different chemical groupings within the groundmass. The semi-quantitative and qualitative analyses, along with the quantitative analyses, will be used to infer copper alloy type and manufacturing techniques. More will be said of these techniques in the Methods section.

## METHODS

The slag samples examined in this study vary in size from roughly 2 to 10 cm in diameter (Appendices B, C). They were selected by Dr. Vincent Serneels in June of 2005 from a larger assemblage recovered during excavations at *Insula* 56 in Avenches during the excavations of 1997-1998. After receipt from the University of Fribourg, the slags were counted and assigned accession numbers. During accession, some samples were counted out of order, leading to skipped accession numbers. ABR015 and ABR026 were skipped. For the sake of consistency, the original accession numbers were left uncorrected. Some of the samples had already been accessioned at Fribourg, and these numbers were used instead of assigning new numbers. These samples have accession numbers beginning with AVS instead of ABR.

All samples were first examined and described as hand samples. Samples were then classified by hand sample appearance according to the estimated amount of vitrification, color, amount of metal present versus slag, presence of oxidation, and texture. Based on these characteristics, they could then be classified as members of three basic categories: predominantly metal, predominantly slag, predominantly ceramic material (Guillaumet, 2003; Mauvilly, et al., 2001). In the case of samples larger than 1" in diameter, sections were cut into pieces small enough to be mounted in 1" (2.54 cm) epoxy round mounts; Samples smaller than 1" (2.54 cm) in diameter were mounted individually. All of the mounted samples were polished using 600 grit and then 1000 grit sandpaper before final polishing using first 10  $\mu\text{m}$ , 5  $\mu\text{m}$  and 1  $\mu\text{m}$   $\text{Al}_2\text{O}_3$  polishing compound.

## Electron Microprobe Analysis (EMPA)

For EMPA, a JEOL 8600 Superprobe was used. For wavelength dispersive spectrometer (WDS) analysis, two analytical routines were created: a slag routine to measure oxide weight percent of the components in the slag/glass areas, and a metal routine to measure elemental weight percent of the metal components within the metallic areas of the samples. The slag routine used oxide standards (Table 1) and the metal routine used metal standards (Table 2). Slag can be very difficult to study using WDS for several reasons: It is often a quenched material akin to a glass, and can be difficult to polish well enough for accurate measurement. Individual phases contained within the slag often vary in hardness especially in comparison to the glassy groundmass, contributing to the polishing problem. Also, it is composed of the waste materials associated with the metal and these can be quite varied; requiring the measurement of a large number of oxides. Fortunately, energy dispersive spectrometer (EDS) analyses from this study combined with data from several previous studies of copper alloy slag make it possible to narrow the field of oxide components. In particular, a set of standards used by Lyle in her study of Roman period copper alloy slags from Carthage (Lyle, 2002) were modified to include additional oxides found during bulk composition analysis of the sample suite (Serneels, et al., 1999). As noted above, the final polishing stages were done using 10  $\mu\text{m}$ , 5  $\mu\text{m}$  and 1  $\mu\text{m}$   $\text{Al}_2\text{O}_3$  polishing compound grits using an automated polishing wheel, and samples were re-polished if initial analysis showed unacceptably low totals.

For all analyses, beam conditions were as follows: A 15 nA beam current was used with an accelerating potential of 15 KeV. A beam diameter of 5 microns was used. For WDS analysis, the Armstrong matrix correction was used for the slag quantitative routine and the Heinrich matrix correction was used for the metal routine. The Armstrong correction matrix accounts for the presence of oxygen within the molecular structure of the various components within the slag.

Table 1: Oxide standards used for oxide analyses

Title: Slag		KV=15		
name	Line	Standard name		Crystal
SiO <sub>2</sub>	K	Siq	Quartz	TAP
Al <sub>2</sub> O <sub>3</sub>	K	Al3	Spinel	TAP
FeO	K	Fe4	Hematite	LIF
CaO	K	Ca2	Sphene	PET
K <sub>2</sub> O	K	K	Orthoclase:	PET
PbO	M	PB2	PBSgood - galena	PET
SnO <sub>2</sub>	L	SN	Sn	PET
CuO	K	CUO	CuO	LIF
Na <sub>2</sub> O	K	NA1	ABOX – Amelia Albite	TAP
As	L	AS1	INAS – Iridium Arsenide	TAP
Sb	L	SB	Sb	PET
MgO	K	MG3	Olivine	TAP
S	K	S	Pyrite	PET

Table 2: Element standards used in WDS analysis of metal.

Title: Metal		KV=15		
name	line	Standard name		Crystal
Cu	K	Cu	Cu	LIF
Sn	L	Sn	Sn	PET
Pb	M	PbMetal	Pb	PET
Fe	K	FEM	Fe	LIF
As	L	AS1	INAS – Iridium Arsenide	TAP
Sb	L	SB	Sb	PET
Cr	K	CrM	Cr	LIF
Ni	K	Ni	Ni	LIF

In this study, EDS was used to characterize metallic areas within the groundmass of the samples, suggest possible identification of mineral grains within the samples, and approximate elemental concentrations within the groundmass in preparation for WDS analysis. WDS analysis was then performed on all of the samples for oxide weight percents; no fewer than two points were analyzed on each sample, and in most cases at least five points were analyzed in order to increase the precision and accuracy of the data. All totals were normalized. In some samples, WDS analysis rendered unacceptably low totals for the groundmass points, and these totals were discarded. Totals



that were representative of individual mineral phases were also discarded for analyses of the groundmass itself.

With respect to imaging in this study, backscattered electron imaging (BEI) was generally more useful than secondary electron imaging (SEI). During the analysis of each sample, when an area of mineralogical interest was found, an image at the appropriate level of magnification was taken. In most cases, the BEI image was combined with an SEI image. In the case of unknown minerals, imaging was combined with EDS data in order to suggest possible identifications for those minerals.

### **X-ray Diffraction (XRD)**

Two samples were chosen for X-ray Diffraction (XRD) analysis: a slag fragment from AVS722, and a ceramic fragment from AVS722. AVS722 showed a gradient from slag on one side to ceramic on the other and was chosen in order to examine the changes between the ceramic material and the slag. The sample was cut into two pieces representative of the two areas noted above and the pieces were prepared as randomly oriented powder mounts.

The X-ray source for the analysis was cobalt, not copper. There is an inherent difference between the X-rays generated by a cobalt source and those generated by a copper source; the wavelength of the X-rays generated by a cobalt source is 1.788965 Å (angstroms). This will change the 2θ angles but not the d-spacings, so for analysis, d-spacings were chosen in order to identify phases, and the 2θ angles were not used for interpretation of the results.

XRD machine settings were as follows: The start angle was 5 degrees, and the stop angle was 70 degrees with a step size of 0.01 degrees. The scan rate was 0.4 degrees 2θ per minute in a continuous mode at a wavelength of 1.788965 Å. The X-ray tube and detector both used fixed slits. After the raw data were collected, peaks with less than 5% relative intensity were discarded, and the remaining peaks were assessed for matches using the Hannawalt search method.

### **Modern Metal Casting Observations**

During the Spring of 2008, the author was enrolled as student in a metal casting class taught at the Lamar Dodd School of Art at the University of Georgia under James Buonaccorsi. The class was required to fabricate cast metal sculpture from the first modeling to the final finishing of the item, including the actual casting itself. During the course of this class, the author was able to observe these steps in the chain of manufacture. This has allowed the author to infer some of the less archaeologically visible activities and choices of materials at *Insula* 56 in the hope that this may piece together a more complete picture of this workshop.

## RESULTS

### **Rough sorting of sample types by hand sample**

The samples were sorted into these three categories: ceramic fragments, metals, and vitreous slag (Table 3). Ceramic fragments showed gradations in color. Some were orange to red on their exterior portions with vitrification on the interior. Some were gray on their exterior portions with vitrification and/or metals adhered to interior. Metal samples were heavily corroded on their exteriors and were initially identified by their greater density and weight. All metal samples appeared to be some form of Cu alloy, based on their green tarnish or “patina”. One sample was also coated with ceramic on one side. The vitreous slag varied in porosity and color. Some were vesicular and tended towards a greenish-gray color. Other samples showed streaks of reddish bands. Other samples were darker and denser, with the main portion of the groundmass colored black, but streaked in places with the same red banding. All slag samples displayed abundant visible quartz grains. See Appendix C for photographs of all samples.

Ceramic fragments were found in ABR027, ABR028, ABR029, AVS722, and AVS905. In all cases, the fragments had a gray-green slag coating on one side; the ceramic layers varied in color between red-brown (AVS722) and dark gray (ABR027, ABR028, ABR029, AVS905). Their texture was gritty with silt and sand sized grains. The slag coating was highly vitrified with visible quartz grains and metal oxides. The ceramic fragments were around 10 cm thick.

Metal was the primary constituent of samples AVS901, AVS902, and AVS903. Samples AVS905 and ABR025 also had a significant metal component. All showed signs of corrosion by oxidation, and in the case of AVS905 its metal composition was not immediately apparent due to the presence of a coating of ceramic and slag. These samples were all heavier than crucible or slag

fragments of comparable size. Their greater density suggested a more metallic composition, and when cut they showed a metallic luster.

The third group, composed of slag, varied in appearance. The largest group had a vitreous, mottled gray and green surface appearance and tended to be vesicular in texture. Most had observable copper oxides, quartz grains, and iron oxides within their groundmass. These samples included ABR006, ABR008, ABR009, ABR010, ABR011, ABR012, ABR013, ABR014, ABR017, ABR018, ABR019, ABR020, ABR021, ABR022, and ABR025. Another group consisted of slag with a greenish gray appearance that was less vesicular but retained a vitreous luster. These were ABR001, ABR002, ABR003, ABR004, ABR005, ABR016, and ABR023. There were observable copper oxides present in these as well. The last group consisted of only two samples, ABR007 and ABR024. These were colored a mottled green, with less gray. These were also had copper oxide corrosion and were vitreous in appearance with fewer vesicles than the first group.

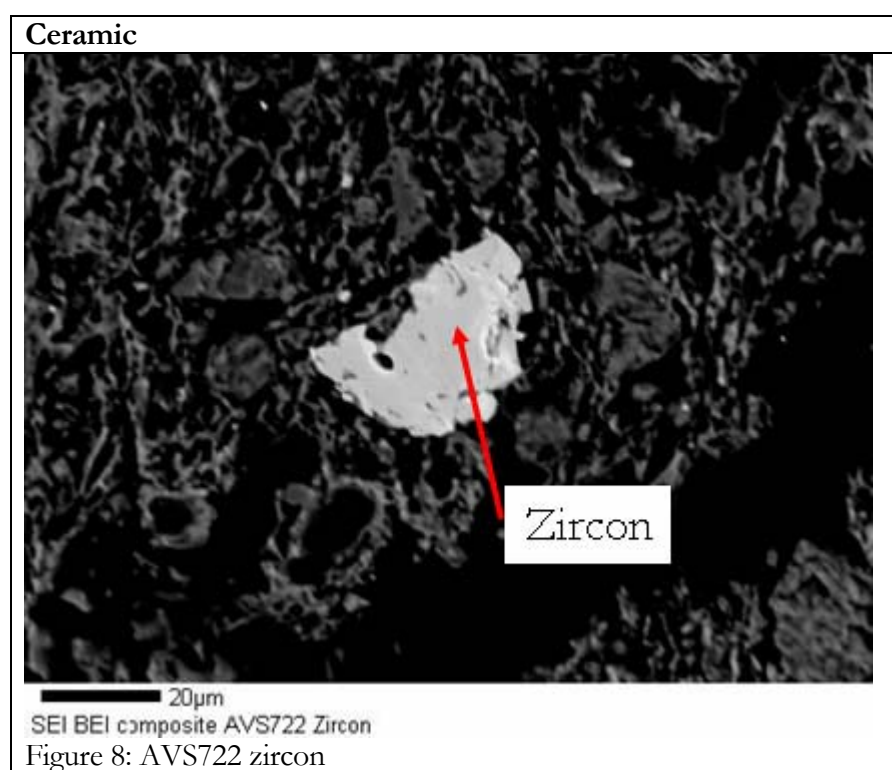
Table 3: Hand sample results and descriptions

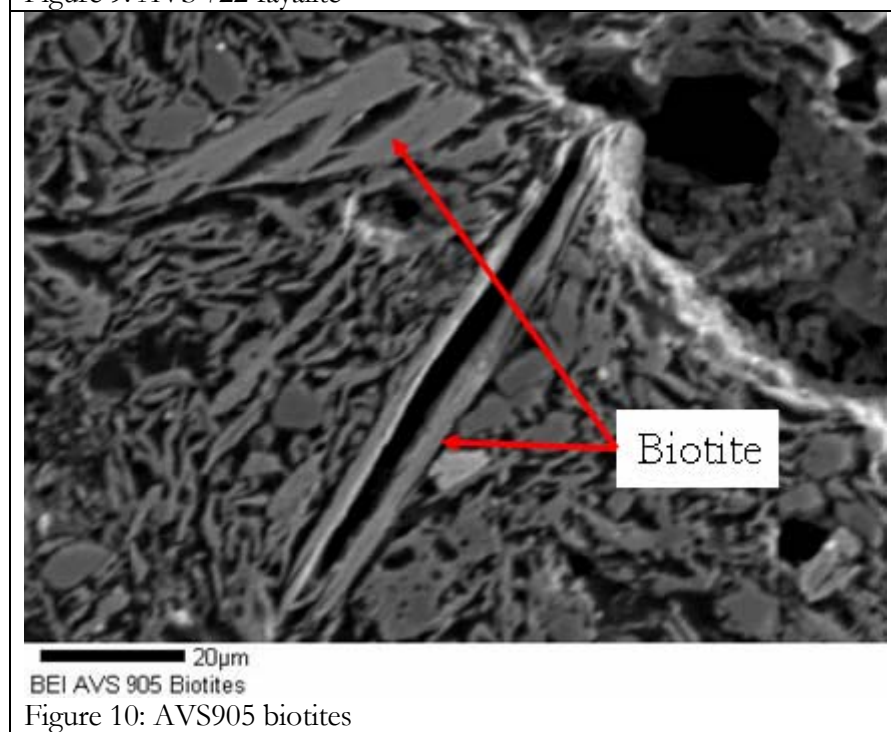
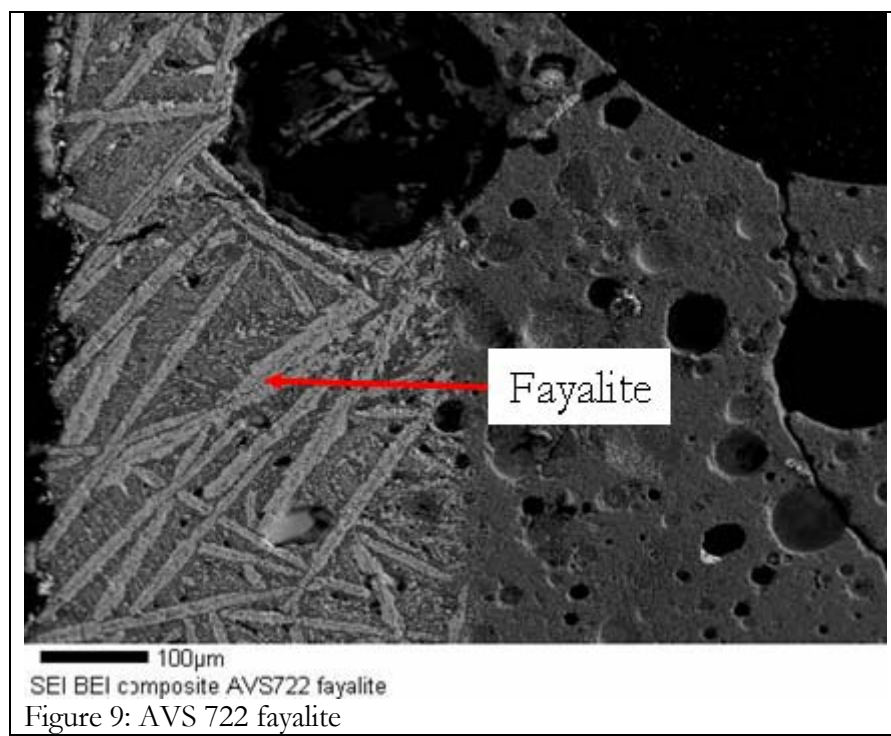
Sample number	Color	Hand sample descriptions	Type
<b>AVS722</b>	Reddish outer layer	Has a distinct ceramic layer bounded by a slag layer.	Ceramic
<b>ABR027</b>	gray brown with green	Slag material on one side, ceramics on the other. Corroded copper visible on slag side. Vesicular appearance on slag side	
<b>ABR028</b>	gray brown with green	Ceramic layer with slag layer on the other side. Slag is very vesicular, dark color, with some corroded copper.	
<b>ABR029</b>	gray brown with green	Darker slag side has smaller amounts of corroded copper, and is considerably more glassy as well as darker in color than most of the other samples. It also has a darker ceramic layer on the back side.	
<b>AVS905</b>	Gray outer layer	Ceramic outer layer, with inner side appearing more like the slag. Some corroded copper visible on the slag side, with vesicles shot through the layer. Some metal components.	
<b>AVS901</b>	mottled green/ red	Metal prill	Metal
<b>AVS902</b>	mottled gray green	Metal prill	
<b>AVS903</b>	mottled gray green	Metal prill	

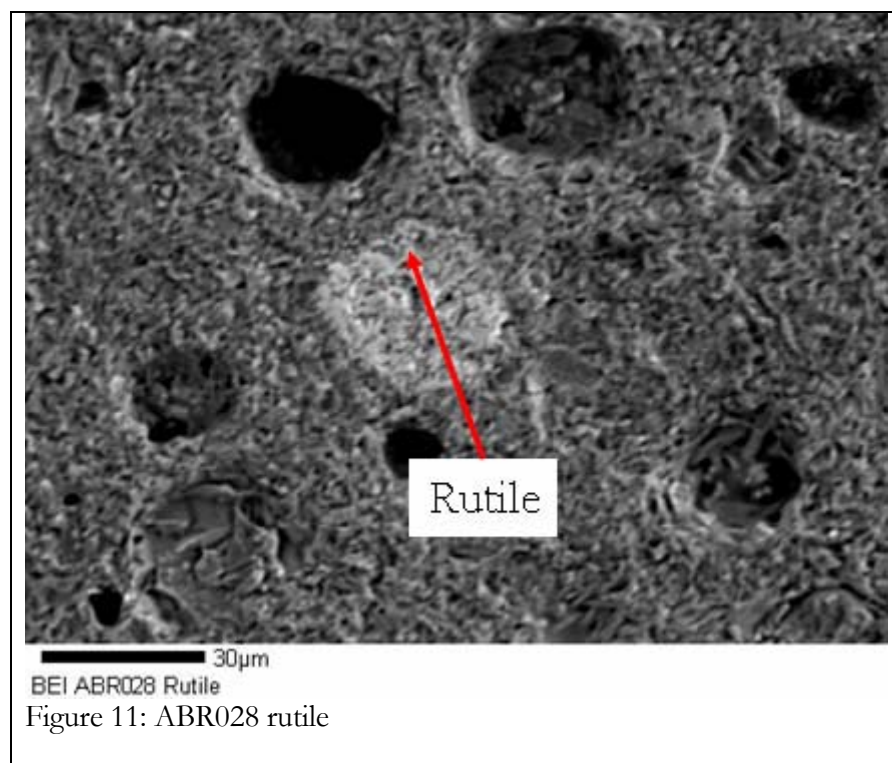
<b>ABR001</b>	green-grey	Slag	Slag
<b>ABR002</b>	green-grey	Slag	
<b>ABR003</b>	green-grey	Slag	
<b>ABR004</b>	green-grey	Slag	
<b>ABR005</b>	green-grey	Slag	
<b>ABR006</b>	Green-gray	Slag	
<b>ABR007</b>	mottled green	Slag: glassy w/ corrosion	
<b>ABR008</b>	Gray green	Slag	
<b>ABR009</b>	Gray green	Slag	
<b>ABR010</b>	Gray green	Slag	
<b>ABR011</b>	mottled green and red	Slag	
<b>ABR012</b>	mottled green and red	Slag	
<b>ABR013</b>	mottled green and red	Slag	
<b>ABR014</b>	mottled green and red	Slag; Vesicular, glass-like slag with corroded copper and quartz grains.	
<b>ABR016</b>	green-grey	Slag : Gritty with corrosion	
<b>ABR017</b>	mottled green and red	Slag	
<b>ABR018</b>	mottled green and red	Slag :Vesicular, with corroded copper.	
<b>ABR019</b>	mottled green and red	Slag	
<b>ABR020</b>	mottled green and red	Slag: Very vesicular, with oxides visible on one side.	
<b>ABR021</b>	mottled green and red	Slag fragment with dark glassy appearance speckled with copper oxide, copper, and quartz grains	
<b>ABR022</b>	mottled green and red	Slag: Very vesicular, with both copper and copper oxide visible on the surface.	
<b>ABR023</b>	green-grey	Slag: Less glassy than 021 or 025, and covered in thin ceramic layer. Underneath this layer, dark glassy slag is visible, with some copper oxide apparent.	
<b>ABR024</b>	mottled green	Slag: glassy w/ corrosion	
<b>ABR025</b>	mottled green and red	Slag: Very vitrified, with extensive copper corrosion, vesicles and quartz grains. Some metal components.	

## Images with EDS spectra

A combination of both backscattered and secondary electron images was generally more useful for all image data. Because quartz is common throughout the sample suite and was readily identifiable in images and EDS, image analysis focused on other mineral phases. Within the ceramic matrix, zircon (Figures 8, 12), fayalite (Figure 9), biotite (Figures 10, 13), and rutile were found (Figure 11). The biotite was very common, as was feldspar and to a lesser extent, zircon. The fayalite only occurred along a sharp boundary between the ceramic and a more vitrified section of the sample AVS722. The rutile was only present in trace amounts.









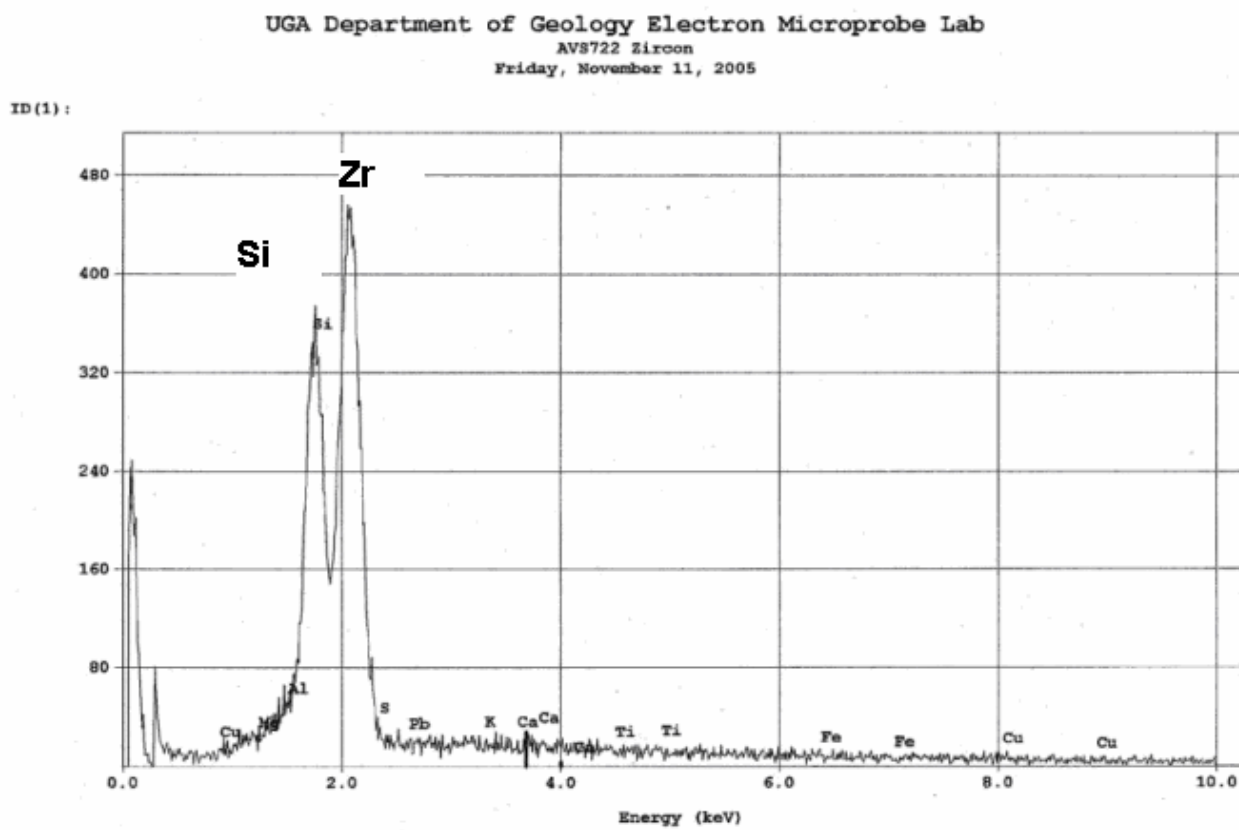


Figure 12: AVS722 zircon

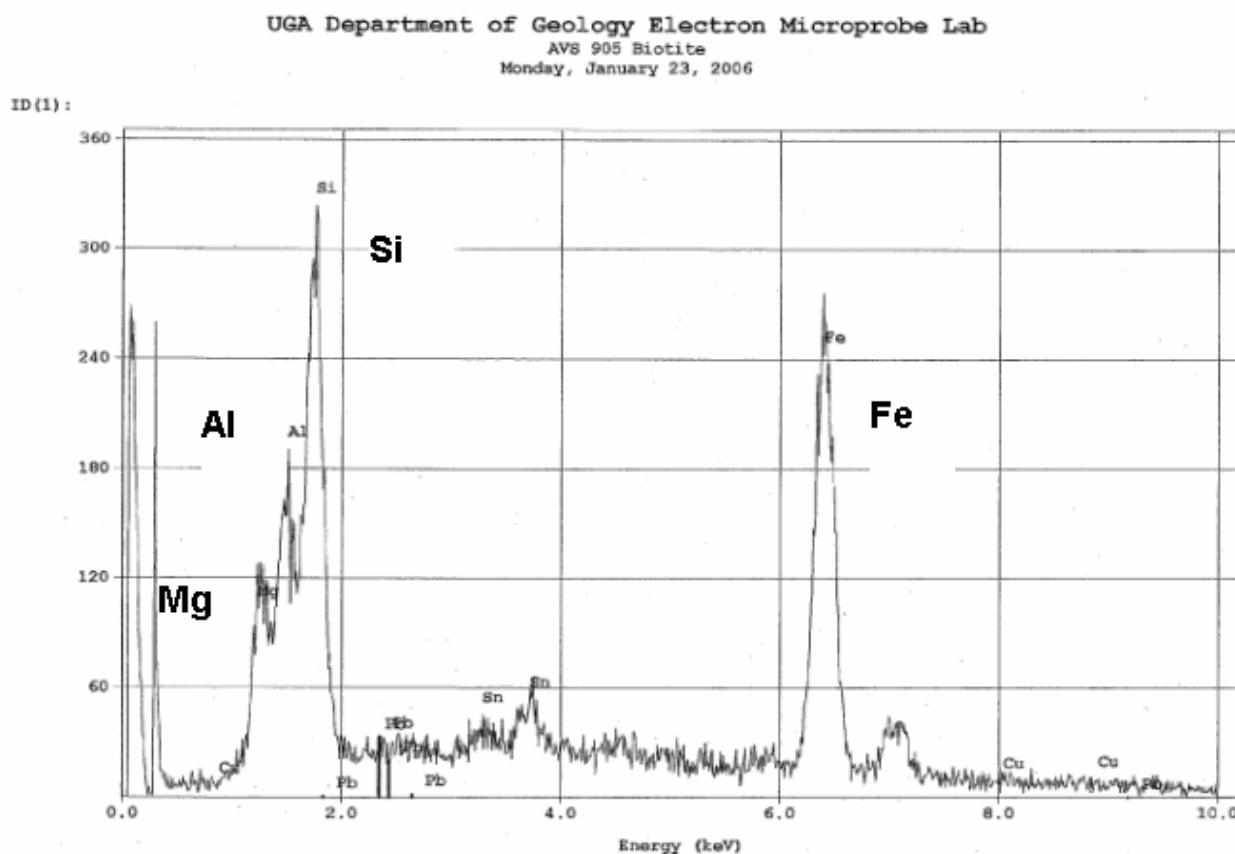


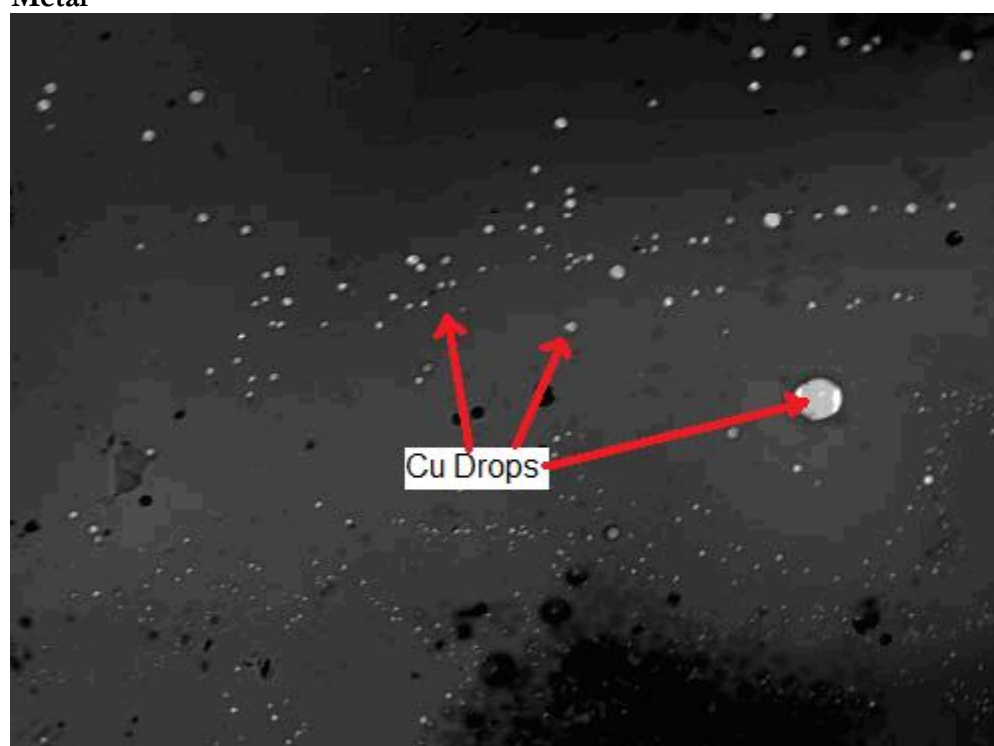
Figure 13: AVS905 biotite

Image data were taken of metal prills within the groundmass of the samples as well as of incomplete reactions between the alloy components and the silicate slag. Metal prills are easily identifiable due to their greater brightness in BEI that was a result of their greater density than the silicate groundmass. EDS spectra were used to identify which metals were present within the prills and are discussed below in the section on EDS results. Metal prills were common within all the ceramic and slag samples. Pure Cu appears more commonly as round drops (Figure 14), but Sn and Pb were

not visible as pure metals alone in the image data; instead, the Sn was present as a component of bronze alloy prills (Figure 15) while Pb was present as a separate immiscible phase (Figure 16) .

The areas of incomplete reactions are displayed below, with one image, Figure 16, and one set of EDS spectra included (Figure 17). These are notable for the fact that the metal components have failed to mix completely. It should be observed that the incomplete reactions as shown by EDS between the metal components of the alloy mostly occur within samples classified in hand sample as predominantly metal. The image shown itself comes from ABR025, which was classified as slag in hand sample, but which also showed extensive Cu corrosion in hand sample and was richer in metals than was immediately apparent to the naked eye in hand samples.

### Metal



50µm  
BEI Area1 in ABr002 at 400 mag  
Figure 14: Cu prills in ABR002

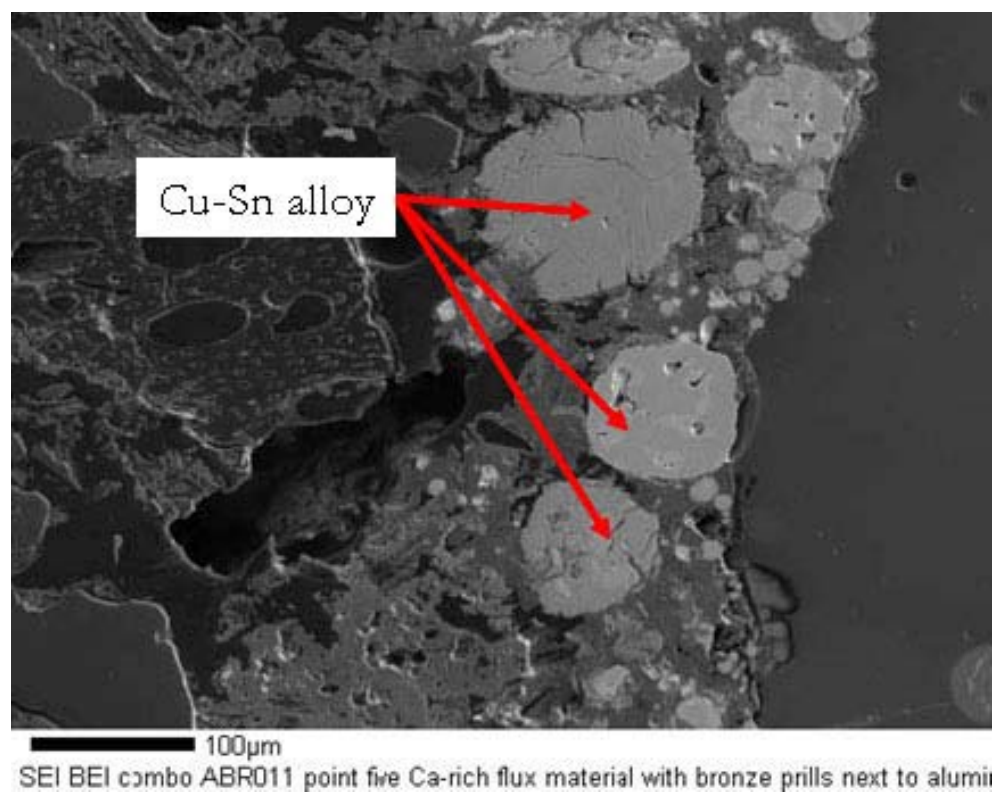


Figure 15: Cu-Sn alloy prills

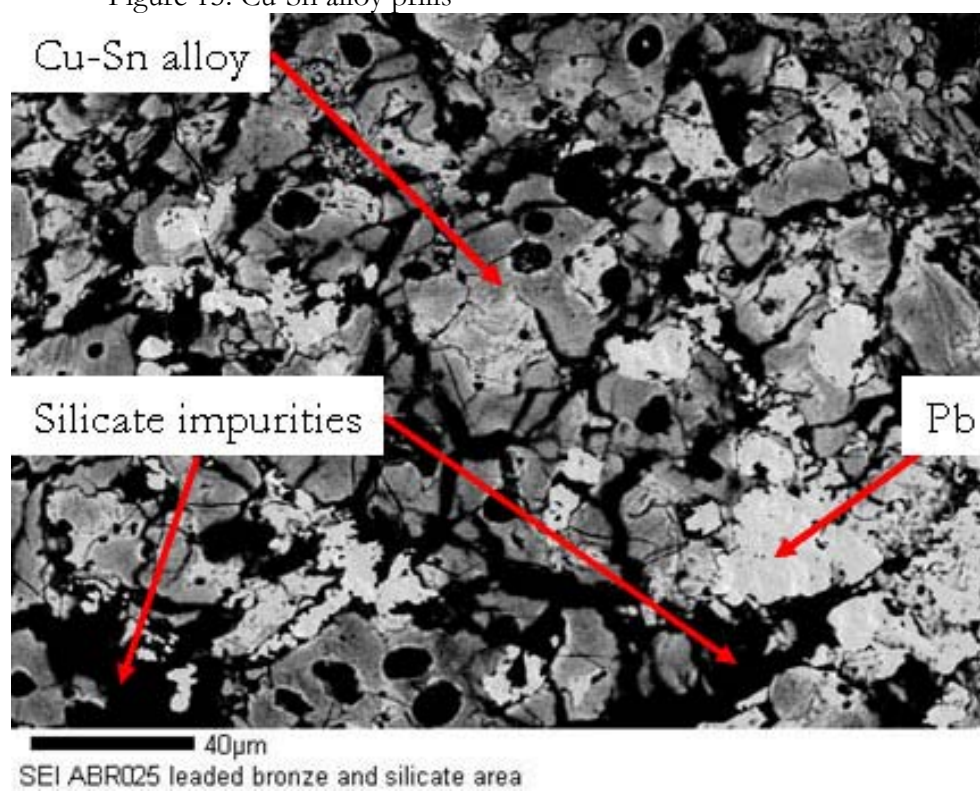


Figure 16: ABR025 leded bronze silicate

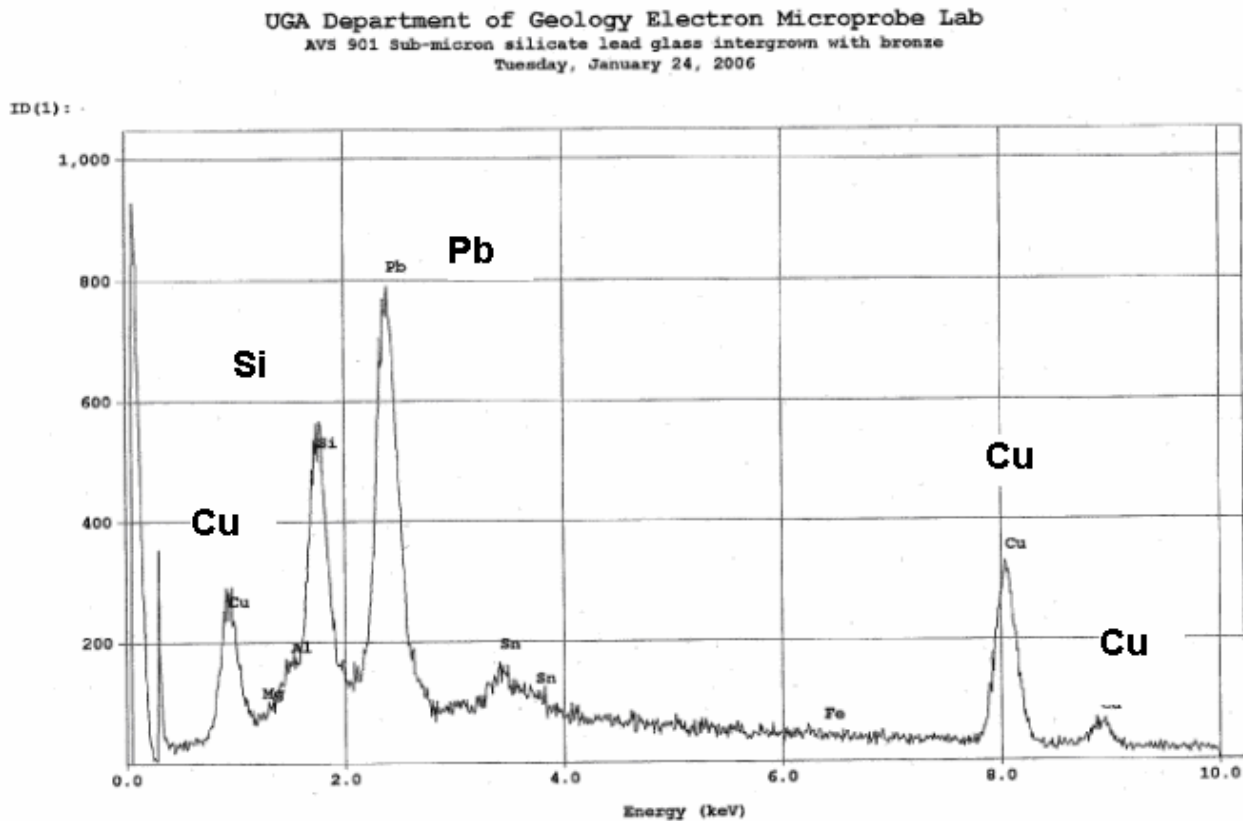


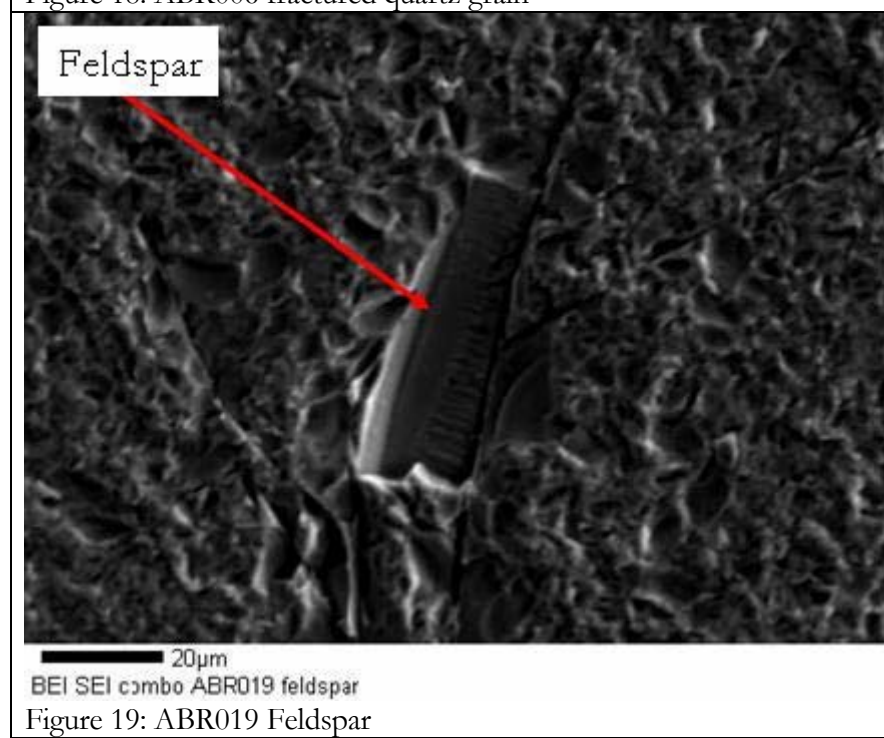
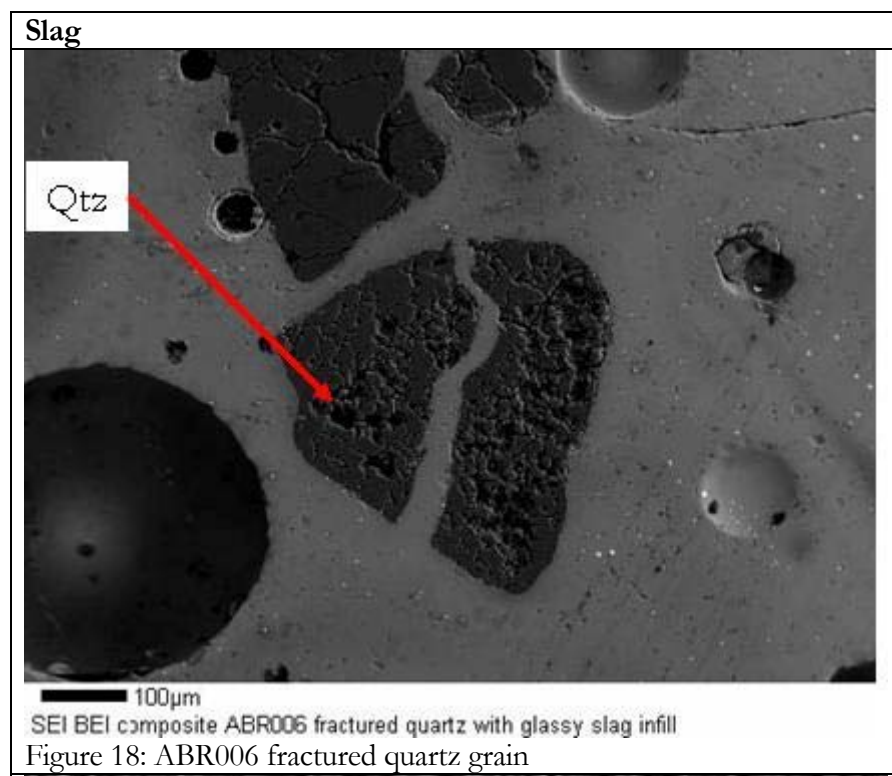
Figure 17: AVS901 silicate groundmass enriched in leaded bronze

Images of the slag groundmass are shown below with accompanying EDS spectra where relevant. In the case of certain phases such as quartz or feldspar that were first identified by EDS, but could then be easily recognized by crystal shape or relative density compared to the rest of the groundmass, EDS spectra have been omitted.

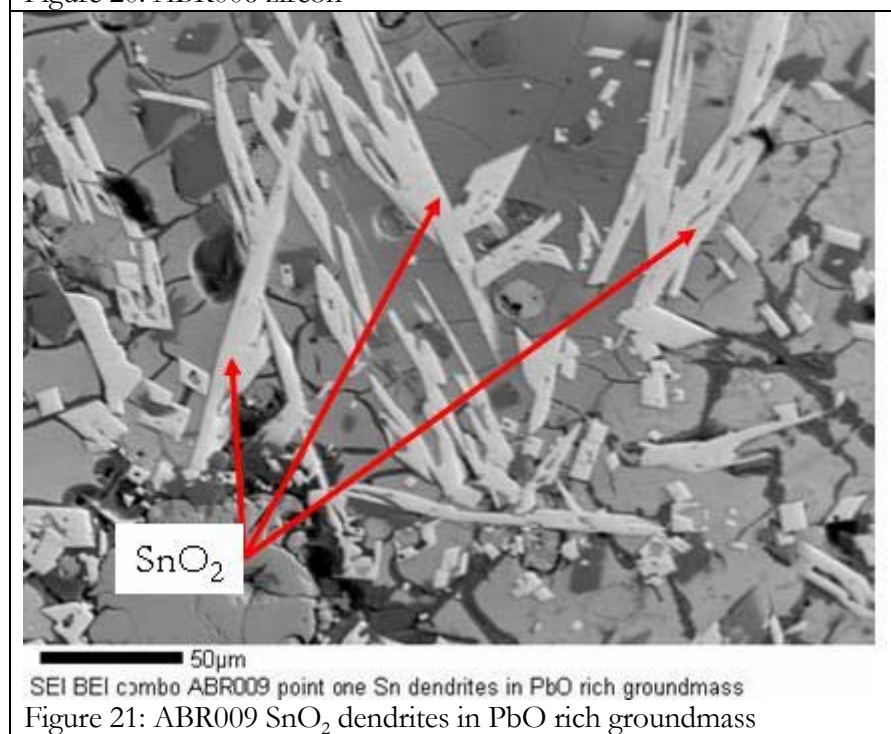
Quartz grains were ubiquitous throughout the groundmass of the slag samples (Figure 18). Zircon also appeared in small quantities (Figures 20), as did some feldspar (Figure 19).  $\text{SnO}_2$ , cassiterite, was extremely common throughout the sample suite as well. It showed two different forms

of crystal habit: rectilinear grains were common in areas of groundmass dominated by PbO (Figure 21), and more equidimensional grains were typical in areas of the groundmass containing FeO (Figures 22, 30). Fayalite was found in the slag groundmass, but it was less common than the SnO<sub>2</sub>. It did not display the dendritic nucleation found in AVS722, however, suggesting a different cooling history (Figures 23). FeO was also detected in other phases that did not display any sort of consistent habit; instead, it appeared as prills within the groundmass (Figure 25) and inside vesicles (Figure 24).

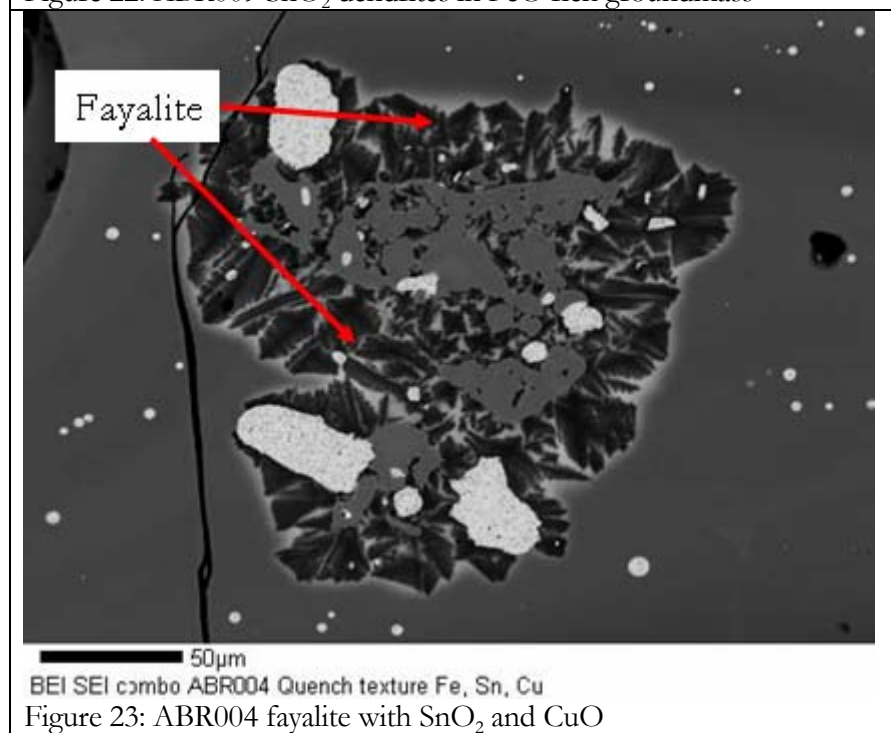
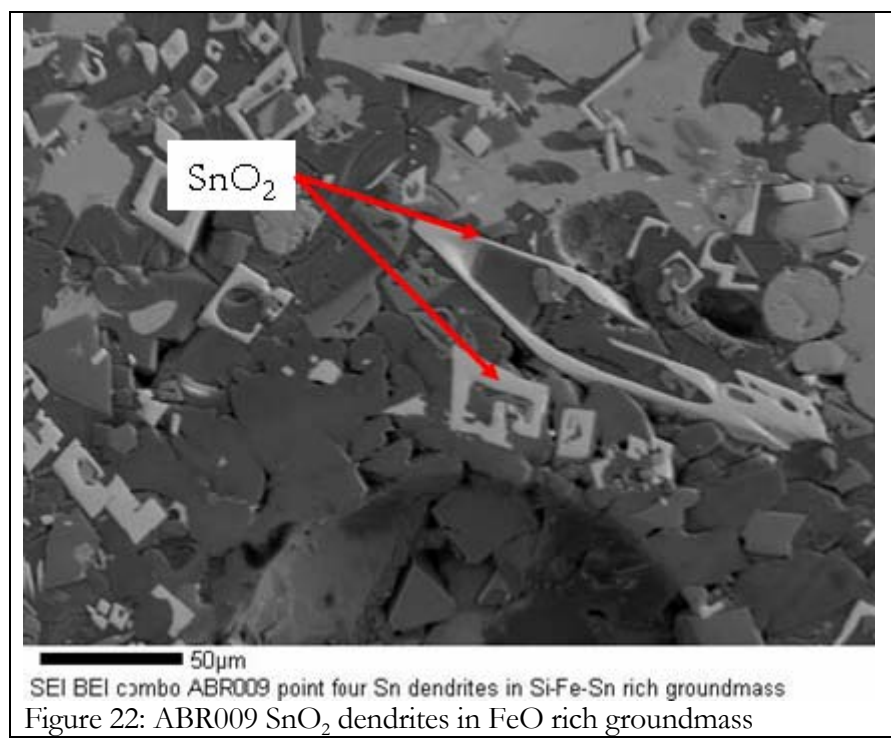
There were also phases that were rare, but interesting in appearance. Iron sulfides were found in ABR019 and ABR029 (Figure 26). An area of high density rendered EDS data that included Cu, Fe, and S, but the lack of crystal habit was not consistent with chalcopyrite (Figure 27). Finally, chrome spinel was detected with crystal habit consistent with the mineral phase (Figure 28), but an area that EDS showed as possible chrome spinel lacked regular crystal habit (Figure 29)

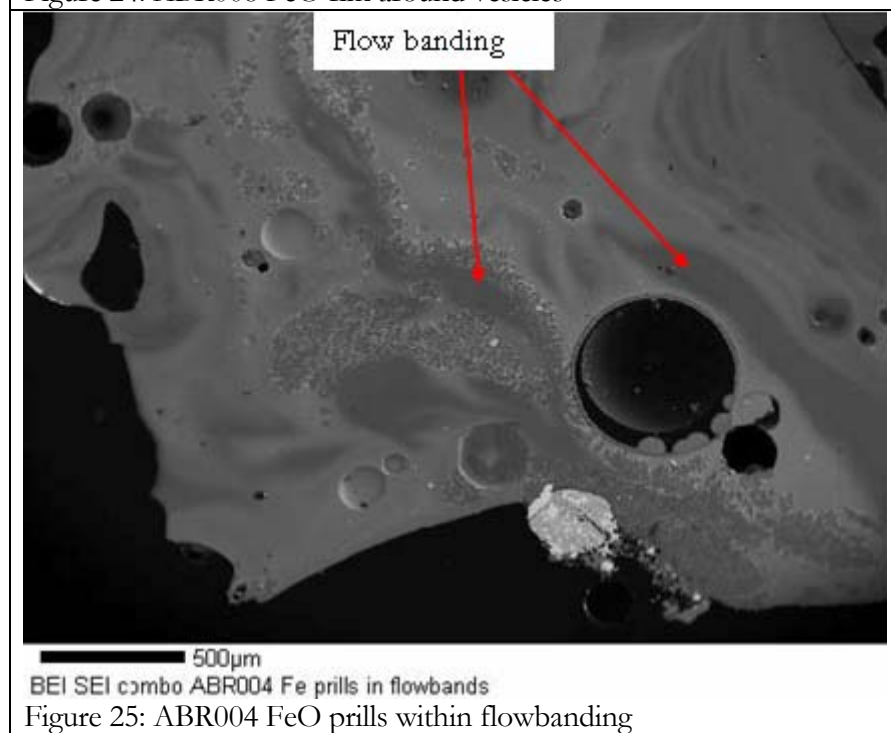
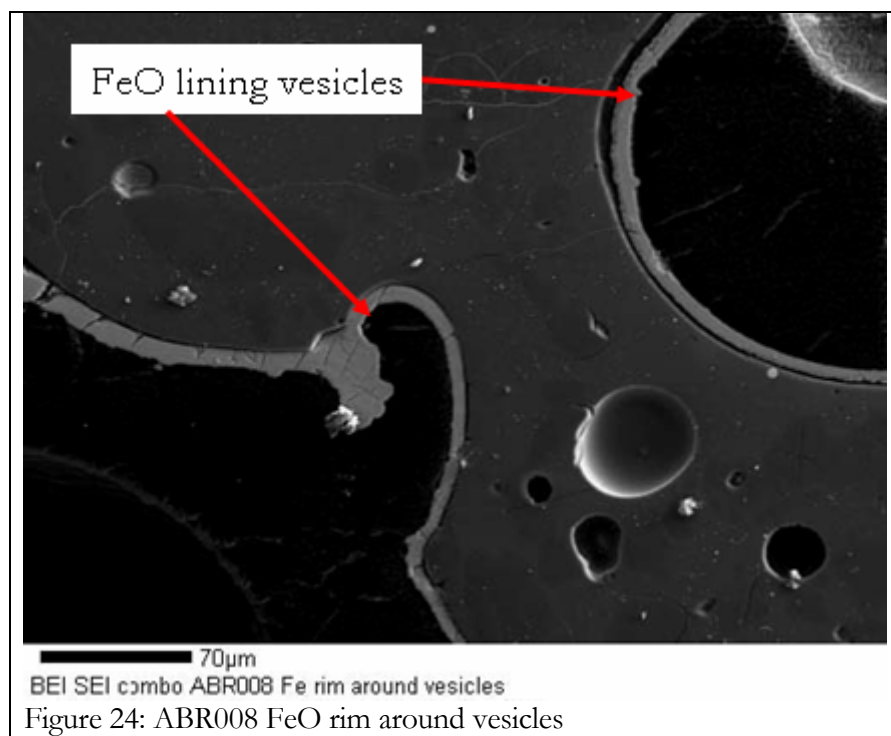


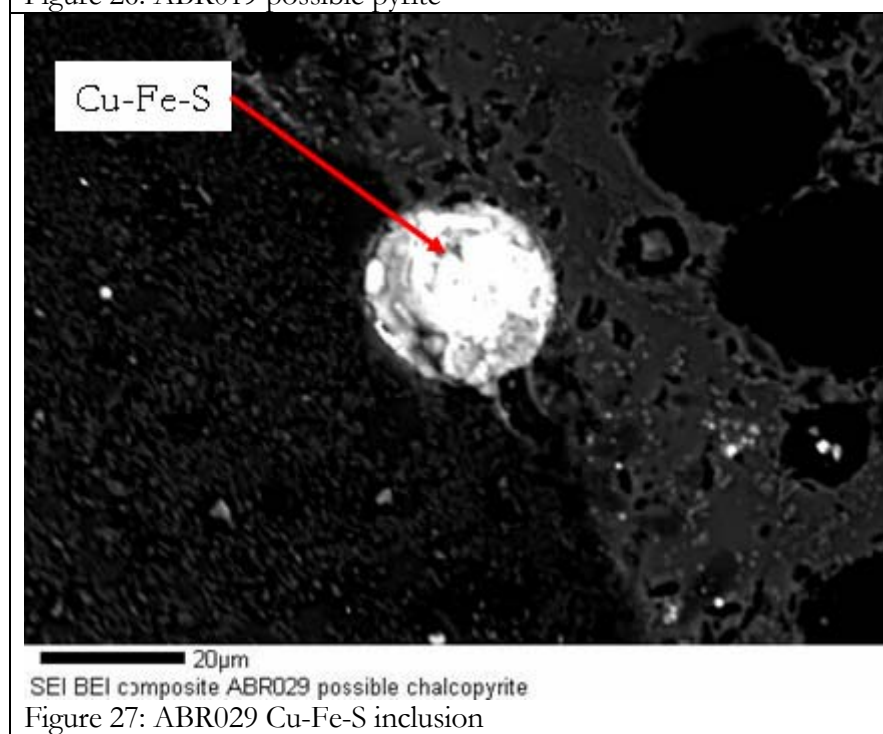
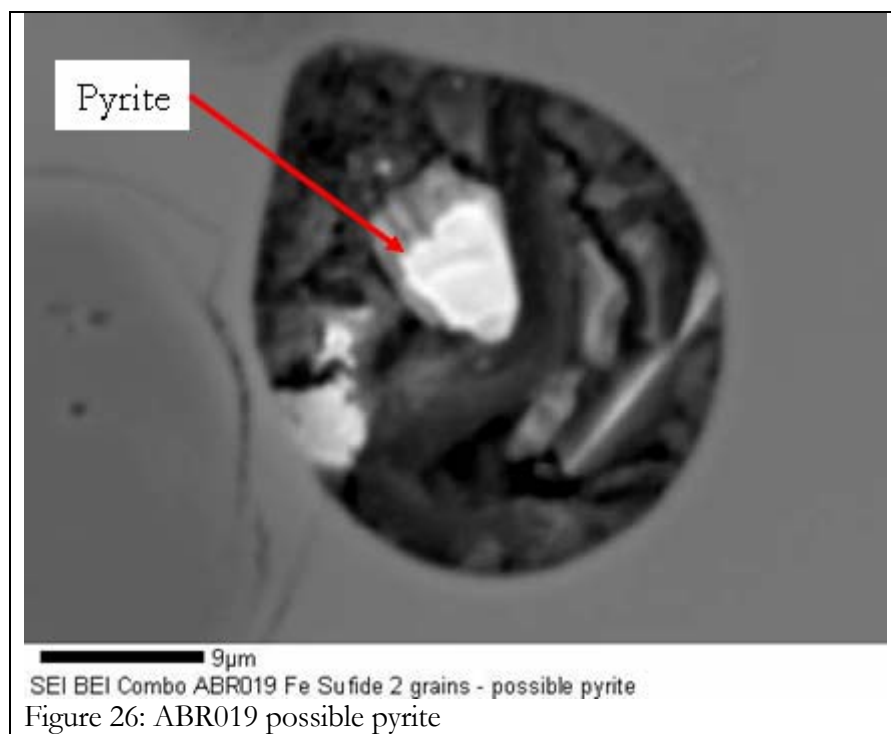


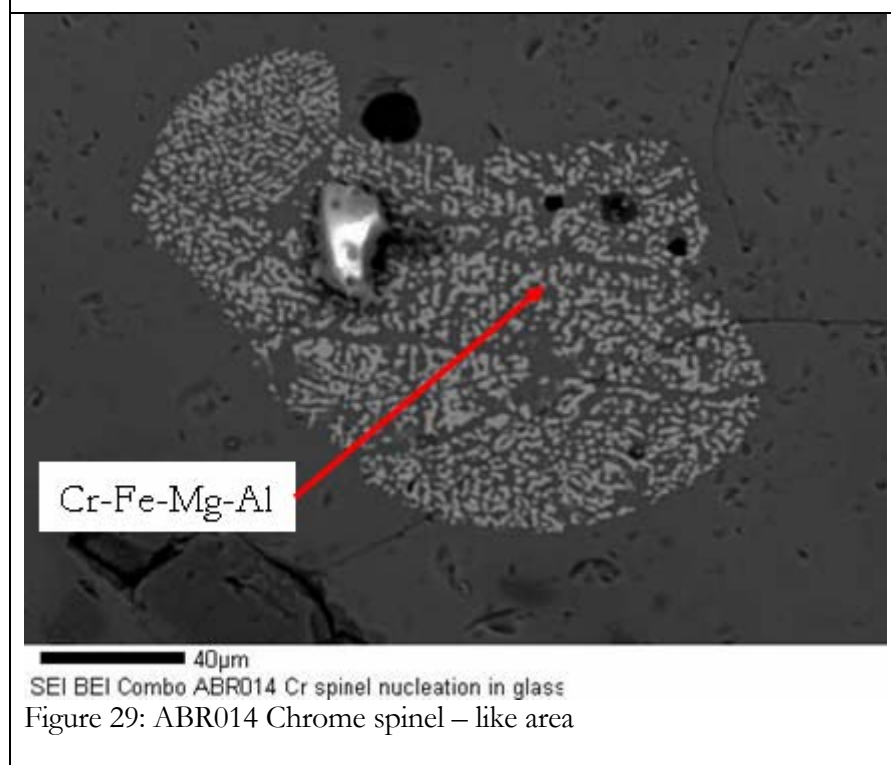
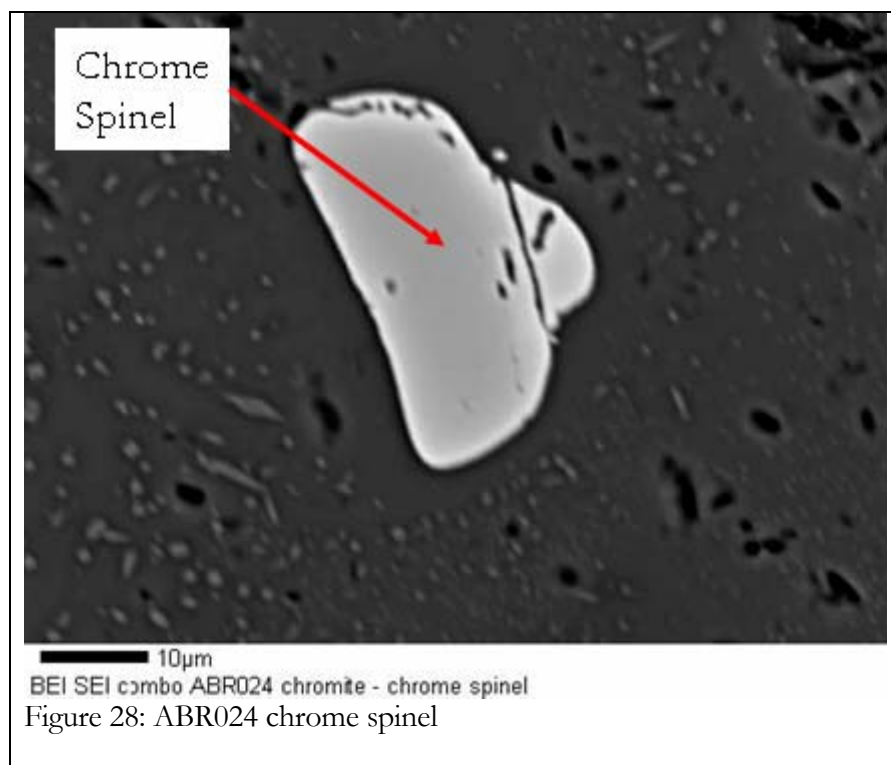












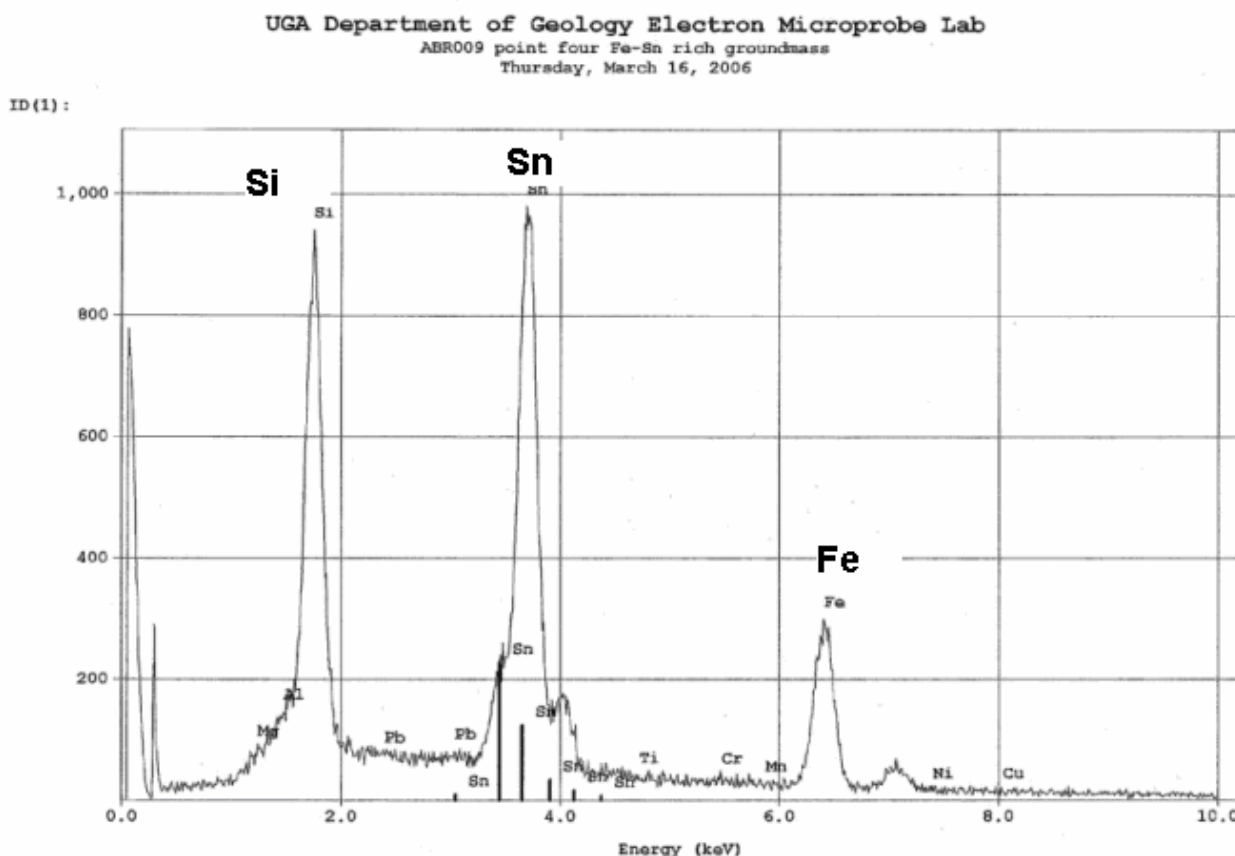


Figure 30: ABR009 SnO<sub>2</sub> in FeO enriched groundmass

### Electron Dispersive Spectrometry Data

EDS data were used to obtain elemental characterization of points within the samples. It is important to note that EDS is only a semi-quantitative analytical method and data obtained by EDS can not be used to securely identify mineral phases. It only offers data on what elements are present within the area targeted by the electron beam.

Fayalite, biotite, potassium feldspar, and zircon were suggested by EDS in the ceramic samples. Within the groundmass of the slag samples, a wide variety of isolated phases were suggested, but not in any significant quantity: Zircon, fayalite, pyrite, sphene, brass, rutile, chromite, biotite,

potassium feldspar, ilmenite, cuprous chloride, garnet, quartz, sylvite (Table 4). Copper, tin, lead, iron, antimony, sulfur and various copper alloy types were all detected within the metal inclusions of the sample suite (Table 5); it should be noted that metal prill inclusions within the group of slag samples were also analyzed by EDS in addition to the metal group of samples. The quartz, feldspar, zircon, fayalite, pyrite, copper sulfide area, and spinel have been discussed above (Figures 18-29)

Table 4: Phases suggested by EDS within the slag groundmass and ceramic

	Zircon	Fayalite	Pyrite	Chalcopyrite	Sphene	Brass	Rutile	Chromite	Biotite	Potassium	Feldspar	Ilmenite	Cu-Cl	Garnet	Quartz	Sylvite
ABR006	Y														Y	Y
ABR004		Y														
ABR009		Y														
ABR010																Y
ABR011		Y														
ABR012	Y												Y		Y	
ABR014	Y				Y	Y		Y	Y							
ABR017	Y															
ABR018	Y	Y								Y					Y	
ABR019	Y		Y							Y						
ABR020							Y									
ABR024								Y								
ABR027		Y					Y									
ABR028	Y				Y		Y									
ABR029		Y	Y	Y												Y
AVS901																
AVS902																
AVS903																
AVS905									Y							
AVS722	Y				Y				Y	Y		Y		Y		
Total	8	6	2	1	3	1	3	2	3	3		1	1	1	3	3

Table 5: Components detected in the metal inclusions within the samples

	<b>Cu</b>	<b>Sn</b>	<b>Pb</b>	<b>Fe</b>	<b>Bronze</b>	<b>Cu-Sn</b>	<b>Sn-Pb</b>	<b>Cu-Pb</b>	<b>S</b>
<b>ABR004</b>	Y			Y		Y			
<b>ABR005</b>		Y		Y	Y		Y		Y
<b>ABR009</b>		Y							
<b>ABR011</b>					Y				
<b>ABR012</b>					Y				
<b>ABR013</b>		Y							
<b>ABR014</b>					Y	Y			
<b>ABR016</b>		Y	Y						
<b>ABR017</b>					Y				
<b>ABR018</b>						Y			
<b>ABR020</b>						Y			
<b>ABR025</b>		Y							
<b>ABR029</b>			Y		Y				
<b>AVS901</b>					Y			Y	
<b>AVS902</b>						Y			
<b>total</b>		3	5	2	7	5	1	1	1

### Wavelength Dispersive Spectrometry Data

All samples were subject to WDS analysis and in samples where specific minerals such as quartz and fayalite were suggested by EDS and imaging data, these phases were also analyzed. Metal prills within the groundmass were also analyzed for weight percentages of the metal components. In some cases, totals were too low to consider reliable and these were discarded; this accounts for the variation in the number of points per sample reported here. Arsenic (As), Na<sub>2</sub>O, MgO and S amounts were below detection limits and were discarded. Antimony (Sb) has also been discarded for the same reason; however, EDS did detect measurable Sb (above minimum detection limits) at several points in the samples. Therefore, it can be considered a trace element: in some samples, but it will not be included in the WDS analysis of the groundmass overall. The rest of the data were normalized.

Only two points of the ceramic groundmass in AVS722 were analyzed. This was due to the difficulty in obtaining a mirror polish on its surface (Table 6).



Table 6: Normalized data for ceramic, minus fayalite analysis

Sample	Pt#	SiO <sub>2</sub>	Al <sub>2</sub> O <sub>3</sub>	FeO	CaO	K <sub>2</sub> O	PbO	SnO <sub>2</sub>	CuO	Na <sub>2</sub> O
AVS722	16	58.51%	22.03%	5.60%	8.69%	2.54%	0.25%	0.00%	0.00%	2.37%
	20	63.80%	20.23%	5.60%	5.58%	3.02%	0.00%	0.00%	0.00%	1.68%
	<b>AVG</b>	<b>61.16%</b>	<b>21.13%</b>	<b>5.60%</b>	<b>7.14%</b>	<b>2.78%</b>	<b>0.00%</b>	<b>0.00%</b>	<b>0.00%</b>	<b>2.03%</b>
	<b>STD</b>	<b>3.75%</b>	<b>1.27%</b>	<b>0.00%</b>	<b>2.20%</b>	<b>0.00%</b>	<b>0.00%</b>	<b>0.00%</b>	<b>0.00%</b>	<b>0.00%</b>
	<b>MDL</b>	<b>0.051</b>	<b>0.05</b>	<b>0.173</b>	<b>0.066</b>	<b>0.036</b>	<b>0.243</b>	<b>0.156</b>	<b>0.202</b>	<b>0.051</b>

Within the metal group weight percentages of copper, tin, lead and iron varied but showed discernable trends. In the metal areas (Table 7) of the samples, Cu varies between 80-100%. Sn varies from 1-20%, but it is impossible to fix a definite percentage of Pb within the alloy due to its immiscibility. Iron varies between 0.0%-0.7%, just above minimum detection limits of 0.12%. The presence of iron within copper alloys is not uncommon (Cooke and Aschenbrenner, 1975).

Table 7: Normalized data for metals

Label	Pt#	Cu	Sn	Pb	Fe	As	Sb	Cr	Ni	Total
ABR001	1	82.84%	10.09%	7.06%	0.01%	0.00%	0.00%	0.00%	0.00%	100.00%
	1	84.84%	9.82%	5.25%	0.09%	0.00%	0.00%	0.00%	0.00%	100.00%
	2	84.15%	10.54%	5.25%	0.06%	0.00%	0.00%	0.00%	0.00%	100.00%
	9	81.65%	16.05%	2.24%	0.06%	0.00%	0.00%	0.00%	0.00%	100.00%
	1	83.81%	10.26%	5.93%	0.00%	0.00%	0.00%	0.00%	0.00%	100.00%
	2	84.19%	9.89%	5.92%	0.00%	0.00%	0.00%	0.00%	0.00%	100.00%
	9	83.04%	15.12%	1.73%	0.10%	0.00%	0.00%	0.00%	0.00%	100.00%
	20	81.56%	10.52%	7.91%	0.01%	0.00%	0.00%	0.00%	0.00%	100.00%
	22	60.73%	39.18%	0.00%	0.09%	0.00%	0.00%	0.00%	0.00%	100.00%
	<b>AVG</b>	<b>80.76%</b>	<b>14.61%</b>	<b>4.59%</b>	<b>0.05%</b>	<b>0.00%</b>	<b>0.00%</b>	<b>0.00%</b>	<b>0.00%</b>	
	<b>SD</b>	<b>7.59%</b>	<b>9.51%</b>	<b>2.65%</b>	<b>0.04%</b>	<b>0.00%</b>	<b>0.00%</b>	<b>0.00%</b>	<b>0.00%</b>	
ABR003	16	98.27%	1.42%	0.31%	0.00%	0.00%	0.00%	0.00%	0.00%	100.00%
	<b>AVG</b>	<b>n/a</b>	<b>n/a</b>	<b>n/a</b>	<b>n/a</b>	<b>n/a</b>	<b>n/a</b>	<b>n/a</b>	<b>n/a</b>	
	<b>SD</b>	<b>n/a</b>	<b>n/a</b>	<b>n/a</b>	<b>n/a</b>	<b>n/a</b>	<b>n/a</b>	<b>n/a</b>	<b>n/a</b>	
ABR028	1	99.95%	0.00%	0.00%	0.05%	0.00%	0.00%	0.00%	0.00%	100.00%
	<b>AVG</b>	<b>n/a</b>	<b>n/a</b>	<b>n/a</b>	<b>n/a</b>	<b>n/a</b>	<b>n/a</b>	<b>n/a</b>	<b>n/a</b>	
	<b>SD</b>	<b>n/a</b>	<b>n/a</b>	<b>n/a</b>	<b>n/a</b>	<b>n/a</b>	<b>n/a</b>	<b>n/a</b>	<b>n/a</b>	
AVS901	5	85.28%	11.40%	3.32%	0.00%	0.00%	0.00%	0.00%	0.00%	100.00%
	6	88.70%	2.83%	8.38%	0.09%	0.00%	0.00%	0.00%	0.00%	100.00%
	7	90.84%	7.35%	1.74%	0.07%	0.00%	0.00%	0.00%	0.00%	100.00%
	8	85.00%	7.10%	7.85%	0.05%	0.00%	0.00%	0.00%	0.00%	100.00%
	9	90.13%	8.96%	0.87%	0.05%	0.00%	0.00%	0.00%	0.00%	100.00%
	10	87.76%	10.83%	1.36%	0.05%	0.00%	0.00%	0.00%	0.00%	100.00%
	12	71.70%	2.59%	25.70%	0.00%	0.00%	0.00%	0.00%	0.00%	100.00%
	13	75.05%	1.97%	22.94%	0.04%	0.00%	0.00%	0.00%	0.00%	100.00%
AVS901	53	80.54%	2.25%	17.14%	0.06%	0.00%	0.00%	0.00%	0.00%	100.00%
	54	82.78%	9.64%	7.53%	0.05%	0.00%	0.00%	0.00%	0.00%	100.00%

Label	Pt#	Cu	Sn	Pb	Fe	As	Sb	Cr	Ni	Total
AVS902	55	77.35%	4.40%	18.16%	0.10%	0.00%	0.00%	0.00%	0.00%	100.00%
	56	66.89%	3.47%	29.60%	0.04%	0.00%	0.00%	0.00%	0.00%	100.00%
	57	92.40%	7.10%	0.43%	0.07%	0.00%	0.00%	0.00%	0.00%	100.00%
	58	91.48%	8.08%	0.40%	0.04%	0.16%	0.00%	0.00%	0.00%	100.00%
	<b>AVG</b>	<b>83.28%</b>	<b>6.28%</b>	<b>10.39%</b>	<b>0.05%</b>	<b>0.01%</b>	<b>0.00%</b>	<b>0.00%</b>	<b>0.00%</b>	
	<b>SD</b>	<b>7.96%</b>	<b>3.32%</b>	<b>10.31%</b>	<b>0.03%</b>	<b>0.04%</b>	<b>0.00%</b>	<b>0.00%</b>	<b>0.00%</b>	
	22	99.78%	0.01%	0.20%	0.01%	0.00%	0.00%	0.00%	0.00%	100.00%
	23	99.72%	0.00%	0.28%	0.00%	0.00%	0.00%	0.00%	0.00%	100.00%
	25	99.69%	0.02%	0.20%	0.09%	0.00%	0.00%	0.00%	0.00%	100.00%
	26	99.71%	0.02%	0.28%	0.00%	0.02%	0.00%	0.00%	0.00%	100.00%
AVS903	27	99.72%	0.03%	0.23%	0.02%	0.05%	0.00%	0.00%	0.00%	100.00%
	<b>AVG</b>	<b>99.72%</b>	<b>0.02%</b>	<b>0.24%</b>	<b>0.02%</b>	<b>0.01%</b>	<b>0.00%</b>	<b>0.00%</b>	<b>0.00%</b>	
	<b>SD</b>	<b>0.03%</b>	<b>0.01%</b>	<b>0.04%</b>	<b>0.04%</b>	<b>0.02%</b>	<b>0.00%</b>	<b>0.00%</b>	<b>0.00%</b>	
	38	94.87%	4.51%	0.44%	0.18%	0.00%	0.00%	0.00%	0.00%	100.00%
	39	92.13%	6.76%	1.00%	0.11%	0.00%	0.00%	0.00%	0.00%	100.00%
	40	93.04%	5.72%	1.13%	0.10%	0.12%	0.00%	0.00%	0.00%	100.00%
	41	92.25%	6.60%	1.04%	0.12%	0.00%	0.00%	0.00%	0.00%	100.00%
	42	96.13%	2.59%	1.09%	0.19%	0.00%	0.00%	0.00%	0.00%	100.00%
	43	77.37%	3.55%	18.97%	0.11%	0.00%	0.00%	0.00%	0.00%	100.00%
	44	88.27%	5.69%	5.91%	0.14%	0.53%	0.77%	0.59%	0.00%	100.00%
AVS905	45	71.58%	5.76%	22.55%	0.11%	0.13%	0.00%	0.00%	0.00%	100.00%
	46	88.25%	8.13%	3.43%	0.19%	0.00%	0.00%	0.00%	0.00%	100.00%
	47	94.28%	4.55%	0.94%	0.24%	0.00%	0.00%	0.00%	0.00%	100.00%
	48	13.06%	0.77%	86.15%	0.02%	0.00%	0.00%	0.00%	0.00%	100.00%
	49	90.93%	6.05%	2.84%	0.17%	0.00%	0.00%	0.00%	0.00%	100.00%
	50	89.69%	4.82%	5.28%	0.21%	0.00%	0.00%	0.00%	0.00%	100.00%
	51	87.97%	11.44%	0.59%	0.00%	0.00%	0.00%	0.00%	0.00%	100.00%
	52	89.83%	6.73%	3.31%	0.14%	0.00%	0.00%	0.00%	0.00%	100.00%
	<b>AVG</b>	<b>83.98%</b>	<b>5.58%</b>	<b>10.31%</b>	<b>0.14%</b>	<b>0.05%</b>	<b>0.05%</b>	<b>0.04%</b>	<b>0.00%</b>	
	<b>SD</b>	<b>20.67%</b>	<b>2.45%</b>	<b>22.03%</b>	<b>0.07%</b>	<b>0.14%</b>	<b>0.20%</b>	<b>0.15%</b>	<b>0.00%</b>	
AVS905	14	93.11%	6.02%	0.72%	0.15%	0.00%	0.00%	0.00%	0.00%	100.00%
	18	93.08%	6.31%	0.46%	0.15%	0.05%	0.05%	0.04%	0.00%	100.00%
	29	92.36%	7.12%	0.39%	0.13%	0.00%	0.00%	0.00%	0.00%	100.00%
	30	93.39%	6.21%	0.16%	0.24%	0.10%	0.00%	0.00%	0.00%	100.00%
	31	94.05%	5.62%	0.19%	0.15%	0.00%	0.00%	0.00%	0.00%	100.00%
	32	94.13%	5.50%	0.17%	0.20%	0.00%	0.00%	0.00%	0.00%	100.00%
	33	94.21%	5.40%	0.19%	0.20%	0.00%	0.00%	0.00%	0.00%	100.00%
	34	92.90%	6.41%	0.49%	0.20%	0.00%	0.00%	0.00%	0.00%	100.00%
	35	92.15%	7.42%	0.30%	0.13%	0.00%	0.00%	0.00%	0.00%	100.00%
	37	93.78%	5.86%	0.14%	0.23%	0.00%	0.00%	0.00%	0.00%	100.00%
	<b>AVG</b>	<b>93.32%</b>	<b>6.19%</b>	<b>0.32%</b>	<b>0.18%</b>	<b>0.02%</b>	<b>0.01%</b>	<b>0.00%</b>	<b>0.00%</b>	
	<b>SD</b>	<b>0.73%</b>	<b>0.67%</b>	<b>0.19%</b>	<b>0.04%</b>	<b>0.03%</b>	<b>0.02%</b>	<b>0.01%</b>	<b>0.00%</b>	
MDL		0.15	0.10	0.32	0.11	0.09	0.11	0.15	0.16	

Histograms were created to display the variation within the alloy composition. Cu, Sn, Pb, and Fe were all plotted. The Cu histogram (Figure 31) demonstrates well that copper percentages averaged

between 80% and 100%, with some outliers that can be explained by the boundaries between the Cu-Sn alloy phase and the immiscible Pb phase. The Sn histogram showed the same kind of skewed distribution for Sn, only in reverse proportions (Figure 32), as would be expected given that Cu and Sn should appear in a high to low percentage distribution. Again, the outliers can be explained by the same phenomenon as the Cu outliers. The Pb histogram appears to be slightly skewed with the outliers being representative of the pure phase (Figure 33). However, because these numbers were not generated by bulk analysis of the bronze alloy, they can not be used to determine the proportions of Cu, Sn, and Pb in the solid alloy accurately; an approximation will be proposed in the Discussion section, however. Iron was a minor part of the alloy but above detection limits (0.12%) varying between 0.13% and just below 0.70%.

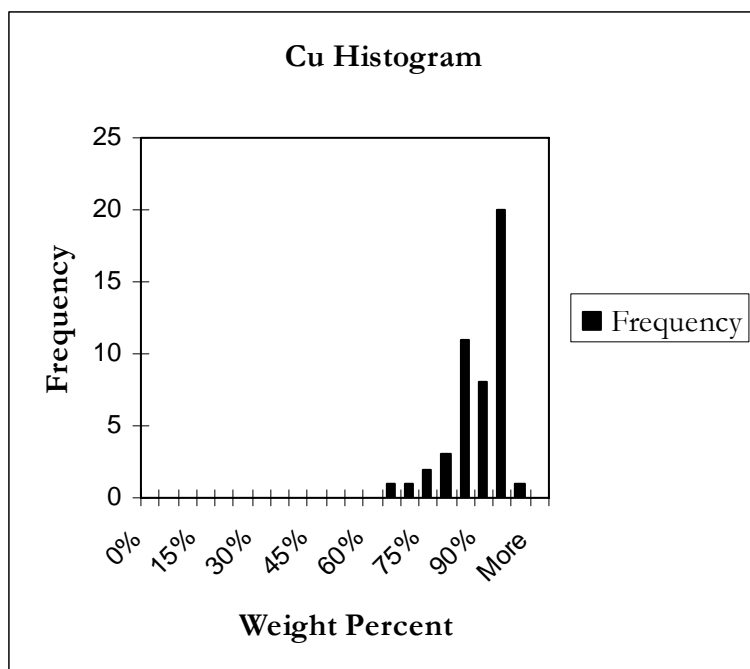


Figure 31: Cu Distribution, all metal samples

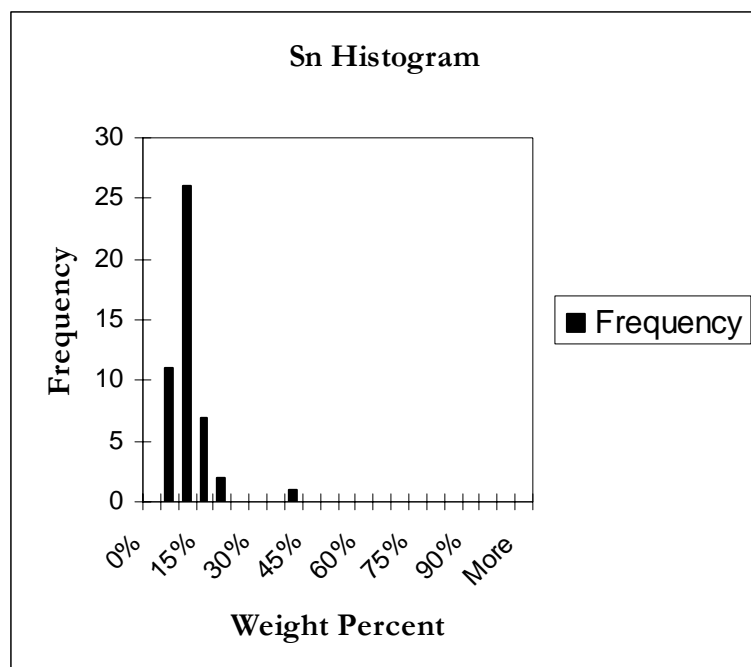


Figure 32: Sn distribution, all metal areas

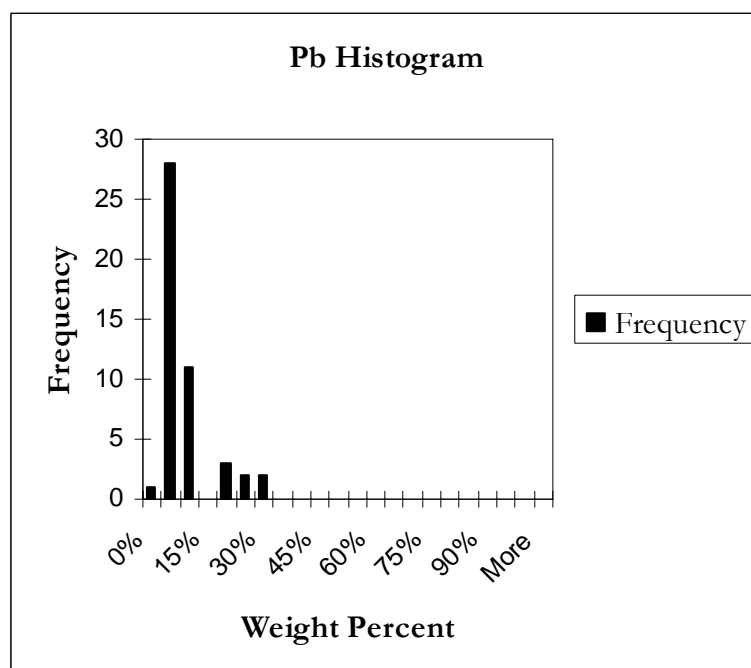


Figure 33: Pb in the metal portions of the samples

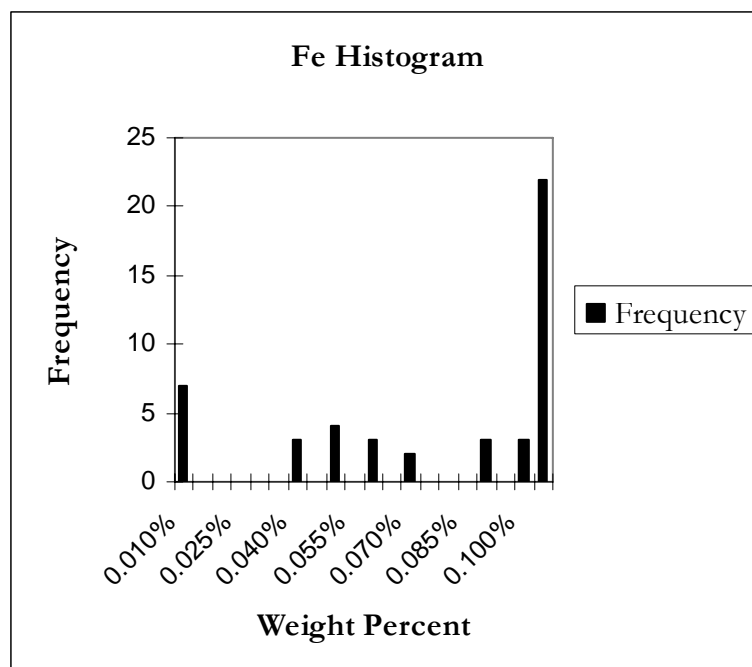


Figure 34: Fe distribution, all metals

WDS analyses of the slag groundmass were assessed for data points that were representative of mineral phases; these were removed. Then, all data for oxides that were below minimum detection limits (MDL) were removed. Finally, the data were normalized (Table 8).

Table 8: WDS data for slag groundmass, normalized

Label	Pt#	SiO <sub>2</sub>	Al <sub>2</sub> O <sub>3</sub>	Fe <sub>2</sub> O <sub>3</sub>	CaO	K <sub>2</sub> O	PbO	SnO <sub>2</sub>	CuO	Total
ABR001	25	36.96%	10.10%	4.47%	3.88%	3.24%	17.13%	24.22%	0.01%	100.00%
	27	41.02%	8.70%	7.30%	13.97%	2.02%	20.73%	6.10%	0.16%	100.00%
	28	40.45%	9.11%	5.98%	7.53%	2.44%	27.09%	7.30%	0.09%	100.00%
	Avg.	39.48%	9.30%	5.92%	8.46%	2.57%	21.65%	12.54%	0.08%	
	S.D.	2.20%	0.72%	1.42%	5.11%	0.62%	5.05%	10.14%	0.08%	
ABR002	13	43.74%	7.74%	10.44%	10.74%	1.96%	22.23%	2.94%	0.23%	100.00%
	25	36.96%	10.10%	4.47%	3.88%	3.24%	17.13%	24.22%	0.01%	100.00%
	27	41.02%	8.70%	7.30%	13.97%	2.02%	20.73%	6.10%	0.16%	100.00%
	28	40.45%	9.11%	5.98%	7.53%	2.44%	27.09%	7.30%	0.09%	100.00%
	1	52.13%	10.70%	5.14%	9.79%	4.17%	11.80%	4.92%	1.35%	100.00%
	2	46.18%	9.34%	7.16%	10.53%	2.98%	18.32%	5.00%	0.48%	100.00%
	3	42.19%	8.98%	7.24%	9.71%	3.18%	22.46%	5.95%	0.29%	100.00%

Label	Pt#	SiO <sub>2</sub>	Al <sub>2</sub> O <sub>3</sub>	Fe <sub>2</sub> O <sub>3</sub>	CaO	K <sub>2</sub> O	PbO	SnO <sub>2</sub>	CuO	Total
ABR002	4	47.43%	9.49%	7.13%	9.83%	3.57%	17.51%	4.58%	0.45%	100.00%
	5	48.70%	9.03%	5.77%	9.59%	3.50%	17.30%	5.81%	0.30%	100.00%
	Avg.	44.31%	9.24%	6.74%	9.51%	3.00%	19.40%	7.42%	0.37%	
	S.D.	4.72%	0.84%	1.72%	2.70%	0.74%	4.34%	6.41%	0.40%	
ABR003	1	69.43%	20.08%	0.00%	0.81%	8.43%	0.11%	0.00%	1.14%	100.00%
	2	57.10%	12.73%	5.25%	6.97%	5.21%	4.17%	1.51%	7.04%	100.00%
	3	56.25%	7.75%	6.55%	12.14%	3.24%	4.38%	3.59%	6.10%	100.00%
	1	63.47%	17.68%	0.00%	11.22%	5.93%	0.14%	0.00%	1.56%	100.00%
	5	55.14%	7.56%	13.76%	19.94%	2.94%	0.19%	0.45%	0.01%	100.00%
	6	68.22%	19.31%	0.08%	0.32%	10.12%	0.13%	0.00%	1.82%	100.00%
	7	58.45%	10.62%	6.32%	11.84%	3.86%	3.78%	2.23%	2.89%	100.00%
	8	68.70%	20.28%	1.18%	1.49%	7.37%	0.28%	0.00%	0.71%	100.00%
	9	63.59%	7.88%	4.44%	4.78%	2.57%	11.52%	5.06%	0.15%	100.00%
	10	65.63%	9.83%	2.67%	2.48%	3.19%	11.35%	4.40%	0.46%	100.00%
	11	62.30%	5.80%	6.17%	6.36%	2.00%	11.80%	4.94%	0.64%	100.00%
	8	82.93%	3.40%	3.19%	3.22%	1.57%	3.08%	0.67%	1.93%	100.00%
	11	54.50%	7.36%	13.31%	17.55%	3.54%	1.73%	1.23%	0.78%	100.00%
	17	57.95%	7.79%	12.55%	15.83%	2.55%	2.49%	0.85%	0.00%	100.00%
	Avg.	63.12%	11.29%	5.39%	8.21%	4.47%	3.94%	1.78%	1.80%	
	S.D.	7.68%	5.72%	4.84%	6.55%	2.59%	4.41%	1.92%	2.19%	
ABR004	56	51.34%	9.98%	11.22%	12.38%	2.68%	9.15%	3.17%	0.09%	100.00%
	57	51.07%	10.35%	8.32%	11.60%	2.66%	11.86%	3.80%	0.35%	100.00%
	58	47.01%	8.97%	13.76%	10.62%	2.30%	13.28%	4.07%	0.00%	100.00%
	59	46.84%	8.91%	15.77%	11.24%	2.37%	11.62%	3.01%	0.24%	100.00%
	60	48.42%	9.03%	13.27%	10.40%	2.56%	12.44%	3.69%	0.18%	100.00%
	61	45.33%	8.32%	15.10%	10.01%	2.26%	14.29%	4.52%	0.16%	100.00%
	62	46.61%	8.85%	14.40%	10.71%	2.31%	12.04%	4.68%	0.40%	100.00%
	63	48.00%	9.00%	15.36%	11.56%	2.48%	10.60%	2.94%	0.05%	100.00%
	Avg.	48.08%	9.18%	13.40%	11.06%	2.45%	11.91%	3.74%	0.18%	
	S.D.	2.14%	0.66%	2.51%	0.77%	0.16%	1.57%	0.67%	0.14%	
ABR005	42	53.89%	9.84%	10.10%	17.94%	2.19%	3.81%	2.00%	0.23%	100.00%
	44	57.09%	11.03%	9.20%	15.61%	2.46%	2.77%	1.53%	0.31%	100.00%
	45	53.72%	8.76%	8.31%	20.69%	2.74%	3.12%	2.42%	0.24%	100.00%
	46	45.94%	8.40%	14.97%	20.69%	1.67%	6.18%	2.01%	0.14%	100.00%
	47	54.26%	9.96%	9.20%	19.74%	2.77%	2.36%	1.67%	0.04%	100.00%
	48	61.00%	10.49%	6.58%	11.60%	3.79%	3.93%	2.61%	0.00%	100.00%
	49	51.94%	9.40%	15.03%	11.37%	2.76%	7.46%	1.95%	0.08%	100.00%
	50	64.74%	12.59%	4.70%	8.36%	3.34%	4.43%	1.52%	0.30%	100.00%
	51	65.45%	12.36%	4.78%	8.18%	3.29%	4.02%	1.71%	0.21%	100.00%

Label	Pt#	SiO <sub>2</sub>	Al <sub>2</sub> O <sub>3</sub>	Fe <sub>2</sub> O <sub>3</sub>	CaO	K <sub>2</sub> O	PbO	SnO <sub>2</sub>	CuO	Total
ABR005	52	67.11%	9.17%	5.38%	9.61%	3.36%	3.42%	1.68%	0.27%	100.00%
	54	54.36%	12.25%	8.30%	15.21%	2.72%	4.63%	2.06%	0.48%	100.00%
	55	57.08%	11.40%	7.71%	14.36%	2.74%	4.70%	1.77%	0.25%	100.00%
	Avg.	57.22%	10.47%	8.69%	14.45%	2.82%	4.24%	1.91%	0.21%	
	S.D.	6.27%	1.45%	3.44%	4.64%	0.57%	1.43%	0.34%	0.13%	
ABR006	30	55.25%	9.06%	13.35%	11.30%	2.44%	5.95%	1.97%	0.67%	100.00%
	31	68.89%	8.76%	6.00%	4.96%	4.02%	4.05%	2.98%	0.34%	100.00%
	32	65.05%	21.38%	1.34%	4.07%	7.69%	0.20%	0.01%	0.24%	100.00%
	33	66.90%	15.17%	2.88%	10.61%	4.42%	0.01%	0.00%	0.00%	100.00%
	34	63.60%	10.84%	6.11%	6.47%	4.01%	6.84%	1.82%	0.30%	100.00%
	35	64.37%	14.28%	4.57%	5.21%	5.01%	4.78%	1.03%	0.75%	100.00%
	36	57.87%	9.46%	14.98%	11.59%	2.48%	2.46%	0.95%	0.20%	100.00%
	37	59.69%	10.69%	10.77%	12.02%	2.94%	2.52%	1.19%	0.18%	100.00%
	Avg.	62.71%	12.46%	7.50%	8.28%	4.13%	3.35%	1.24%	0.34%	
	S.D.	4.67%	4.31%	4.97%	3.40%	1.71%	2.51%	1.00%	0.25%	
ABR007	14	52.33%	10.12%	12.61%	18.39%	2.07%	2.92%	1.34%	0.23%	100.00%
	15	51.45%	10.23%	10.82%	10.13%	2.83%	7.83%	4.43%	2.27%	100.00%
	Avg.	51.89%	10.17%	11.72%	14.26%	2.45%	5.37%	2.89%	1.25%	
	S.D.	0.62%	0.08%	1.26%	5.84%	0.54%	3.47%	2.18%	1.44%	
ABR008	22	53.88%	11.53%	9.23%	13.59%	3.06%	2.20%	5.69%	0.83%	100.00%
	23	56.44%	11.78%	7.65%	12.48%	3.37%	2.18%	5.52%	0.59%	100.00%
	24	58.79%	13.96%	5.10%	10.88%	3.85%	2.46%	4.81%	0.15%	100.00%
	26	78.09%	17.76%	0.58%	0.94%	2.51%	0.00%	0.00%	0.12%	100.00%
	27	74.22%	21.40%	0.60%	1.28%	2.49%	0.00%	0.01%	0.00%	100.00%
	1	50.60%	11.34%	6.33%	15.47%	3.52%	9.40%	1.84%	1.50%	100.00%
	2	58.61%	14.77%	8.21%	9.47%	1.90%	2.61%	4.36%	0.08%	100.00%
	3	59.26%	14.91%	6.07%	9.27%	2.93%	2.49%	4.06%	1.01%	100.00%
	5	48.99%	9.88%	7.92%	19.14%	3.95%	7.14%	2.84%	0.14%	100.00%
	6	47.08%	8.62%	7.54%	14.55%	2.27%	12.31%	7.35%	0.29%	100.00%
	7	31.34%	7.04%	3.41%	5.59%	1.84%	6.90%	3.96%	39.91%	100.00%
	9	46.87%	10.13%	7.55%	11.19%	2.80%	14.53%	6.32%	0.60%	100.00%
	Avg.	55.35%	12.76%	5.85%	10.32%	2.87%	5.19%	3.90%	3.77%	
	S.D.	12.41%	4.04%	2.90%	5.50%	0.71%	4.82%	2.34%	11.39%	
ABR009	21	37.48%	6.65%	26.68%	23.46%	0.04%	2.12%	3.42%	0.15%	100.00%
	22	63.92%	18.46%	4.98%	7.45%	4.99%	0.06%	0.03%	0.10%	100.00%
	23	64.11%	18.81%	4.75%	7.59%	4.59%	0.00%	0.09%	0.06%	100.00%
	25	64.09%	17.21%	5.23%	7.41%	5.63%	0.12%	0.15%	0.16%	100.00%
	Avg.	57.40%	15.28%	10.41%	11.48%	3.81%	0.57%	0.92%	0.12%	
	S.D.	13.28%	5.80%	10.85%	7.99%	2.55%	1.03%	1.67%	0.05%	

Label	Pt#	SiO <sub>2</sub>	Al <sub>2</sub> O <sub>3</sub>	Fe <sub>2</sub> O <sub>3</sub>	CaO	K <sub>2</sub> O	PbO	SnO <sub>2</sub>	CuO	Total
ABR010	29	50.90%	10.49%	6.63%	8.47%	2.89%	12.15%	5.86%	2.60%	100.00%
	30	50.11%	10.04%	6.42%	9.42%	2.36%	14.49%	6.79%	0.36%	100.00%
	31	50.88%	10.36%	6.21%	9.16%	2.89%	13.80%	6.31%	0.39%	100.00%
	32	52.20%	10.66%	6.07%	8.79%	2.82%	13.14%	6.12%	0.21%	100.00%
	33	66.72%	18.64%	0.59%	3.54%	5.07%	3.22%	1.47%	0.74%	100.00%
	34	55.84%	11.37%	5.26%	9.53%	3.42%	8.87%	5.29%	0.41%	100.00%
	35	55.42%	13.03%	4.94%	4.09%	3.11%	15.44%	3.42%	0.54%	100.00%
	33	64.58%	18.61%	6.46%	6.33%	3.57%	0.27%	0.00%	0.17%	100.00%
	16	65.46%	17.39%	5.82%	5.48%	5.69%	0.04%	0.01%	0.13%	100.00%
	17	68.26%	16.70%	5.48%	5.35%	4.01%	0.05%	0.11%	0.04%	100.00%
	Avg.	58.04%	13.73%	5.39%	7.02%	3.58%	8.15%	3.54%	0.56%	
	S.D.	7.37%	3.67%	1.77%	2.32%	1.06%	6.54%	2.87%	0.75%	
ABR011	19	47.97%	8.61%	7.56%	33.10%	2.12%	0.27%	0.37%	0.00%	100.00%
	Avg.	n/a	n/a	n/a	n/a	n/a	n/a	n/a	n/a	
	S.D.	n/a	n/a	n/a	n/a	n/a	n/a	n/a	n/a	
ABR012	14	54.16%	11.00%	7.42%	13.03%	3.84%	7.69%	2.71%	0.15%	100.00%
	15	50.06%	9.15%	9.92%	10.94%	2.63%	11.72%	5.30%	0.28%	100.00%
	16	47.54%	8.46%	7.76%	7.55%	2.76%	19.24%	6.13%	0.55%	100.00%
	17	46.77%	8.52%	5.67%	7.66%	2.86%	18.99%	2.16%	7.37%	100.00%
ABR012	18	60.94%	11.82%	5.42%	10.40%	4.02%	4.78%	2.40%	0.22%	100.00%
	56	48.18%	9.76%	9.35%	11.37%	2.61%	13.92%	3.96%	0.85%	100.00%
	58	52.75%	10.62%	8.86%	13.89%	3.10%	7.54%	2.93%	0.31%	100.00%
	60	63.47%	9.99%	5.38%	10.87%	3.53%	3.95%	2.48%	0.33%	100.00%
	61	48.82%	9.21%	3.94%	8.10%	3.02%	20.15%	1.37%	5.39%	100.00%
	62	52.68%	11.05%	8.27%	13.81%	3.62%	7.34%	3.07%	0.15%	100.00%
	63	51.74%	11.32%	7.80%	13.90%	3.41%	7.94%	3.40%	0.49%	100.00%
	64	51.49%	10.66%	7.45%	12.70%	3.33%	7.75%	2.92%	3.70%	100.00%
	65	62.48%	11.20%	5.02%	10.24%	4.49%	4.44%	1.87%	0.26%	100.00%
	66	44.19%	9.99%	7.23%	10.71%	2.52%	20.74%	3.68%	0.92%	100.00%
	67	61.42%	13.37%	5.18%	8.13%	4.27%	5.09%	2.05%	0.49%	100.00%
	69	46.06%	10.14%	12.80%	12.48%	2.61%	12.47%	3.26%	0.18%	100.00%
	70	46.58%	9.82%	12.50%	13.05%	2.69%	12.00%	3.06%	0.29%	100.00%
	71	46.02%	10.16%	13.84%	13.64%	2.88%	10.80%	2.47%	0.17%	100.00%
	72	45.62%	8.67%	8.90%	9.00%	2.22%	19.96%	5.19%	0.44%	100.00%
	Avg.	51.63%	10.26%	8.04%	11.13%	3.18%	11.40%	3.18%	1.19%	
	S.D.	6.20%	1.23%	2.77%	2.23%	0.64%	5.88%	1.24%	2.02%	
ABR013	16	45.19%	7.68%	5.90%	6.44%	2.13%	24.84%	5.31%	2.49%	100.00%
	17	49.25%	10.67%	12.28%	12.98%	3.11%	8.87%	2.52%	0.33%	100.00%
	18	53.69%	10.17%	9.79%	13.66%	3.38%	6.75%	2.19%	0.37%	100.00%



Label	Pt#	SiO <sub>2</sub>	Al <sub>2</sub> O <sub>3</sub>	Fe <sub>2</sub> O <sub>3</sub>	CaO	K <sub>2</sub> O	PbO	SnO <sub>2</sub>	CuO	Total
ABR013	19	44.51%	9.52%	10.79%	10.31%	2.47%	17.59%	4.58%	0.23%	100.00%
	20	43.05%	9.41%	5.75%	7.50%	1.37%	30.42%	1.93%	0.58%	100.00%
	Avg.	47.14%	9.49%	8.90%	10.18%	2.49%	17.69%	3.31%	0.80%	
	S.D.	4.32%	1.13%	2.95%	3.21%	0.80%	10.13%	1.53%	0.95%	
ABR014	50	67.21%	20.08%	4.63%	3.72%	4.21%	0.02%	0.05%	0.09%	100.00%
	52	63.82%	20.14%	6.25%	5.56%	3.92%	0.02%	0.01%	0.28%	100.00%
	53	66.49%	15.32%	5.23%	8.26%	4.28%	0.03%	0.17%	0.22%	100.00%
	54	70.43%	17.02%	4.54%	3.45%	4.37%	0.13%	0.00%	0.05%	100.00%
	55	66.98%	19.09%	5.68%	4.22%	3.69%	0.15%	0.00%	0.19%	100.00%
	1	61.11%	15.75%	6.92%	13.50%	2.42%	0.06%	0.10%	0.14%	100.00%
	2	67.05%	18.86%	4.82%	5.30%	3.63%	0.14%	0.00%	0.20%	100.00%
	3	60.23%	14.48%	6.13%	14.52%	2.94%	0.38%	0.19%	1.13%	100.00%
	4	69.33%	17.59%	5.00%	3.85%	4.02%	0.02%	0.00%	0.20%	100.00%
	5	66.09%	16.25%	5.07%	8.01%	4.20%	0.08%	0.15%	0.15%	100.00%
	Avg.	65.87%	17.46%	5.43%	7.04%	3.77%	0.10%	0.07%	0.27%	
	S.D.	3.27%	2.02%	0.79%	4.05%	0.63%	0.11%	0.08%	0.31%	
ABR016	6	46.12%	11.75%	7.88%	2.56%	2.11%	9.82%	2.47%	17.29%	100.00%
	7	56.03%	18.96%	10.16%	2.37%	3.01%	4.44%	1.20%	3.84%	100.00%
	8	58.08%	18.75%	8.82%	2.35%	2.86%	4.00%	0.92%	4.20%	100.00%
	9	55.62%	10.67%	4.79%	1.80%	2.42%	15.39%	7.20%	2.10%	100.00%
	14	53.54%	10.70%	4.59%	1.92%	2.37%	18.72%	7.20%	0.95%	100.00%
	16	38.91%	23.74%	12.69%	24.61%	0.00%	0.00%	0.00%	0.06%	100.00%
	Avg.	51.38%	15.76%	8.16%	5.94%	2.13%	8.73%	3.17%	4.74%	
	S.D.	7.38%	5.49%	3.13%	9.15%	1.09%	7.25%	3.22%	6.35%	
ABR017	12	45.67%	8.76%	20.70%	15.13%	2.80%	4.04%	2.86%	0.03%	100.00%
	13	41.15%	8.10%	21.53%	13.90%	2.61%	7.66%	4.76%	0.27%	100.00%
	14	66.22%	18.46%	5.31%	6.18%	3.78%	0.03%	0.00%	0.00%	100.00%
	15	65.02%	17.27%	3.39%	8.20%	5.30%	0.32%	0.07%	0.43%	100.00%
	Avg.	54.52%	13.15%	12.74%	10.85%	3.62%	3.01%	1.93%	0.18%	
	S.D.	12.96%	5.48%	9.72%	4.34%	1.23%	3.60%	2.31%	0.20%	
ABR018	25	65.71%	22.05%	6.05%	1.77%	4.31%	0.08%	0.02%	0.02%	100.00%
	26	54.88%	17.45%	5.32%	20.12%	2.03%	0.06%	0.00%	0.13%	100.00%
	27	61.80%	24.77%	6.86%	2.33%	4.09%	0.00%	0.02%	0.13%	100.00%
	28	65.14%	21.01%	5.93%	3.16%	4.63%	0.13%	0.00%	0.00%	100.00%
	29	58.21%	29.43%	1.85%	8.20%	2.17%	0.06%	0.00%	0.07%	100.00%
	Avg.	61.15%	22.94%	5.20%	7.12%	3.44%	0.07%	0.01%	0.07%	
	S.D.	4.61%	4.48%	1.95%	7.70%	1.24%	0.05%	0.01%	0.06%	
ABR019	36	61.43%	21.05%	7.16%	6.29%	3.00%	0.18%	0.00%	0.89%	100.00%
	37	63.09%	15.54%	4.85%	13.42%	2.00%	0.21%	0.00%	0.90%	100.00%



Label	Pt#	SiO <sub>2</sub>	Al <sub>2</sub> O <sub>3</sub>	Fe <sub>2</sub> O <sub>3</sub>	CaO	K <sub>2</sub> O	PbO	SnO <sub>2</sub>	CuO	Total
ABR023	Avg.	53.76%	12.21%	12.40%	10.76%	4.09%	4.41%	1.99%	0.39%	
	S.D.	5.05%	3.01%	4.07%	1.61%	3.07%	1.33%	1.00%	0.51%	
ABR024	31	59.65%	14.83%	10.59%	10.73%	3.66%	0.46%	0.06%	0.01%	100.00%
	32	54.32%	13.64%	19.64%	8.90%	2.91%	0.51%	0.06%	0.02%	100.00%
	43	56.59%	24.74%	3.86%	13.72%	0.80%	0.15%	0.06%	0.08%	100.00%
	44	64.52%	20.88%	6.60%	3.82%	3.79%	0.14%	0.00%	0.25%	100.00%
	45	68.13%	19.38%	5.95%	3.01%	3.41%	0.08%	0.00%	0.04%	100.00%
	46	74.16%	15.84%	3.75%	2.17%	3.69%	0.10%	0.07%	0.22%	100.00%
	47	68.93%	19.68%	4.24%	3.03%	3.92%	0.13%	0.02%	0.06%	100.00%
	48	58.25%	15.93%	10.24%	11.29%	3.74%	0.23%	0.21%	0.11%	100.00%
	Avg.	63.07%	18.12%	8.11%	7.08%	3.24%	0.22%	0.06%	0.10%	
	S.D.	6.95%	3.71%	5.38%	4.57%	1.03%	0.17%	0.07%	0.09%	
ABR025	1	52.97%	10.38%	15.24%	15.46%	2.53%	1.82%	1.46%	0.14%	100.00%
	2	64.16%	12.67%	5.45%	12.37%	2.92%	0.41%	1.91%	0.12%	100.00%
	3	61.00%	12.69%	6.82%	13.70%	2.96%	0.79%	1.57%	0.47%	100.00%
	4	45.79%	7.98%	9.21%	19.54%	1.92%	11.66%	2.60%	1.31%	100.00%
	5	66.88%	14.85%	3.75%	10.64%	3.69%	0.13%	0.06%	0.00%	100.00%
	Avg.	58.16%	11.71%	8.10%	14.34%	2.80%	2.96%	1.52%	0.41%	
	S.D.	8.66%	2.62%	4.47%	3.40%	0.65%	4.90%	0.93%	0.54%	
ABR028	24	65.38%	11.33%	8.73%	8.93%	5.54%	0.07%	0.01%	0.00%	100.00%
	25	64.62%	17.02%	5.64%	9.32%	3.28%	0.10%	0.03%	0.00%	100.00%
	26	62.57%	18.59%	4.74%	11.11%	2.91%	0.08%	0.01%	0.00%	100.00%
	27	51.76%	29.63%	1.42%	16.14%	1.01%	0.05%	0.00%	0.00%	100.00%
	28	65.14%	15.96%	5.86%	8.52%	4.38%	0.12%	0.02%	0.00%	100.00%
	Avg.	61.89%	18.50%	5.28%	10.80%	3.42%	0.08%	0.02%	0.00%	
	S.D.	5.77%	6.78%	2.63%	3.14%	1.70%	0.03%	0.01%	0.00%	
ABR029	20	68.17%	19.07%	0.08%	0.04%	12.55%	0.04%	0.00%	0.05%	100.00%
	21	74.64%	22.18%	0.04%	1.84%	1.31%	0.00%	0.00%	0.00%	100.00%
	22	64.91%	18.41%	0.22%	0.03%	16.36%	0.04%	0.02%	0.00%	100.00%
	23	70.61%	22.36%	0.32%	2.61%	4.03%	0.00%	0.07%	0.00%	100.00%
	2	69.96%	20.99%	1.71%	3.75%	3.54%	0.00%	0.00%	0.05%	100.00%
	3	67.13%	18.90%	7.15%	2.40%	4.27%	0.02%	0.00%	0.14%	100.00%
	4	69.67%	19.92%	3.83%	1.67%	4.86%	0.06%	0.00%	0.00%	100.00%
	5	36.10%	45.62%	15.40%	0.96%	1.49%	0.17%	0.00%	0.25%	100.00%
	6	67.90%	14.54%	6.29%	7.04%	4.11%	0.07%	0.05%	0.00%	100.00%
	7	61.72%	17.55%	8.69%	8.38%	3.45%	0.00%	0.01%	0.20%	100.00%
	Avg.	65.08%	21.95%	4.37%	2.87%	5.60%	0.04%	0.02%	0.07%	
	S.D.	10.75%	8.63%	5.06%	2.81%	4.89%	0.05%	0.03%	0.09%	
AVS 905	37	54.18%	20.18%	17.34%	4.26%	3.42%	0.58%	0.04%	0.00%	100.00%

Label	Pt#	SiO <sub>2</sub>	Al <sub>2</sub> O <sub>3</sub>	Fe <sub>2</sub> O <sub>3</sub>	CaO	K <sub>2</sub> O	PbO	SnO <sub>2</sub>	CuO	Total
<b>AVS905</b>	38	66.34%	19.69%	0.19%	0.62%	13.16%	0.00%	0.00%	0.00%	100.00%
	39	57.76%	23.48%	7.71%	8.47%	2.07%	0.51%	0.00%	0.00%	100.00%
	40	83.64%	15.00%	0.40%	0.33%	0.28%	0.14%	0.02%	0.20%	100.00%
	<b>Avg.</b>	<b>65.48%</b>	<b>19.59%</b>	<b>6.41%</b>	<b>3.42%</b>	<b>4.73%</b>	<b>0.31%</b>	<b>0.01%</b>	<b>0.05%</b>	
	<b>S.D.</b>	<b>13.14%</b>	<b>3.49%</b>	<b>8.08%</b>	<b>3.81%</b>	<b>5.76%</b>	<b>0.28%</b>	<b>0.02%</b>	<b>0.10%</b>	
<b>MDL</b>		<b>0.051</b>	<b>0.05</b>	<b>0.173</b>	<b>0.066</b>	<b>0.036</b>	<b>0.243</b>	<b>0.156</b>	<b>0.202</b>	

The slag analyses were assessed for evidence of distinct chemical groupings in order to ascertain if they were created by one or more technologies. First, ternary plots were created to look for trends within the groundmass. Two systems were used: SiO<sub>2</sub>-FeO-CaO (Figure 35) and SiO<sub>2</sub>-Al<sub>2</sub>O<sub>3</sub>-FeO (Figure 36). SiO<sub>2</sub> was used in all the plots because it is largest component by weight percentage. CaO was used because this study assumes that it was an intentional addition to the melt in the form of a lime flux. Al<sub>2</sub>O<sub>3</sub> was used because it is commonly found with the SiO<sub>2</sub> within the slag groundmass. FeO was used because the working hypothesis is that an iron crucible was used. Both plots show only that there are no clear, multiple groups within the groundmass.

Aventicum Slag Groundmass  
 $\text{SiO}_2\text{-FeO-CaO}$

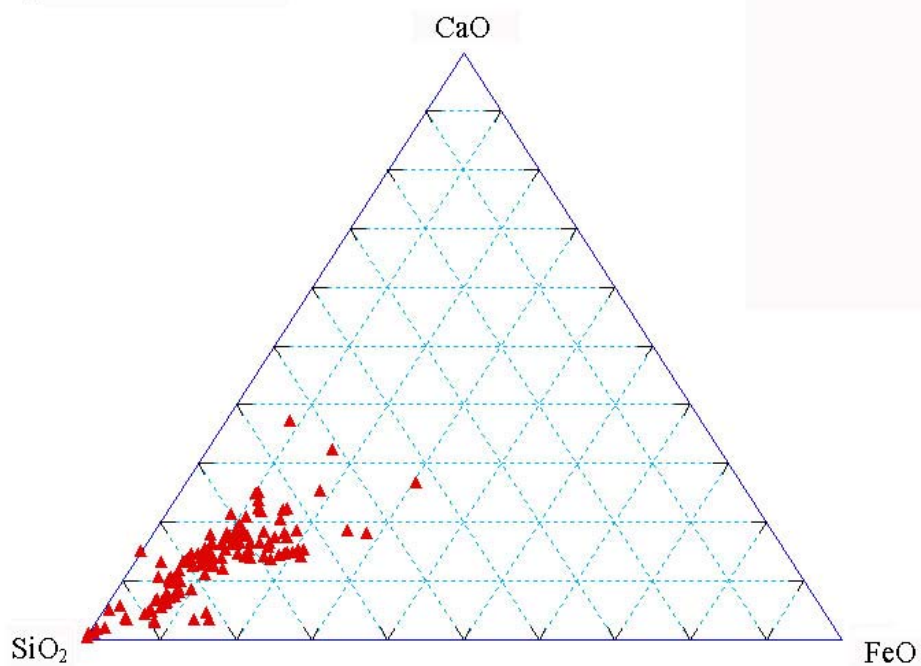


Figure 35:  $\text{SiO}_2\text{-FeO-CaO}$  ternary system

Aventicum Slag Groundmass  
 $\text{SiO}_2\text{-FeO-Al}_2\text{O}_3$

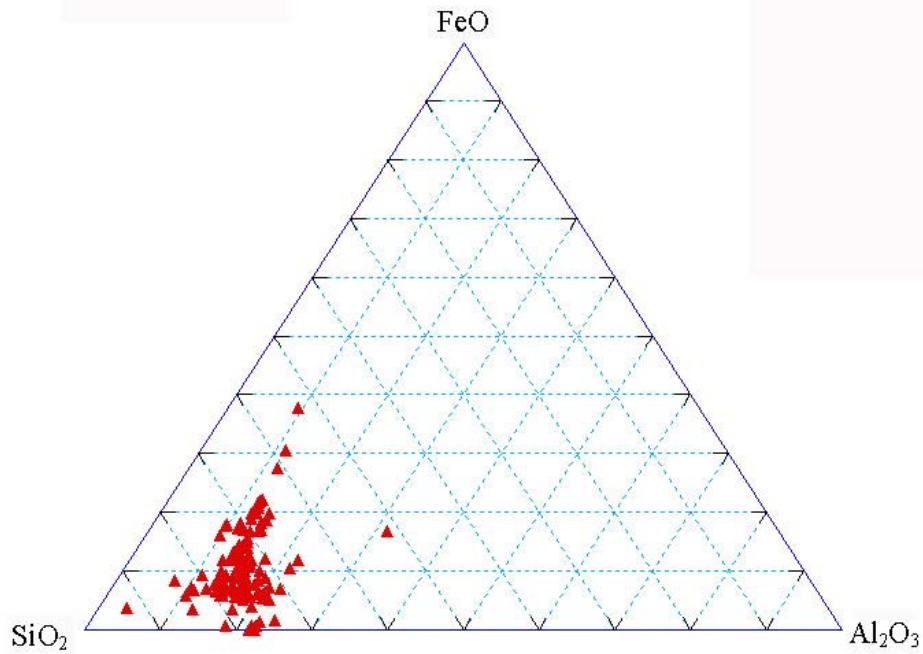


Figure 36:  $\text{SiO}_2\text{-FeO-Al}_2\text{O}_3$  ternary system

Binary x-y scatter plots were then created using FeO, CaO, and  $\text{SiO}_2$  in order to look for groups within the groundmass. When FeO and  $\text{SiO}_2$  were plotted against one another, the data points cluster together with no true outliers (Figure 37). When FeO and CaO are plotted against one another, the same pattern is evident (Figure 38). This is again the case when  $\text{SiO}_2$  was plotted against CaO (Figure 39). The tightest cluster of data points was observed in the Feo-CaO diagram.

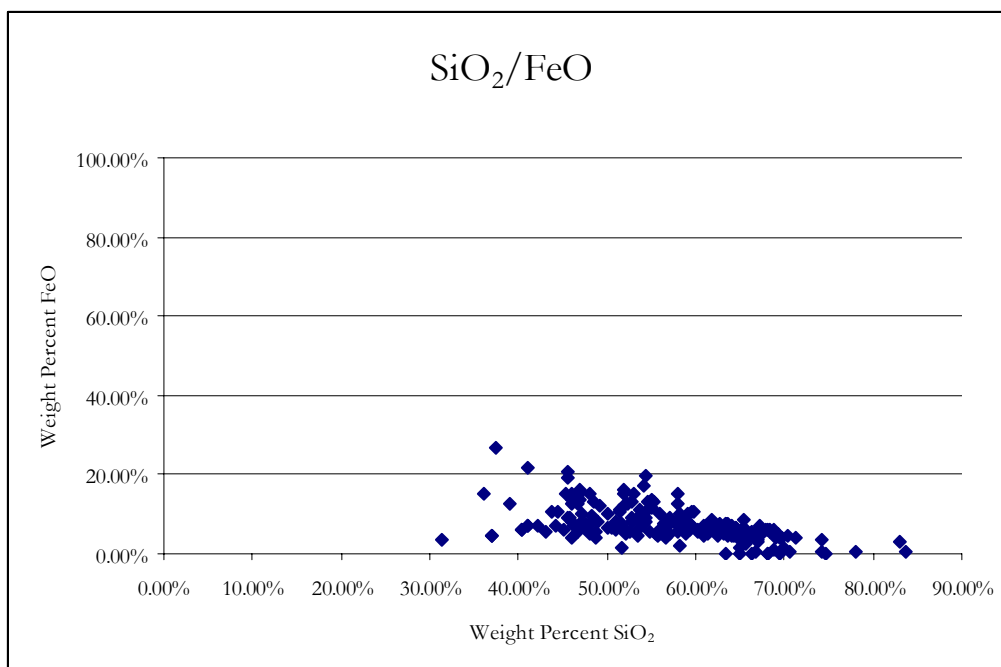


Figure 37: SiO<sub>2</sub>-FeO weight percentages  $R^2 = 0.337956$

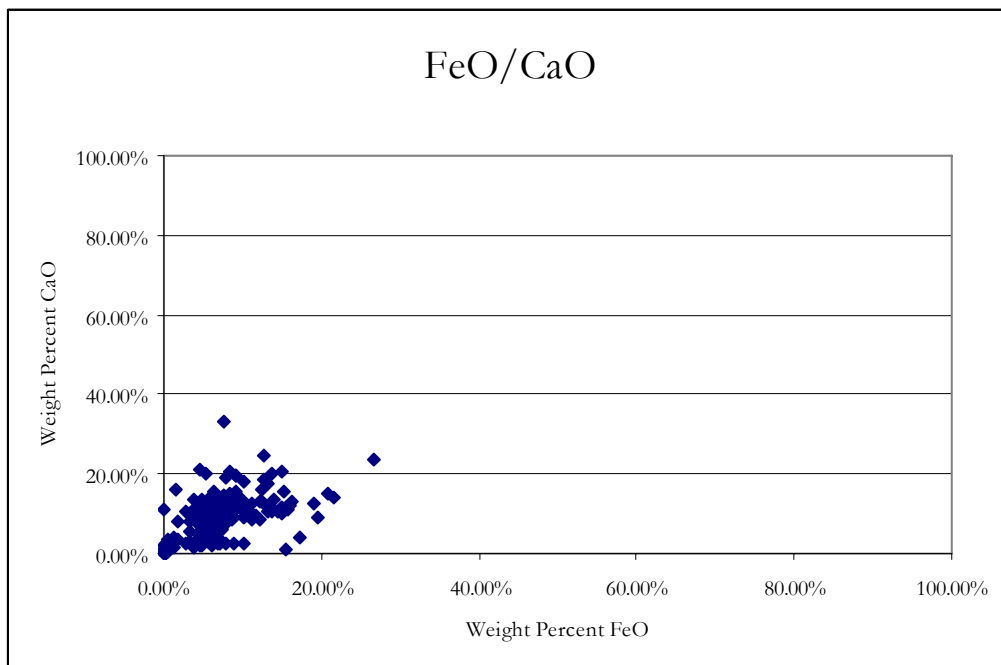


Figure 38: FeO-CaO weight percentages  $R^2 = 0.249305$

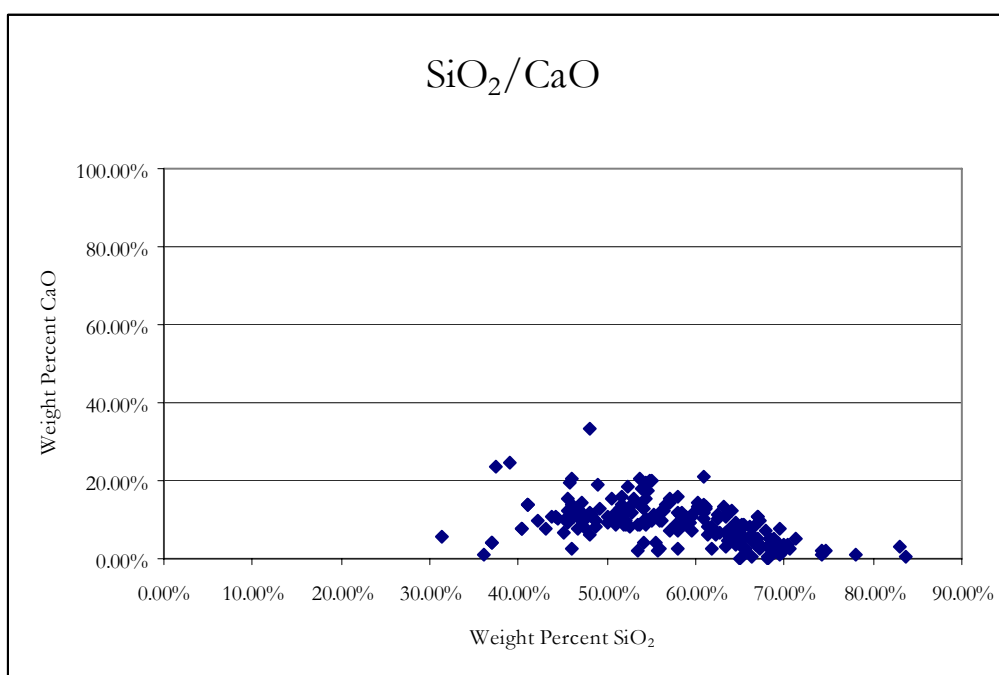


Figure 39: SiO<sub>2</sub>-CaO weight percentages  $R^2 = 0.211299$

Because the ternary and binary plots showed only one chemical groups, correlation tests were performed to determine if there are groups within the slag that are not obvious using the above plotting methods. Specifically correlation analysis and cluster analysis were used. 199 points were used from all slag samples; again, any points that were clearly mineral phases such as quartz or fayalite were discarded and only points representing analyses of the glassy materials were used. The results showed two subgroups within the slag: alumino-silicate rich material low in metal oxides, and material with higher amounts of metal oxides. This is seen in the way that SiO<sub>2</sub> has a negative correlation to FeO, PbO, and SnO<sub>2</sub>. In other words, the trend is one where the heavier oxides such as SnO<sub>2</sub> and PbO tend to increase together at the expense of the SiO<sub>2</sub> (Table 9). For example, the correlation coefficient between SnO<sub>2</sub> and PbO is 0.619848, a positive correlation. The correlation coefficient between SiO<sub>2</sub> and FeO is -0.52688, showing that FeO and SiO<sub>2</sub> are negatively correlated in the samples. The



correlation coefficients between  $\text{SiO}_2$  and  $\text{PbO}$ , and  $\text{SiO}_2$  and  $\text{SnO}_2$ , are -0.59042 and -0.50677, respectively, supporting the hypothesis that the metal oxides increase at the expense of the  $\text{SiO}_2$ . Interestingly, the correlation between  $\text{CaO}$  and  $\text{FeO}$  was 0.512594, which is weakly positive. The most important aspect of this correlation matrix is that both types of slag appear to be present in all the slag samples within the sample suite.

Table 9: Correlation coefficients for WDS data, groundmass points only

	$\text{SiO}_2$	$\text{Al}_2\text{O}_3$	$\text{FeO}$	$\text{CaO}$	$\text{K}_2\text{O}$	$\text{PbO}$	$\text{SnO}_2$
<b><math>\text{SiO}_2</math></b>	1						
<b><math>\text{Al}_2\text{O}_3</math></b>	0.383107	1					
<b><math>\text{FeO}</math></b>	-0.52688	-0.34583	1				
<b><math>\text{CaO}</math></b>	-0.41416	-0.3748	0.512594	1			
<b><math>\text{K}_2\text{O}</math></b>	0.335284	0.269588	-0.35888	-0.35766	1		
<b><math>\text{PbO}</math></b>	-0.59042	-0.56738	0.153509	0.0826	-0.26346	1	
<b><math>\text{SnO}_2</math></b>	-0.50677	-0.45866	0.109143	0.049262	-0.18114	0.619848	1

Cluster analysis was performed using the centroid method using PlotIt, a Windows based software for statistical analyses. Cluster analysis calculates the presence of statistically significant groups within the sample and seeks to find the point at which one group diverges from another. The assignment of a given point to a group is dependent on its numerical distance from a given point, known as the centroid. It was hoped that this method would quantify the actual number of possible groupings within the slag data as well as the number of analyses that actually fell into each individual group.

The statistically correct number of potential clusters must be chosen or the results are not valid. This number is reached by using criterion values. First, a cluster analysis was run using 5 potential clusters in order to obtain criterion values. These criterion values were then plotted on a simple line graph and the “elbow” method was used to arrive at a cut-off point for number of true clusters (Figure 40). When the line graph was calculated, it showed that the data can only be reasonably clustered into two groups with any certainty.

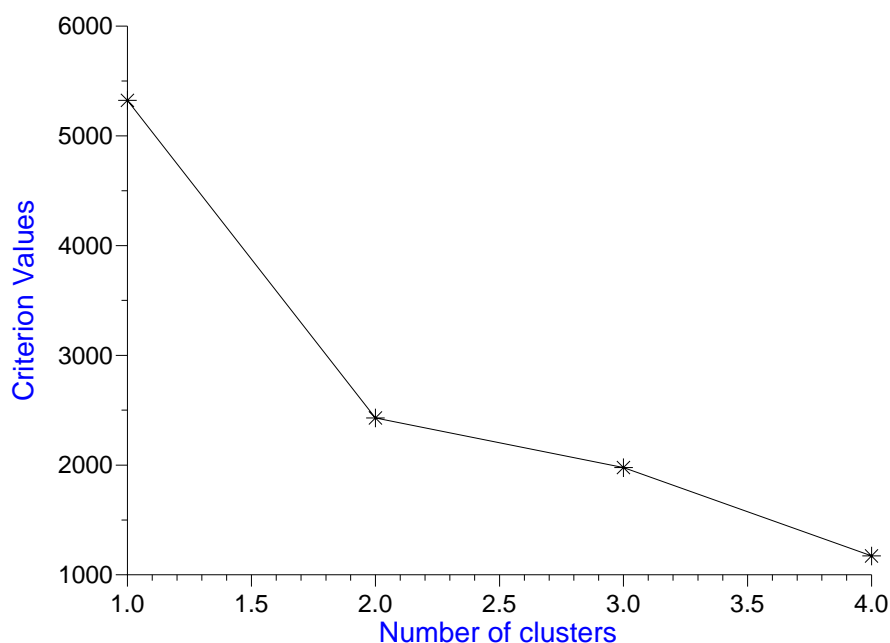


Figure 40: Cluster analysis: “Elbow” Method. Criterion values are plotted against potential number of clusters.

Further analysis of the resulting clusters using a dendrogram showed that in fact only one data point fell within group two (Appendix E). This again supports the hypothesis that there are not multiple chemical groups within the slag.

### **X-ray Diffraction (XRD)**

Only two samples were analyzed from the sample suite: A section of the ceramic portion in AVS722 and a vitrified portion of AVS722. The ceramic section was reddish-brown with visible quartz grains and the vitrified portion was grayish-green with visible quartz grains and metal inclusions. Machine failure limited the data set but some observations can be made from what data were collected.

The XRD analysis of the ceramic portion of AVS 722 showed that quartz, feldspar, and mica are present (Table 10). The quartz peaks were the most prominent, but there is one distinct feldspar

peak that can be observed. Feldspar peaks are easily masked by quartz peaks and so it is a reasonable assumption that there are more feldspar peaks that are simple hidden by the quartz peaks.

Table 10: XRD results by d-spacing for AVS722, ceramic portion. UID indicates unidentified phases

Position of Peaks		Intensity	Relative Intensity	ID
Degrees 2 $\theta$	D spacing	Counts per second	% of the total counts	
10.1481	10.114	58.90	6.22	Mica
16.0481	6.4080	28.78	3.04	Quartz
24.2188	4.2639	182.91	19.32	Quartz
30.9811	3.3491	946.60	100	Quartz
31.9825	3.2469	130.56	13.79	Quartz
32.0150	3.2437	75.51	7.98	Feldspar
32.2530	3.2204	54.88	5.8	Quartz
32.4815	3.1913	153.54	16.22	UID
34.2652	3.0364	52.03	5.5	Quartz
42.6571	2.4593	53.40	5.64	Quartz
46.1163	2.2130	61.16	6.46	Quartz
49.6757	2.1295	50.04	5.29	Quartz
58.8933	1.8195	73.52	7.77	Quartz

Within the vitrified portions of AVS722, however, fayalite appears while the mica disappears.

The quartz remains, as does some feldspar (Table 11).

Table 11: XRD results by d-spacing for AVS722, vitrified portion. UID indicates unidentified phases

Position of Peaks		Intensity	Relative Intensity	ID
Degrees 2 $\theta$	D spacing	Counts per second	% of the total counts	
24.2796	4.2534	53.91	16.27	Quartz
25.5715	4.0418	45.27	13.66	Quartz
27.5108	3.7618	16.88	5.09	Fayalite
28.8860	3.5863	18.29	5.52	Fayalite
29.7545	3.4130	17.96	5.42	Quartz
31.0518	3.3417	331.41	100	Quartz
32.0014	3.2450	46.43	14.01	Feldspar
32.3375	3.2122	64.91	19.58	Quartz
32.5586	3.1909	42.38	12.79	UID
34.6826	3.0010	26.90	8.12	UID
35.9272	2.9003	26.07	7.87	UID
41.0646	2.5503	37.01	11.17	Fayalite
41.3136	2.5356	10.15	3.06	Fayalite

Position of Peaks		Intensity	Relative Intensity	ID
Degrees 2 $\theta$	D spacing	Counts per second	% of the total counts	
41.5954	2.5192	25.22	7.61	Fayalite
42.5717	2.4640	21.31	6.43	Quartz
49.7221	2.1276	23.88	7.21	Quartz
50.8206	2.0846	17.41	5.25	Feldspar
58.9850	1.8169	33.86	10.22	Quartz
64.7333	1.6709	16.77	5.06	Quartz
67.9065	1.6015	18.35	5.54	Quartz

### Modern Metal Casting Work

The focus of the work observed by the author in spring 2008 was iron, not bronze casting. Therefore, no analogies with the chemistry of the resulting slags will be attempted, only qualitative information. The basic goals are the same in any case: the production of a piece of cast metal suitable for use or display.

In order to accomplish this goal, the subject of the piece must first be created using a plastic material such as wax or plasticine, which is a modern modeling clay that does not dry out when exposed to air. The complexity of the positive model determines the complexity of the mold. After the positive is created, several options are available to the sculptor; s/he can use the original positive to create the sand mold, can cast a negative plaster cast of the positive in order to create a negative “mother” mold that is used to make duplicates of the positive, and so on. In any case, the sculptor will eventually end up with at least one positive model that can be used to make the negative mold. Sand bonded together using a resin is packed around the positive; in the case of the simplest, two piece molds, the sand is packed around first one side of the positive, then after the resin cures to a solid, it is turned over and packed around the other side. Once the entire sand mold is complete, it is re-opened, the positive is removed, and the interior of the mold is prepared for casting. The first treatment is the creation of channels that allow the metal to flow into the mold and the channels that allow gases to escape (known as spruing and/or gating). There are other treatments such as “core washing”, which entails brushing the interior of the mold with an ethanol/graphite mixture. Core washing reduces the

amount of so-called “burn-in”, during which the molten metal actually partially melts and bonds with the resin and silica in the sand mold. Burn-in can reduce the quality of a piece that must have a smooth surface after finishing, and so core washing is usually done in these cases. In other circumstances where the anticipated surface treatment does not require as smooth a surface, core washing can be eliminated.

After the interior of the mold is prepared, the pieces are placed in their final configuration and the mold is closed using glue – in this case, construction adhesive was used. The openings to the gates that allow the molten metal into the mold and the risers that allow gas to escape are topped with more resin sand pieces designed to assist these processes; the gate is topped with a piece mold to resemble a wide funnel (known as a “pour cup”) that makes it easier to get the metal into the gate itself, and the risers are topped with cone-shaped resin sand pieces in which holes have been drilled to allow the gases to escape more efficiently (Figure 41).



Figure 41: Molds during an iron pour showing pour cups and risers.

Once the molds are prepared, the metal can be cast. Modern iron casting does involve significant technological differences from ancient bronze casting in some respects: 1) Iron is melted using a blast furnace, involving temperatures above 1500° C; 2) The molten iron is tapped directly from the blast furnace into a container termed a ladle, not a crucible. In other areas, though, the logistics are not so different from bronze casting. Both processes involve working with molten metal, a highly dangerous activity, and both processes have as end goals the production of decent quality artwork at their ends.

A modern iron blast furnace is known as a cupola and depending on its size is capable of tapping over 100 lbs. of iron with every tap. It has a relatively simple construction with tuyeres that feed into the blast zone of the furnace, two taps (one placed higher to allow slag to run off and one lower for tapping the molten iron), and refractory liner made of clay mixed with quartz sand. During operation, the charge is fed into the top by one or more workers. At the minimum the metal tap, and sometimes both taps, are closed off with refractory clay. As the charge travels through the blast zone it becomes molten, with the flux assisting in driving off slag and purifying the iron. The slag flows from the higher slag tap (if closed with refractory clay the clay seal is rammed open with a metal lance when it is time to allow the slag to pour off), and when the charge is completely molten, the lower tap is rammed open in the same fashion as the slag tap and the iron flows into a waiting ladle. The molten iron is then “slagged off” using another fluxing substance that is simply tossed on top of the metal; the resulting slag is less dense and slightly more viscous than the metal and is removed using a metal pole shaped somewhat like a gardening spade. The half-moon spade at the end of the pole is used to skim off the slag, and the metal pole is banged against whatever is convenient to knock off the slag. The ladle is then carried either by hand or by crane from mold to mold, and the crews pour molten metal into each mold until it is completely filled (Figure 42).



Figure 42: Pouring into the molds

Modern metal casting parlance includes the term “hot pour” that designates the use of the hottest molten metal for the largest molds in order to ensure that the molten metal does not begin to solidify before the mold is completely filled. Should the metal cool too quickly, it creates what are called “choke points” today, denoting the fact that the metal has been stalled or stopped from filling up the mold. During modern casting of iron, the ladle is lined on its exterior with refractory materials prior to receiving the molten metal, and is heated prior to tapping the iron.

After the molds have been filled and enough time has elapsed to allow the metal to cool sufficiently, the molds are broken open and the sculptures are removed. They are then subjected to various surface treatments that affect their color and texture; these are based on aesthetic criteria as well as the physical limitations of the metal itself.

Because of the actual pour is such a labor intensive task requiring multiple crews of people to manage charging the furnace, slagging the melt, handling the ladle, and monitoring safety throughout, multiple molds are typically prepared for casting before a pour will be done.



## DISCUSSION

The ceramic portions of the sample suite are mostly consistent with the *cune* discussed by Serneels, et al., in the 1999 study. They are around ~10 cm thick with visible metal inclusions within the vitrified portion of the sample. Quartz grains are abundant, and EMPA data show both feldspar and biotite are present within the ceramic matrix. These data are corroborated by the minimal XRD data. There is a fayalite boundary on the side of the one ceramic fragment labeled AVS722 that suggests rapid cooling. The fayalite in the ceramic of the *cune* and the slag groundmass is not, by itself, an indicator of an iron crucible. However, it is unlikely that there would be enough Fe in a ceramic crucible, or within a copper alloy mixture, to allow for this much fayalite to form in either the ceramic materials or within the poling slag. An additional source for the iron within the  $\text{FeSiO}_4$  is necessary. The crystal structure of the fayalite as well as the sharp boundary between it and the ceramic matrix indicates a very iron rich source in addition to very rapid cooling; these conditions do not seem consistent with the conditions within the rest of the sample suite. At the present time, the fayalite boundary in AVS722 raises more questions than it answers. The copper alloy inclusions, however, could easily be sourced to slag that dripped down between the crucible and the *cune*, and this would also account for at least some of the vitrification along the side of the *cune* in contact with the exterior of the crucible.

The observed weight percentages of the metal constituents of the alloy vary, with broad standard deviations (Table 12).

Table 12: Average weight percentages, metals

Label	Pt#	Cu	Sn	Pb	Fe	As	Sb	Cr	Ni
ABR001	AVG	80.76%	14.61%	4.59%	0.05%	0.00%	0.00%	0.00%	0.00%
	SD	7.59%	9.51%	2.65%	0.04%	0.00%	0.00%	0.00%	0.00%
ABR003	AVG	98.27%	1.42%	0.31%	0.00%	0.00%	0.00%	0.00%	0.00%

Label	Pt#	Cu	Sn	Pb	Fe	As	Sb	Cr	Ni
<b>ABR003</b>	SD	n/a	n/a	n/a	n/a	n/a	n/a	n/a	n/a
<b>ABR028</b>	AVG	99.95%	0.00%	0.00%	0.05%	0.00%	0.00%	0.00%	0.00%
	SD	n/a	n/a	n/a	n/a	n/a	n/a	n/a	n/a
<b>AVS901</b>	AVG	83.28%	6.28%	10.39%	0.05%	0.01%	0.00%	0.00%	0.00%
	SD	7.96%	3.32%	10.31%	0.03%	0.04%	0.00%	0.00%	0.00%
<b>AVS902</b>	AVG	99.72%	0.02%	0.24%	0.02%	0.01%	0.00%	0.00%	0.00%
	SD	0.03%	0.01%	0.04%	0.04%	0.02%	0.00%	0.00%	0.00%
<b>AVS903</b>	AVG	83.98%	5.58%	10.31%	0.14%	0.05%	0.05%	0.04%	0.00%
	SD	20.67%	2.45%	22.03%	0.07%	0.14%	0.20%	0.15%	0.00%
<b>AVS905</b>	AVG	93.32%	6.19%	0.32%	0.18%	0.02%	0.01%	0.00%	0.00%
	SD	0.73%	0.67%	0.19%	0.04%	0.03%	0.02%	0.01%	0.00%
	MDL	0.15	0.1	0.32	0.11	0.09	0.11	0.15	0.16

An approximation of the alloy weight percentages of Cu, Sn, and Pb can be made, however. First, the data from ABR003, ABR028, and AVS902 were removed due to their near-complete lack of Sn and Pb; these analyses were made on points that were within copper prills in the slag groundmass and can not be considered representative of the alloy mixture itself. Then, data points that were clearly representative of the boundary between Cu-Sn grains and the immiscible Pb were removed. Finally, the data were re-averaged and standard deviations were re-calculated. The results showed that Cu averaged approximately 88%, Sn averaged 8 %, and the balance for Pb was 6 % (Table 13, Figure 43). It is important to note that this is only an approximation; however, this is consistent with a typical low tin bronze alloy. While the alloy was not subjected to metallographic examination to determine exactly which Cu-Sn phase is present, the amount of tin present is within the range that forms the Cu-Sn  $\alpha$  phase (Sidot, et al., 2005). Overall, one is left with the impression that these samples do not represent a successful attempt at creating a high quality Cu-Sn-Pb alloy, but that they are more consistent with incomplete reactions that were discarded. Nevertheless, they suggest the general alloy composition, and it is consistent with leaded bronze of the type typically used to cast Roman-style statuary.

Table 13: Normalized Element Weight Percent Alloy Components

Label	Pt#	Cu	Sn	Pb	Fe	As	Sb	Cr	Ni	Total
ABR001	1	82.84%	10.09%	7.06%	0.01%	0.00%	0.00%	0.00%	0.00%	100.00%
	1	84.84%	9.82%	5.25%	0.09%	0.00%	0.00%	0.00%	0.00%	100.00%
	2	84.15%	10.54%	5.25%	0.06%	0.00%	0.00%	0.00%	0.00%	100.00%
	9	81.65%	16.05%	2.24%	0.06%	0.00%	0.00%	0.00%	0.00%	100.00%
	1	83.81%	10.26%	5.93%	0.00%	0.00%	0.00%	0.00%	0.00%	100.00%
	2	84.19%	9.89%	5.92%	0.00%	0.00%	0.00%	0.00%	0.00%	100.00%
	9	83.04%	15.12%	1.73%	0.10%	0.00%	0.00%	0.00%	0.00%	100.00%
	20	81.56%	10.52%	7.91%	0.01%	0.00%	0.00%	0.00%	0.00%	100.00%
	22	60.73%	39.18%	0.00%	0.09%	0.00%	0.00%	0.00%	0.00%	100.00%
AVS901	5	85.28%	11.40%	3.32%	0.00%	0.00%	0.00%	0.00%	0.00%	100.00%
	6	88.70%	2.83%	8.38%	0.09%	0.00%	0.00%	0.00%	0.00%	100.00%
	7	90.84%	7.35%	1.74%	0.07%	0.00%	0.00%	0.00%	0.00%	100.00%
	8	85.00%	7.10%	7.85%	0.05%	0.00%	0.00%	0.00%	0.00%	100.00%
	9	90.13%	8.96%	0.87%	0.05%	0.00%	0.00%	0.00%	0.00%	100.00%
	10	87.76%	10.83%	1.36%	0.05%	0.00%	0.00%	0.00%	0.00%	100.00%
AVS901	54	82.78%	9.64%	7.53%	0.05%	0.00%	0.00%	0.00%	0.00%	100.00%
	57	92.40%	7.10%	0.43%	0.07%	0.00%	0.00%	0.00%	0.00%	100.00%
	58	91.48%	8.08%	0.40%	0.04%	0.16%	0.00%	0.00%	0.00%	100.00%
AVS903	38	94.87%	4.51%	0.44%	0.18%	0.00%	0.00%	0.00%	0.00%	100.00%
	39	92.13%	6.76%	1.00%	0.11%	0.00%	0.00%	0.00%	0.00%	100.00%
	40	93.04%	5.72%	1.13%	0.10%	0.12%	0.00%	0.00%	0.00%	100.00%
	41	92.25%	6.60%	1.04%	0.12%	0.00%	0.00%	0.00%	0.00%	100.00%
	42	96.13%	2.59%	1.09%	0.19%	0.00%	0.00%	0.00%	0.00%	100.00%
	44	88.27%	5.69%	5.91%	0.14%	0.53%	0.77%	0.59%	0.00%	100.00%
	46	88.25%	8.13%	3.43%	0.19%	0.00%	0.00%	0.00%	0.00%	100.00%
	47	94.28%	4.55%	0.94%	0.24%	0.00%	0.00%	0.00%	0.00%	100.00%
	49	90.93%	6.05%	2.84%	0.17%	0.00%	0.00%	0.00%	0.00%	100.00%
	50	89.69%	4.82%	5.28%	0.21%	0.00%	0.00%	0.00%	0.00%	100.00%
AVS905	51	87.97%	11.44%	0.59%	0.00%	0.00%	0.00%	0.00%	0.00%	100.00%
	52	89.83%	6.73%	3.31%	0.14%	0.00%	0.00%	0.00%	0.00%	100.00%
	14	93.11%	6.02%	0.72%	0.15%	0.00%	0.00%	0.00%	0.00%	100.00%
	18	93.08%	6.31%	0.46%	0.15%	0.05%	0.05%	0.04%	0.00%	100.00%
	29	92.36%	7.12%	0.39%	0.13%	0.00%	0.00%	0.00%	0.00%	100.00%
	30	93.39%	6.21%	0.16%	0.24%	0.10%	0.00%	0.00%	0.00%	100.00%
	31	94.05%	5.62%	0.19%	0.15%	0.00%	0.00%	0.00%	0.00%	100.00%
	32	94.13%	5.50%	0.17%	0.20%	0.00%	0.00%	0.00%	0.00%	100.00%
	33	94.21%	5.40%	0.19%	0.20%	0.00%	0.00%	0.00%	0.00%	100.00%
	34	92.90%	6.41%	0.49%	0.20%	0.00%	0.00%	0.00%	0.00%	100.00%
	35	92.15%	7.42%	0.30%	0.13%	0.00%	0.00%	0.00%	0.00%	100.00%
	37	93.78%	5.86%	0.14%	0.23%	0.00%	0.00%	0.00%	0.00%	100.00%

Label	Pt#	Cu	Sn	Pb	Fe	As	Sb	Cr	Ni	Total
AVS905	Avg.	88.80%	8.51%	2.58%	0.11%	0.02%	0.02%	0.02%	0.00%	100.00%
	S.D.	0.062542	0.058107	0.027092	0.000715	0.000903	0.001233	0.000945	0	0

Alloy Composition  
Aventicum

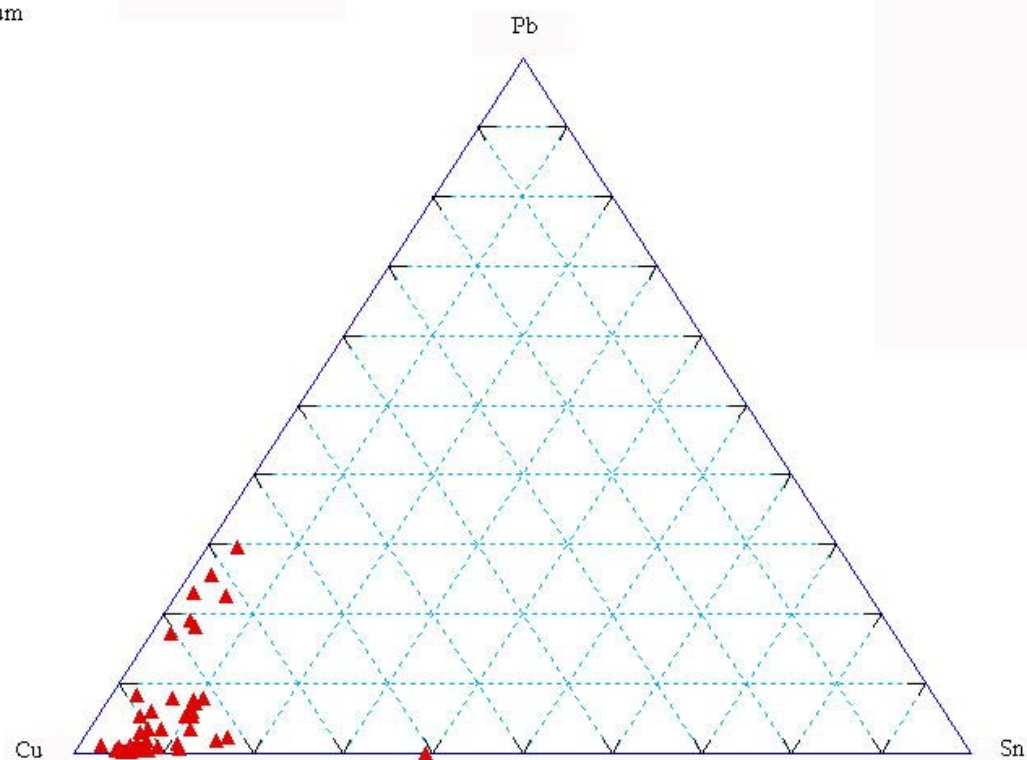


Figure 43: Cu-Pb-Sn ternary plot, metal components

In all of the ternary and binary plots of the oxides present within the slag, only one obvious grouping appears, with the tightest clustering seen in the Feo-CaO binary plot. The biotite, potassium feldspar, quartz, zircon, and rutile, among other random mineral grains seen in image analysis and EDS analysis, are all probably from the heavy mineral fraction in the sand used as a flux material (Kresten et al., 1998). A comparison of the data collected for slag by Serneels and Wolf with the data collected in this study shows some significant differences. The slag data, albeit only three points, from the 1997 study, clusters near the  $\text{SiO}_2$  apex of the ternary system  $\text{CaO-SiO}_2\text{-Al}_2\text{O}_3$  within the ranges

assigned to cristobalite, tridymite, mullite, and anorthite (See Figure 44). The data from this study, however, shows slightly lower  $\text{SiO}_2$  levels, with data points distributed more strongly towards  $\text{CaO}$  and  $\text{Al}_2\text{O}_3$  (Figure 45). The simplest reason that this difference appears may lie with the disparate techniques used; the 1997 study employed bulk analysis that did not remove quartz from the samples under study, whereas the WDS data plotted in this study did in fact remove these mineral grains. EMPA has allowed for a more precise, accurate chemical characterization of the slag groundmass itself in this study, and allows the temperature of the slag melt to be fixed more accurately as well, at approximately  $1350^\circ\text{--}1400^\circ\text{C}$ .

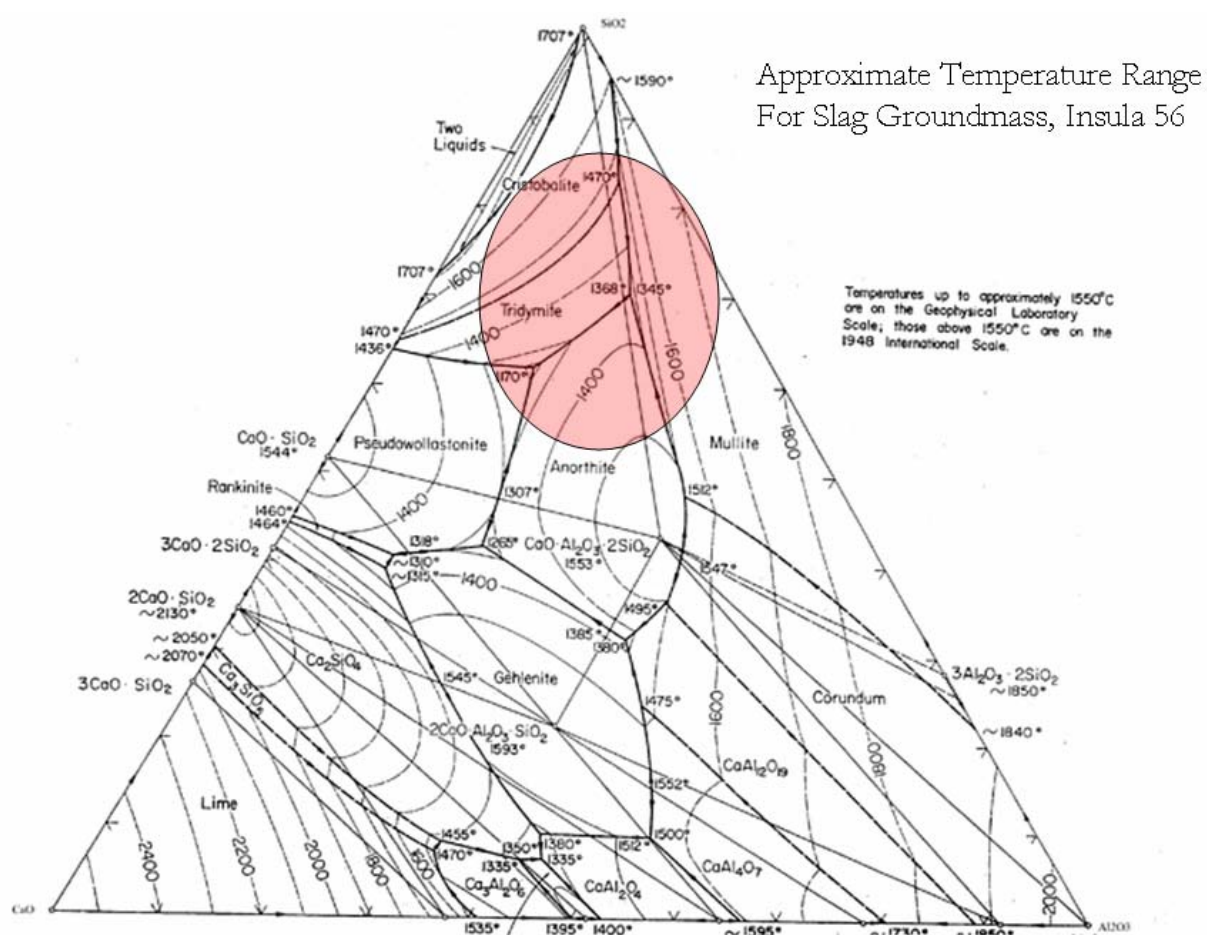


Figure 44:  $\text{CaO-SiO}_2\text{-Al}_2\text{O}_3$  system

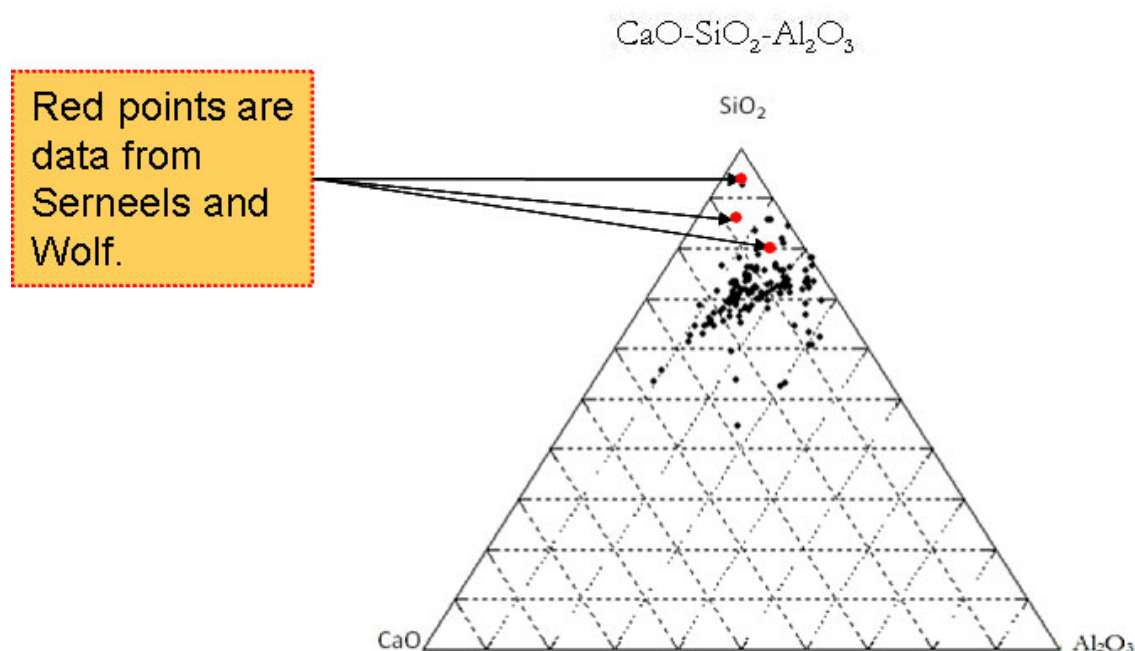


Figure 45:  $\text{CaO-SiO}_2\text{-Al}_2\text{O}_3$  system showing data from Serneels and Wolf, 1997 (in red), compared with Cook Hale, 2008 (in black).

While ternary and binary plots along with statistical analyses did not support the presence of multiple chemical groups within the slag, it is also impossible to ignore the fact that there are flowbands of varying densities with varying amounts of metal oxides within them. It is clear that the slag containing greater amounts of  $\text{PbO}$  and  $\text{FeO}$  did not uniformly mix with slag containing smaller amounts of  $\text{PbO}$  and  $\text{FeO}$ , but this is most likely due to rapid cooling of somewhat immiscible liquid. This hypothesis is further reinforced by the presence of slag of both greater and lesser density within most if not all of the slag samples.

With respect to the fayalite found within the poling slag itself, the iron necessary to form the fayalite can be sourced to the iron crucible itself; the Fe-Sn diagram as well as a Cu-Fe binary phase diagram (Figure 46) show that the temperatures were high enough for some iron to enter the melt.

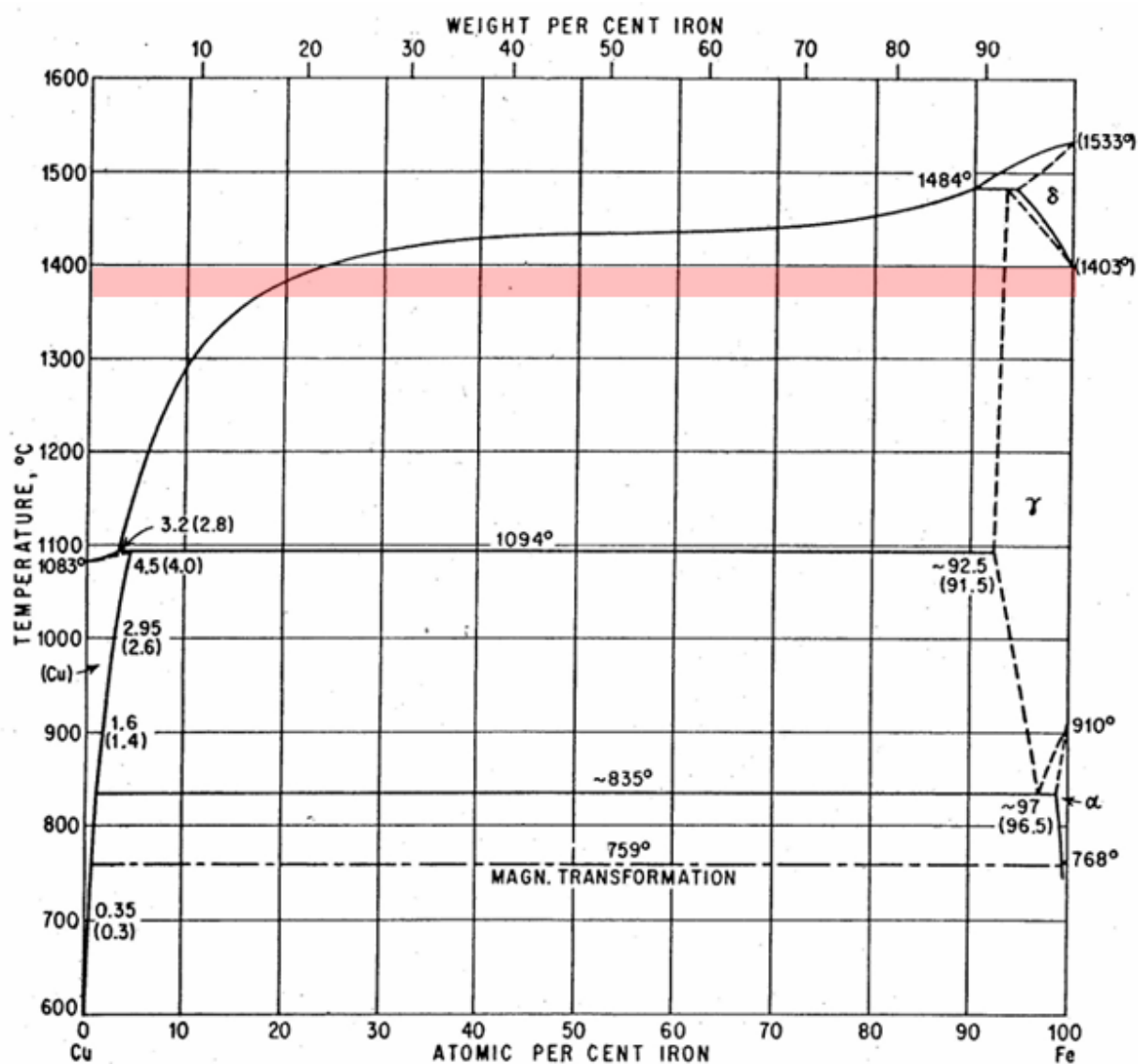


Figure 46: Cu-Fe binary phase diagram

The amount of the Fe present in a slag is also suggestive of the  $pO_2$ : Overly reduced conditions will trap iron within the copper, while overly oxidized conditions lead to high slag viscosity and the

formation of spinel. Low iron in the copper alloy and the minor presence of chrome in the slag suggest that the slag was more oxidized than the alloy. Some Sn remained within the slag as an oxide,  $\text{SnO}_2$ . Cu tends to easily oxidize but when Sn is present, the Sn will oxidize before the Cu (Hamilton, 1996). The  $\text{SnO}_2$  is found in areas within the groundmass that are richer in  $\text{PbO}$  and  $\text{FeO}$ . It is apparent that the Sn component of the alloy was reacting with the Fe in the wall of the crucible, leaving behind  $\text{SnO}_2$ . Figure 47, a binary plot of Fe and Sn, shows that at a temperature of  $1350^\circ\text{C}$ , a mixture containing  $>25\%$  or more Sn will consist of two melts. It is difficult to fix the nature of the cooling history, but it is reasonable to say that the Fe rich slag melt solidified before the Pb rich portions of the melt. Further, due to the higher temperatures at which a Fe rich melt will quench, it seems reasonable that  $\text{SnO}_2$  nucleation will end more quickly in that mixture than in a Pb rich melt.

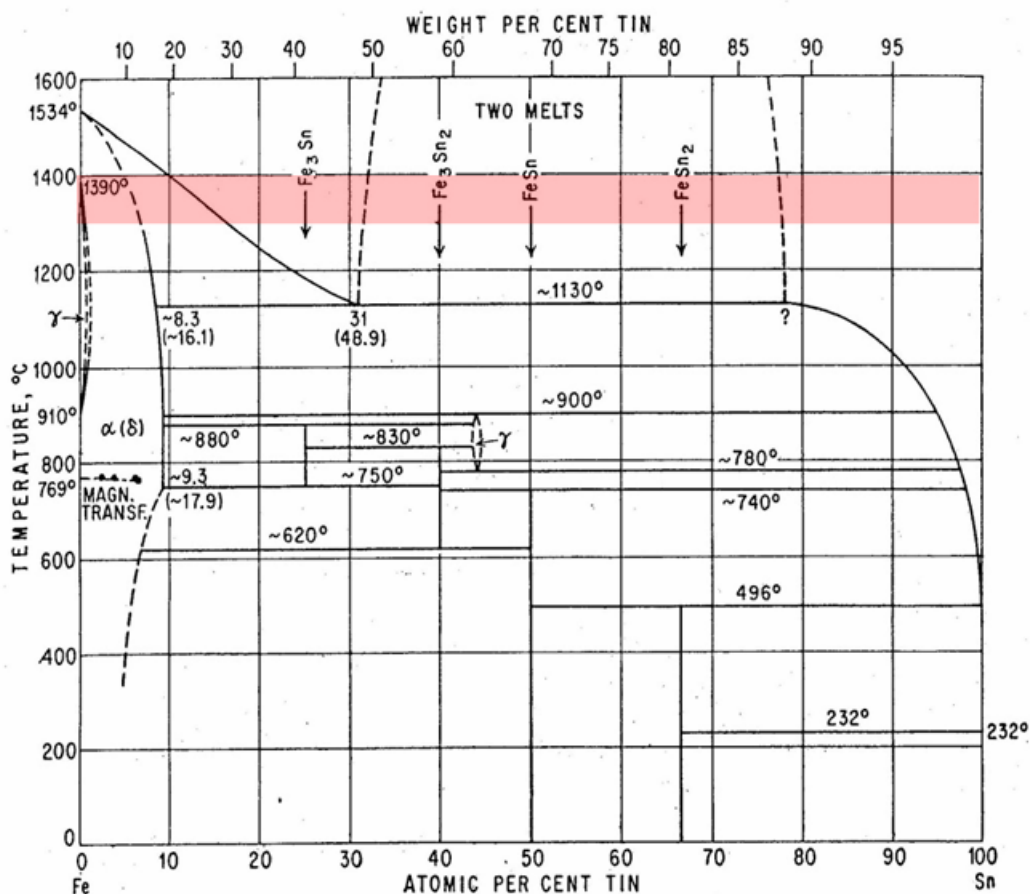


Figure 47: Fe-Sn binary plot



Observation of modern metal casting by the author in spring of 2008 offers some answers to the actual mechanics of the casting process at *Insula 56*. Analysis of the WDS data for the slag groundmass suggests that the slag reached temperatures of around 1350°-1400° C, far hotter than should be necessary to simply melt the metal components of the alloy. This would easily qualify as a hot pour; a hot pour would have been the most effective one for casting large pieces of statuary in terms of the integrity of the final product.

Another requirement to create a hot pour is the refractory liner placed around a modern ladle; it seems quite possible that within an ancient context, refractory clays similar to the ones used in the furnace construction itself might have been used. These refractory external liners serve to prevent the temperature within the ladle from dropping below an undesirable point during the pour. This strongly suggests that the *cune* was not a permanent emplacement within the furnace itself, but was instead molded around the exterior of the crucible/ladle prior to melting. Unlike a modern blast furnace such as is used in artistic iron casting today, the charge used at Insula 56 was not placed directly within the furnace, but was instead placed within the iron crucible that had been lined with the *cune*; the entire assembly was then lowered into the furnace itself. Once the charge was molten, the crucible and *cune* assembly were probably then lifted out of the furnace, and the slag was poled off of the top of the molten bronze. This process results in a slag that is highly vesicular with a general morphology remarkably similar to the slag from Insula 56 (Figure 48). It is important to note here that the data from the current study offers no information about when the fluxes were introduced. They could have been placed in the crucible with the metal components prior to lowering the assembly into the furnace, thrown in after the crucible and *cune* were lifted from the furnace, or any other possible combination of these two scenarios.



Figure 48: Modern Poling Slag, 2/2008, and ABR020 from Insula 56

## CONCLUSIONS

Returning to the four questions raised in the introductory portion of this study, what were the benefits of using a more expensive iron crucible that involved more effort to fabricate than a ceramic crucible? What purpose may have been served by the external crucible lining or “*cuvè*”? What effects can be seen in the slag left behind? Finally, now that these remains have been characterized, what are some unique aspects of this assemblage that can be potentially used to identify the use of iron crucibles in the rest of the Gallo-Roman world?

Based on the high temperatures ( $\sim 1350^{\circ}\text{C}$ ) achieved at the workshop in Insula 56, ceramic crucibles would have been an insufficient, and even potentially dangerous, choice of material. Iron has a higher melting temperature and was probably the best choice for this process. The use of an iron crucible also suggests a permanent foundry in contrast to some workshops in Aventicum that seem to have been temporary (Morel, 2001). Their use strongly suggests that a high volume of copper alloy could have been cast, again consistent with the production of lead bronze statuary.

Despite the fact that the WDS data from the metal analyses were impossible to fix with complete accuracy, it seems reasonable to say that the overall alloy composition was a very pure leaded bronze. This conclusion is supported by the fact that although the melting of the silicate slag was incomplete and there is evidence of some incomplete reactions within the melt, the WDS analyses of the metal show these areas to be a pure copper-tin-lead alloy.

It appears that the artisans of Insula 56 were engaged in a highly industrial casting operation that operated at a high volume of production. The waste materials from this operation show evidence for a consistent alloy that can be detected by EMPA as well as bulk analysis methods; further, the use of EMPA is more useful than bulk analysis in detecting the  $\text{SnO}_2$  and Fe phases that are markers for

an iron, as opposed to a ceramic, crucible. If evidence for iron crucibles can be found at other foundry sites from the Gallo-Roman world, then EMPA analysis of the slag offers considerable promise in accomplishing this task. The groundmass of slag from copper alloy foundries must be analyzed for evidence of a high temperature melt ( $\sim 1350^{\circ}\text{C}$ ) and the distinctive  $\text{SnO}_2$  and Fe phases must be sought in both slag and ceramic fragments. It would be useful also to look for analogs to the as-yet unexplained fayalite along the side of AVS722 in order to explain its appearance in this study. The logical next step in further study would be a re-analysis of waste materials recovered from other sites known to produce copper alloys at a large scale of production, such as Alesia and Autun, both in modern-day France.

## REFERENCES

- [1] Arnold, B. (1990). *Cortaillod-Est et les villages du lac de Neuchâtel au Bronze Final. Structure at l'habitat et proto-urbanism* (Vol. 6).
- [2] Arnold, B. (1990). *un village du Bronze Final Cortaillod-Est. fouilles subaquatique at photographie aérienne*. (Vol. 1).
- [3] Bale (Ed.). (2002). *SPM V: Epoque Romain. Quand Le Suisse N'existant Pas: Les Temps Des Romains* (Vol. V). Corbag, S.A. Montreaux: Societe suisse de Prehistoire et d'archaologie.
- [4] Bayley, J., Mackreth, D.F., & Wallis, H. (2001). Evidence for Romano-British Brooch Production at Old Buckenham, Norfolk. *Britannia*, 32, 93-118.
- [5] Blanc, P., Duvauchelle, A., & Ogay, A. (1999). Avenches/En Selley, rapport sur less investigations realisees en 1997-1998. *Bulletin de L'Association Pro Aventico*, 41, 7-24.
- [6] Blanc, P., Meylan-Krause, M., Hochuli-Gysel, A., Duvauchelle, A., & Ogay, A. (1999). Avenches/En Selley, investigations 1997: quelques reperes sur l'occupation tardive d'un quartier peripherique d'Aventicum (insula 56). Structures et mobilier des III et IV ap. J.-C. *Bulletin de L'Association Pro Aventico*, 41, 25-70.
- [7] Caesar, G.J. (50 B.C.). *Commentariorum De Bello Gallico Cum a. Hirti Supplemento Libri VIII*. In C.H.F. Albert Harkness (Ed.), *Caesar's Commentaries on the Gallic War* (Vol. 1). New York, Cincinnati, Chicago: American Book Company.
- [8] Castella, D. (Ed.). (1998). *Aux Portes d'Aventicum* (Vol. 4). Avenches: Imprimerie Corbaz SA, Montreux.
- [9] Collis, J. (2007). The Politics of Gaul, Britain, and Ireland in the Late Iron Age. In T.M. Colin Haselgrove (Ed.), *The Later Iron Age in Britain and Beyond* (pp. 523-528). Oxford, UK: Oxbow Books.
- [10] Cooke, S.R.B., Aschenbrenner, S. (1975). The Occurrence of Iron in Ancient Copper. *Journal of Field Archaeology*, 2(3).
- [11] Craddock, P.T. (1977). The Composition of the Copper Alloys used by the Greek, Etruscan and Roman Civilisations. *Journal of Archaeological Science*, 4, 103-123.
- [12] Craddock, P.T. (1979). The Copper Alloys of the Medieval Islamic World – Inheritors of the Classical Tradition (Vol. 11, no. 1, *Early Chemical Technology*).
- [13] Craddock, P.T., Lang, J. (Eds.). (2003). Mining and Metal Production Through the Ages. London: *The British Museum Press*.
- [14] Datta, P., Chattopadhyay, P., Ray, A. (2007). New Evidence for High Tin Bronze in Ancient Bengal. *SAS Bulletin*, 30(2), 13-16.
- [15] Dillmann, P., L'Héritier, M. (2007). Slag inclusion analyses for studying ferrous alloys employed in French medieval buildings: supply of materials and diffusion of smelting processes. *Journal of Archaeological Science*, 34(11), 1810-1823.
- [16] Dungworth, D. (1997). Roman Copper Alloys: Analysis of Artefacts from Northern Britain. *Journal of Archaeological Science*, 24, 901-910
- [17] Durman, A. (2004). *Vučedolski Hromi Bog: Zašto Svi Metalurški Bogovi Šepaju? (The Lame God of Vucedol: Why Do All the Gods of Metallurgy Limp?)* Vukovar.

- [18] Duvauchelle, A., Ogay, A. (1999). Avenches/En Selley investigations 1997-1998: un artisanat du fer et du brinze aux I et II s. ap. J.-C. Le petit mobilier. *Bulletin de L'Association Pro Aventico*, 41, 125-132.
- [19] Edmondson, J.C. (1989). Mining in the Later Roman Empire and beyond: Continuity or Disruption? *The Journal of Roman Studies*, 79, 84-102.
- [20] Eramo, G. (2006). The Glass Melting Crucibles of Derriere Sairoche (1699-1714 AD, Ct. Bern, Switzerland): a petrological approach. *The Journal of Archaeological Science*, 33, 440-452.
- [21] Farley, M., Henig, M., Taylor, J.W. (1988). A Hoard of Late Roman Bronze Bowls and Mounts from the Misbourne Valley, near Amersham, Bucks. *Britannia*, 19, 357-366.
- [22] Fasnacht, W., Hack, E., Jauch, V., Rechenmacher, D., Senn, M., & Vontobel, P. (2005). Vier Öfen, zwölf Düsen - Archäometallurgie und dreidimensionale Erfassung römischer Schmiedeöfen. *Mitteilungsblatt der Schweizerischen Gesellschaft für Ur- und Frühgeschichte – SGUF (Bulletin de la Société suisse de préhistoire et d'archéologie – SSPA, Bollettino della Società svizzera di preistoria e d'archeologia – SSPA)*. 20-27.
- [23] Fellman, R. (1988, 1992). *La Suisse Gallo-Romaine: Cinq Siècles D'Histoire* Konrad Theiss Verlag GmbH & Co.
- [24] Giumlia-Mair, A. (2005). Copper and Copper Alloys in the Southeastern Alps: An overview. *Archaeometry*, 47(2).
- [25] Goodway, M. (1989). Etruscan Mirrors: a Reinterpretation. *MASCA Research Papers in Science and Archaeology, (History of Technology: The Role of Metals)*.
- [26] Gosden, C. (1985). Gifts and Kin in Iron Age Europe. *Man*, 20(3), 475-493.
- [27] Gostencnik, K. (2002). Agathangelus the Bronzesmith: The British Finds in Their Continental Context. *Britannia*, 33, 227-256.
- [28] Guillaumet, J.-P. (2003). *Paleomanufacture Metallique: methode d'etude*. Gollion, CH: Infolio editions.
- [29] Hamilton, E.G. (1996). Technology and Social Change in Belgic Gaul: Copper Working at the Titelberg, Luxembourg, 125 B.C. to A.D. 300. *MASCA Research Papers in Science and Archaeology*, 13.
- [30] Hein, A., Kilikoglou, V., Kassianidou, V. (2007). Chemical and mineralogical examination of metallurgical ceramics from a Late Bronze Age copper smelting site in Cyprus. *Journal of Archaeological Science*, 34, 141-154.
- [31] Holland, T. (2003). *Rubicon* Anchor Books.
- [32] Ingo, G.M., Caro, T.D., Riccucci, C., & Khosroff, S. (2006). Uncommon corrosion phenomena of archaeological bronze alloys. *Applied Physics A: Materials Science & Processing*, 83(4), 581-588.
- [33] James, S. (1993). *The World of the Celts*. London, UK: Thames and Hudson Ltd.
- [34] Kaenal, G., Curdy, P., Carrard, F. (2004). *L'oppidum du Mont Vully. Un bilan des recherches, 1978-2003*. Fribourg, CH: Archeologie fribourgeoise.
- [35] Kleiner, F.S. (1973). Gallia Graeca, Gallia Romana and the Introduction of Classical Sculpture in Gaul. *American Journal of Archaeology*, 77(4), 379-390.
- [36] Kramer, H.G. (1940). Aventicum. *The Classical Journal*, 36(3), 155-163.
- [37] Kresten, Peter; Hjärthner-Holdar, Eva; Larsson, Lena. Geochemistry in Archaeometallurgy. Paper presented at Buma IV, Matsue, Japan, 1998.
- [38] Lawson, A.K., Oddy, W.A., Craddock, P.T. (1986). A Fragment of Life-Size Bronze Equine Statuary from Ashill, Norfolk. *Britannia*, 17, 333-333p.
- [39] Lechtman, H. (1996). Arsenic Bronze: Dirty Copper or Chosen Alloy? A View from the Americas. *Journal of Field Archaeology*, 23(4), 477-514.
- [40] Lönnqvist, K.K.A. (2003). A Second Investigation into the Chemical Composition of the Roman Provincial (Procuratorial) Coinage of Judaea, AD 6–66. *Archaeometry*, 45(1), 45-60.

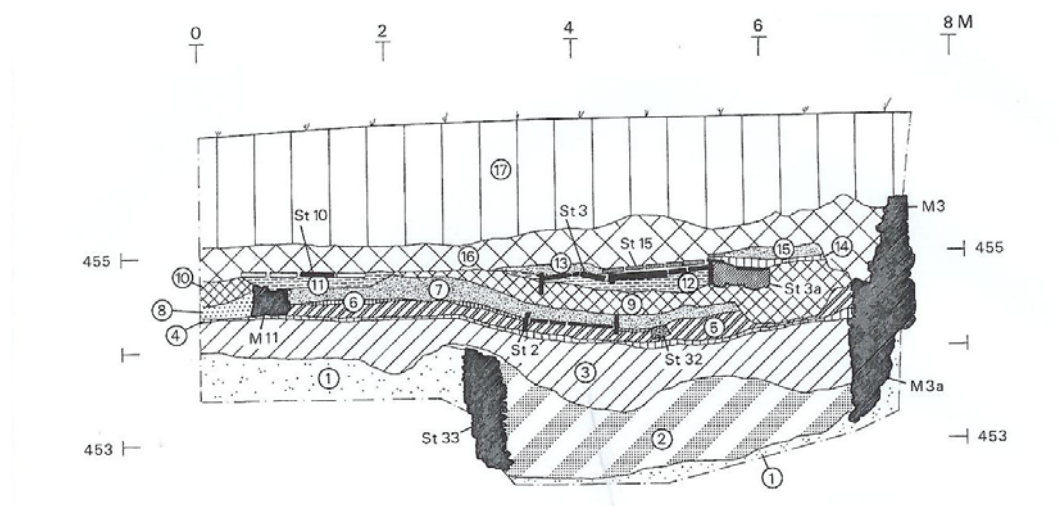
- [41] Lyle, N. (2002). The use of geological methods for the characterization of Roman metallurgical slag from the excavations of the Yasmina Cemetery in Carthage, Tunisia. Unpublished master's thesis, University of Georgia, Athens.
- [42] Mattusch, C.C. (1977). Bronze- and Ironworking in the Area of the Athenian Agora. *Hesperia*, 46(4), 340-379.
- [43] Mattusch, C.C. (1995). Two Bronze Herms: Questions of Mass Production in Antiquity. *Art Journal*, 54 (No. 2, Conservation and Art History), 53-59.
- [44] Mauvilly, M., Christobal, E.G., Peiry, C., & Serneels, V. (2001). La metallurgie du bronze au milieu de l'âge du fer. *Archeologie Suisse*, 24(3).
- [45] Morel, J., Chevalley, C., & Castella, D. (2001). Le Fabrication de Grand Bronzes a Aventicum: une fosse de coulee dans L'insula 12. *Bulletin Pro Aventicum*, 43, 141-162.
- [46] Ottaway, B., & Strahm, C. (1975). Swiss Neolithic Copper Beads: Currency, Ornament or Prestige Items? *World Archaeology*, 6(3), 307-321.
- [47] Pare, C.F.E. (Ed.). (2000). *Bronze and the Bronze Age*. Oxford, UK: Oxbox Books.
- [48] Paynter, S. (2006). Regional Variations in Bloomery Smelting Slag of the Iron Age and Romano-British Periods. *Archaeometry*, 48(2), 271-292.
- [49] Pliny. (75 A.D.). *The Natural History*. In J.R. Bostock, H. T. (Ed.) (Vol. XXXIV).
- [50] Ponting, M. (2002). Keeping up with the Romans? Romanisation and copper alloys in First Revolt Palestine. *Institute for Archaeo-Metallurgical Studies* (22), 3-6.
- [51] Ponting, M. (2002). Roman Military Copper-Alloy Artefacts from Israel: Questions of Organization and Ethnicity. *Archaeometry*, 44(4), 555-571.
- [52] Ponting, M., & Segal, I. (1998). Inductively Coupled Plasma-Atomic Emission Spectroscopy Analyses of Roman Military from the Excavations at Masada, Israel. *Archaeometry*, 40(1), 109-122.
- [53] Pryce, T.O., Bassiakos, Y., Catapotis, M., & Doonan, R.C. (2007). 'De Caerimoniae' Technological Choices in Copper-Smelting Furnace Designs at Early Bronze Age Chrysokamino, Crete. *Archaeometry*, 49(3), 543-557.
- [54] Ramseyer, D. (1992). Les Cites Lacustres: Le Neolithique dans le canton de Fribourg, Suisse, de 3867 a 2462 avant J.-C. Catalogue de l'exposition créée au Musée du Malgré-Tout du 6 juin au 20 décembre par le CEDARC at le Service Archéologique Cantonal de Fribourg.
- [55] Rehren, T. (1999). Small Size, Large Scale Roman Brass Production in Germania Inferior. *Journal of Archaeological Science*, 26, 1083-1087.
- [56] Rehren, T. (2003). Crucibles as Reaction Vessels in Ancient Metallurgy. In P.T. Craddock & J. Lang (Eds.), *Mining and Metal Production Through the Ages*. London: The British Museum Press.
- [57] Rehren, T. & Pernicka, E. (2008). Coins, Artefacts, and Isotopes – Archaeometallurgy and Archaeometry. *Archaeometry*, 50, 232-248.
- [58] Renfrew, C. (1969). Trade and Culture Process in European Prehistory. *Current Anthropology*, Vol. 10(2/3).
- [59] Renfrew, C. (Ed.). (1975). *Trade as Action at a Distance: Questions of Integration and Communication*. Albuquerque: University of New Mexico Press.
- [60] Rostoker, W., & Gebhard, E.R. (1980). The Sanctuary of Poseidon at Isthmia: Techniques of Metal Manufacture. *Hesperia*, 49(4), pp. 347-363.
- [61] Rychner, V. Le cuivre et les alliages du bronze final en suisse Occidentale. Extrait du Musée Neuchâtelois, 3, 81.
- [62] Rychner, V. (1988). Les bracelets de Sursee at la metallurgie de Suisse centrale a 'âge du Bronze final. *Archeologie Suisse*, 11 (2).
- [63] Rychner, V., Klanstchi, N. (1995). *Arsenic, Nickel, et Antimoine* (Vol. 63). Lausanne.
- [64] Sauter, M.R. (1976). Switzerland from Earliest Times to the Roman Conquest. Thames and Hudson Ltd.

- [65] Serneels, V., & Wolf, S. (1999). Les temoignages du travail du fer at du bronze provenant des fouilles En Selley a Avenches en 1997. *Bulletin de L'Association Pro Aventico*, 41.
- [66] Sidot, E., Kahn-Harari, A., Cesari, E., Robbiola, L. (2005). The lattice parameter of  $\alpha$ -bronzes as a function of solute content: application to archaeological materials. *Materials Science and Engineering, A* (393), 147-156
- [67] Tumiatì, S., Casartelli, P., Mambretti, A., Martin, S. (2005). The Ancient Mine of Servette (Saint Marcel, Val D'Aosta, Western Italian Alps): A Mineralogical, Metallurgical, and Charcoal Analysis of Furnace Slags. *Archaeometry*, 47(2), 317-340.
- [68] Webster, J. (2001). Creolizing the Roman Provinces. *American Journal of Archaeology*, 105(2), 209-225.
- [69] Weisgerber, G. (2003). Spatial Organisation of Mining and Smelting at Feinan, Jordan: Mining Archaeology Beyond the History of Technology. In P.L. Craddock, Janet (Ed.), *Mining and Metal Production Through the Ages* (pp. 76-89). London: British Museum Press.
- [70] Wells, P. (1980). Contact and Change: an example on the fringes of the Classical World. *World Archaeology*, 12(1).
- [71] Wells, P. (1984). *Farms, Villages and Cities*. Ithaca, New York, United States, and London, UK: Cornell University Press.
- [72] Wells, P. (Ed.). (2001). *Beyond Celts, Germans, and Scythians*. London: Gerald Duckworth & Co.
- [73] Wingheart, S. (2000). Mining, Processing and Distribution of Bronze: Reflections on the Organization of Metal Supply between the Northern Alps and the Danube Region. From *Metals Make the World Go Round*. Oxford, UK: Oxbox Books.
- [74] Zaghis, F., Molin, G., Salviulo, G., Calliari, I., Ramous, E., & Gangemi, G. (2005). A New Setting for the Northern Border of the Veneti: Metallic Finds from the Venetic Site of Monte Calvario, Auronzo di Cadore. *Archaeometry*, 47(2), 341-349.
- [75] Zivkovic, D., Štrbac, N., Trujic, V., Zivkovic, Z., Vuksan, M., Zivkovic, Z. (2004). Physico-Chemical Investigation of Slag Occurrences, Rgotski Kamen Timok region, Eastern Serbia. *Journal of Thermal Analysis and Calorimetry*, 76, 227-253



## APPENDIX A

## Stratigraphic profile of Insula 56



1: Sterile soil- reddish sandy silt

Phase 2 (2nd – 3rd century AD)

St 1: excavation that could have served as a storage site. This depression is bounded by the low wall St 33 (fragments of tegulae and limestone fragments not used for construction)

2: lower fill of St. 1 (grayish silt, very charred at the base, with fragments of tegulae and mounds of clay, K10285): occupation/abandonment layer.

3: Discarded clay rubble St 1. Numerous slags and sandy clay materials (kiln brick, crucibles, molds) associated with copper alloy metallurgy

4: Intermediate activity layer (charred silt)

Phase 3 (2nd half of the 3rd century AD)

St.2: Hearth

St32: low sand pit marking an internal subdivision of local L3

M11: low wall forming the northern limit of local L3

5: Construction debris (brownish-beige silt), K 10266

6: Circulation layer (mortar, whitewash, and gravel), K10302

7: Occupation layer and demolition (fire), K10264 and 10283.

8: Occupation layer and the exterior limit of local 3 (charred silt and organics)

9-10: Destruction layer (limestone cinder blocks and numerous fragments of tegulae) disarranged architectural materials. Observed over the entire surface that was surveyed, these attest to a demolition phase affecting all construction within this district.

Phase 4a (end of the 3rd century AD – around 320 AD)

St 3, St 10: hearths

St3a: Work surface laid out before the heart St3 (fragment of tegulae arranged horizontally on top of a limestone sill)

11: blanket of reddish clay and gravel serving as a base for St10

12: Blanket of clay serving as a base for St3

13: Occupation/abandonment layer, K10245

Phase 4b (around 320 AD – 330/335 AD)

St. 15: hearth

14: Circulation layer (beaten earth)

15: Occupation/abandonment layer, K10268

Phase 5 (abandonment in the 4th century AD)

16: Final destruction, never rebuilt, K10247, 10249, 10250, 10269, 10301.

General destruction layer overburden

17: Post-Roman sediments containing materials of ancient destruction and vegetal cover, K10279

### Standards used for EMPA WDS analysis

Table 14: Oxide Standards

Title: Slag		KV=15	Number of Elements=22		
name	line	mode	Mode value	Standard by elemental or oxide weight percent	Crystal
SiO <sub>2</sub>	K	WDS	Siq	Quartz: Ox% SiO <sub>2</sub> =100	TAP
Al <sub>2</sub> O <sub>3</sub>	K	WDS	Al3	Spinel: El% Mg=17.09 Al=37.93 O=44.98	TAP
FeO	K	WDS	Fe4	Hematite: Ox% Fe <sub>2</sub> O <sub>3</sub> =100	LIF
CaO	K	WDS	Ca2	Sphene: El% Si= 14.41 Ti=22.66 Al=0.72 Fe=0.51 Ca=20.6 Mn=0.04 P=0.01 F=0.08 O=40.63	PET
K <sub>2</sub> O	K	WDS	K	Orthoclase: El% Si=30.1 Al=9.129 K=12.39 Fe=0.02 Na=0.846 Ba=0.7 O=46.05	PET
PbO	M	WDS	PB2	PBSgood – Galena: El% Pb=86.6 S=13.4	PET
SnO <sub>2</sub>	L	WDS	SN	Sn: El% Sn=100	PET
CuO	K	WDS	CUO	CuO: Ox% CuO=100	LIF
Na <sub>2</sub> O	K	WDS	NA1	ABOX – Amelia Albite: Ox% SiO <sub>2</sub> =68.07 Al <sub>2</sub> O <sub>3</sub> =19.78 FeO=0.08 Na <sub>2</sub> O=11.4 K <sub>2</sub> O=0.26	TAP
As	L	WDS	AS1	INAS – Iridium Arsenide: El% In=60.51 As=39.49	TAP
Sb	L	WDS	SB	Sb: El% Sb=100	PET
MgO	K	WDS	MG3	Olivine: El%: Si=19.24 Fe=5.92 Mg=30.62 Mn=0.08 Ni=0.23 Cr=0.01 O=43.86	TAP
S	K	WDS	S	Pyrite: El%: Fe=46.549 S=53.541	PET

Table 15: Element Standards

Title: Metal		KV=15	Number of Elements=9		
name	line	mode	Mode value	Standard by element weight percent	Crystal
Cu	K	WDS	Cu	El% Cu=100	LIF
Sn	L	WDS	Sn	El% Sn=100	PET
Pb	M	WDS	PbMetal	El% Pb =100	PET
Fe	K	WDS	FEM	El% Fe=100	LIF
As	L	WDS	AS1	INAS – Iridium Arsenide: El% In=60.51 As=39.49	TAP
Sb	L	WDS	SB	Sb: El% Sb=100	PET
Cr	K	WDS	CrM	El% Cr=100	LIF
Ni	K	WDS	Ni	El% Ni=100	LIF

## APPENDIX B

## Sample suite by accession

Type	Samples	
Crucible	AVS722, ABR027, ABR028, ABR029, AVS905	
Metal prill	AVS901, AVS902, AVS903	
slag	ABR001, ABR002, ABR003, ABR004, ABR005, ABR006, ABR007, ABR008, ABR009, ABR010, ABR011, ABR012, ABR013, ABR014, ABR016, ABR017, ABR018, ABR019, ABR020, ABR021, ABR022, ABR023, ABR024, ABR025	
Hand sample descriptions		
AVS722	Reddish outer layer	This sample also has a distinct ceramic layer bounded by a slag layer.
ABR026	gray brown with green	Gritty
ABR027	gray brown with green	Slag material on one side, ceramics on the other. Corroded copper visible on slaggy side. Vesicular appearance on slag side
ABR028	gray brown with green	Ceramic layer with slag layer on the other side. Slag is very vesicular, dark color, with some corroded copper.
ABR029	gray brown with green	Darker slag side has smaller amounts of corroded copper, and is considerably glassier as well as darker in color than most of the other samples. It also has a ceramic layer on the back side, which is also darker than other ceramic layers.
AVS905	Gray outer layer	Ceramic outer layer, with inner side appearing more like the slag. Some corroded copper visible on the slag side, with vesicles shot through the layer.
AVS901	mottled green and red	Metal prill
AVS902	mottled gray green	Metal prill
AVS903	mottled gray green	Metal prill
ABR001	green-grey	Casting slag
ABR002	green-grey	Casting slag
ABR003	green-grey	Casting slag
ABR004	green-grey	Casting slag
ABR005	green-grey	Casting slag
ABR006	Green-gray	Casting slag
ABR007	mottled green	Casting slag ; glassy w/ corrosion
ABR008	Gray green	Casting slag
ABR009	Gray green	Casting slag
ABR010	Gray green	Casting slag
ABR011	mottled green and red	Casting slag
ABR012	mottled green and red	Casting slag
ABR013	mottled green and red	Casting slag

ABR014	mottled green and red	Casting slag ; Vesicular, slaggy glass-like chunk with corroded copper, copper, and quartz grains present.
ABR016	green-grey	Gritty with corrosion
ABR017	mottled green and red	Casting slag
ABR018	mottled green and red	Vesicular, with corroded copper.
ABR019	mottled green and red	Casting slag
ABR020	mottled green and red	Very vesicular, with high amounts of copper oxides visible on one side. See Figures 75.76.
ABR021	mottled green and red	Slag fragment with dark glassy appearance speckled with copper oxide, copper, and what appear to be quartz grains
ABR022	mottled green and red	Very vesicular, with both copper and copper oxide visible on the surface.
ABR023	green-grey	Less glassy than 021 or 025, and covered in thin ceramic layer. Underneath this layer, dark glassy slag is visible, with some copper oxide apparent.
ABR024	mottled green	glassy w/ corrosion
ABR025	mottled green and red	Very vitrified, with extensive copper corrosion, vesicles and several chunks of quartz grains.

## APPENDIX C

## Photographic Data



Figure 49: ABR001, ABR002, ABR003



Figure 50: ABR004



Figure 51: ABR005



Figure 52: ABR006



Figure 53: ABR007



Figure 54: ABR008



Figure 55:ABR009



Figure 56:ABR010



Figure 57:ABR011



Figure 58:ABR012



Figure 59:ABR013



Figure 60:ABR014





Figure 61:ABR016



Figure 62:ABR017



Figure 63:ABR018



Figure 64:ABR019



Figure 65:ABR020



Figure 66:ABR021





Figure 67:ABR022



Figure 68:ABR023



Figure 69:ABR024



Figure 70:ABR025



Figure 71:ABR027



Figure 72:ABR028



Figure 73:ABR029



Figure 74:AVS901



Figure 75:AVS902



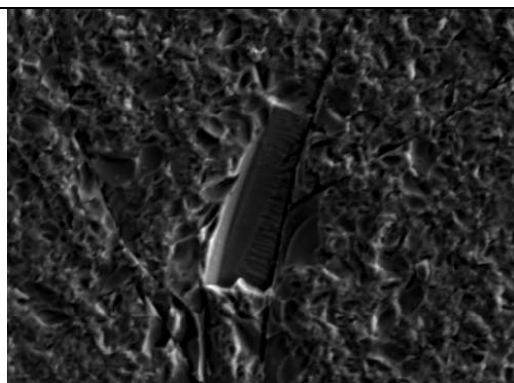
Figure 76:AVS903



Figure 77:AVS905

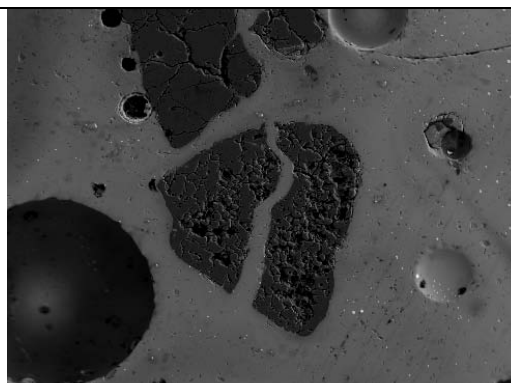


Figure 78:AVS722



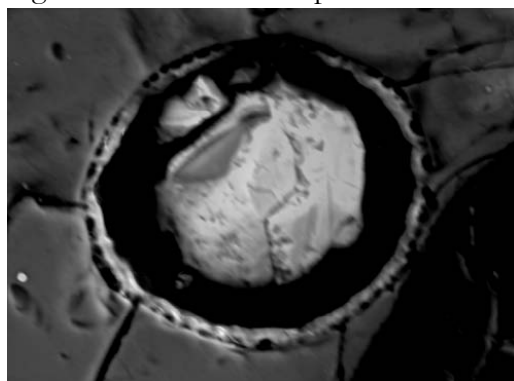
20µm  
BEI SEI combo ABR019 feldspar

Figure 79: ABR019 Feldspar



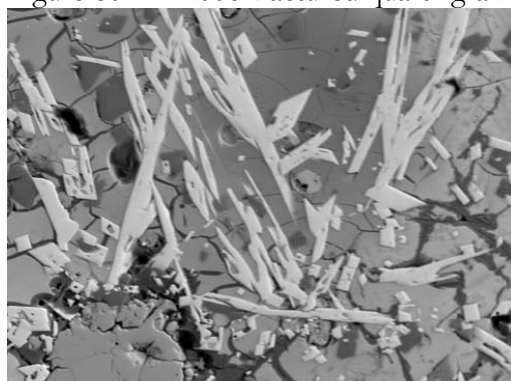
100µm  
SEI BEI composite ABR006 fractured quartz with glassy slag infill

Figure 80: ABR006 fractured quartz grain



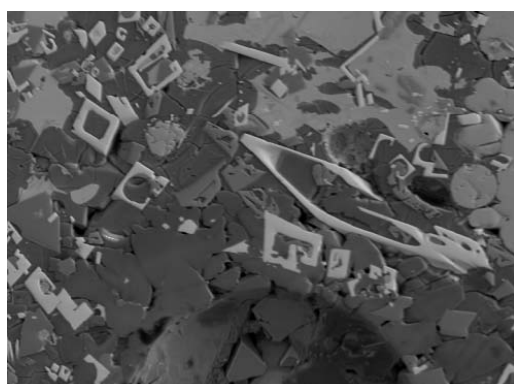
10µm  
SEI BEI composite ABR006 Zircon

Figure 81: ABR006 zircon



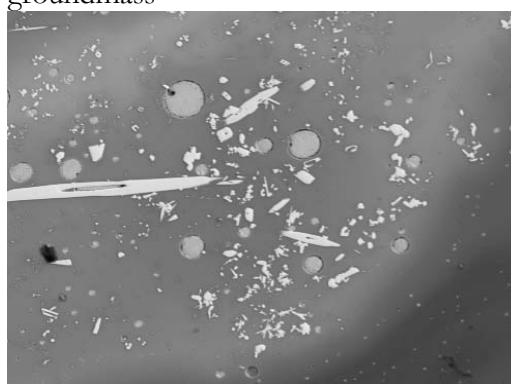
50µm  
SEI BEI combo ABR009 point one Sn dendrites in PbO rich groundmass

Figure 82: ABR009 SnO<sub>2</sub> dendrites in PbO rich groundmass



50µm  
SEI BEI combo ABR009 point four Sn dendrites in Si-Fe-Sn rich groundmass

Figure 83: ABR009 SnO<sub>2</sub> dendrites in SiO<sub>2</sub>-FeO-SnO<sub>2</sub> groundmass



70µm  
SEI BEI combo ABR012 point two Cu prills in Sn-Pb rich groundmass with Sn dendrite

Figure 84: ABR012 SnO<sub>2</sub> in PbO groundmass with Cu prills (round)

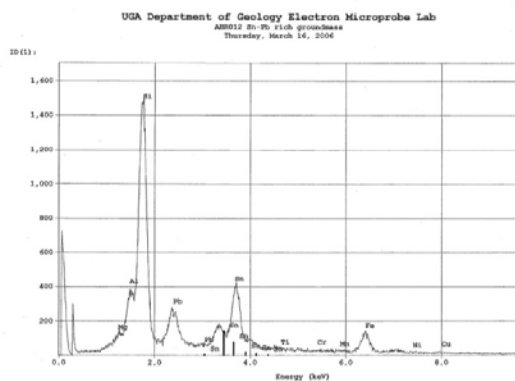
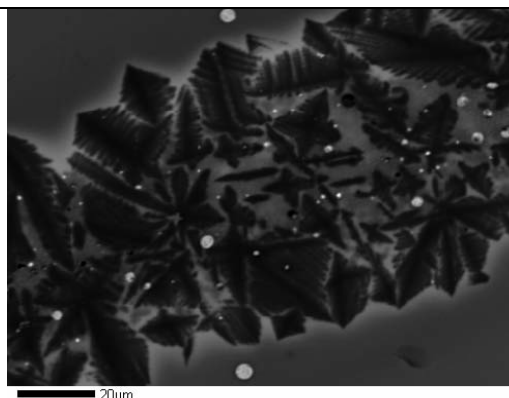
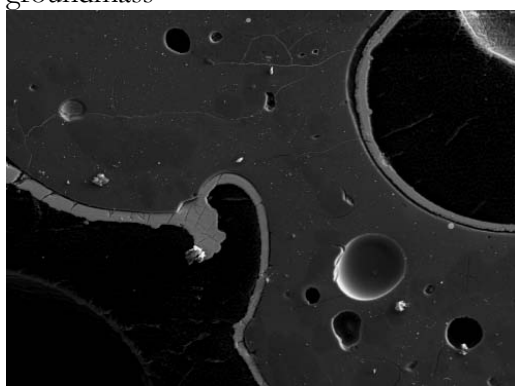


Figure 85: ABR012 SnO<sub>2</sub>-PbO enriched groundmass



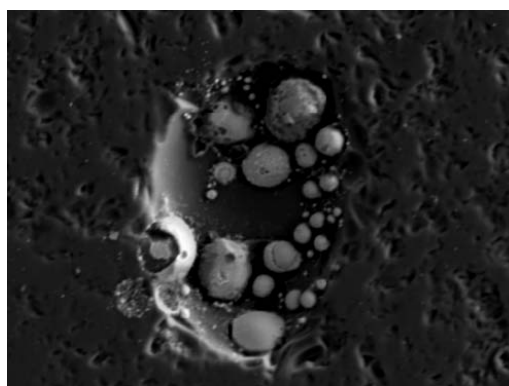
BEI SEI combo ABR004 Quench texture Fe, Sn, Si, Pb

Figure 86: ABR004 fayalite within SnO<sub>2</sub>, PbO silicate groundmass



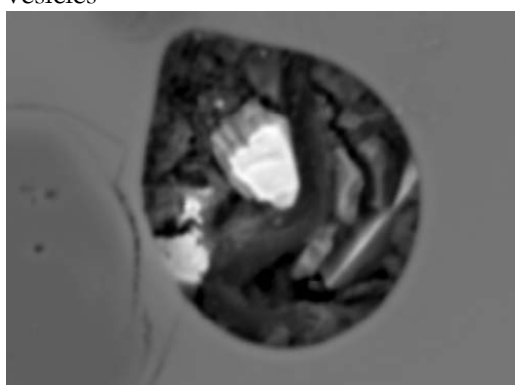
BEI SEI combo ABR008 Fe rim around vesicles

Figure 87: ABR008 FeO rim around vesicles



BEI SEI combo ABR008 Fe prills

Figure 88: ABR008 FeO prills



SEI BEI Combo ABR019 Fe Sulfide 2 grains - possible pyrite

Figure 89: ABR019 possible pyrite

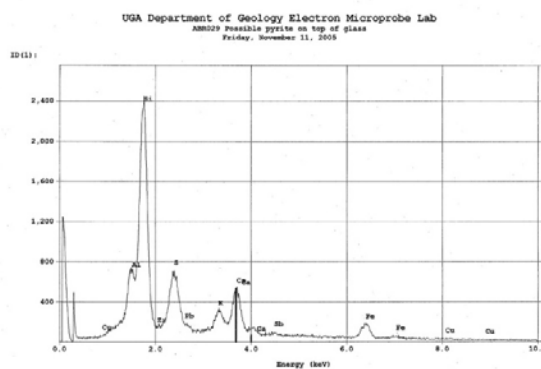
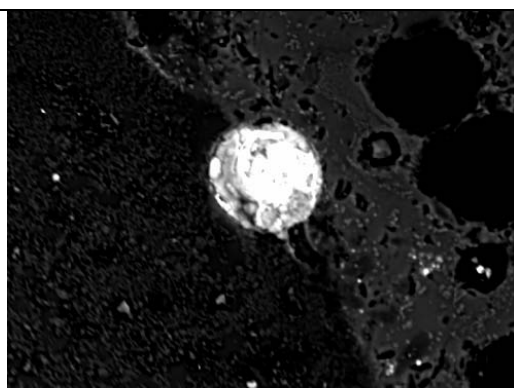


Figure 90: ABR029 pyrite



SEI BEI composite ABR029 possible chalcopyrite

Figure 91: ABR029 Cu-Fe-S inclusion

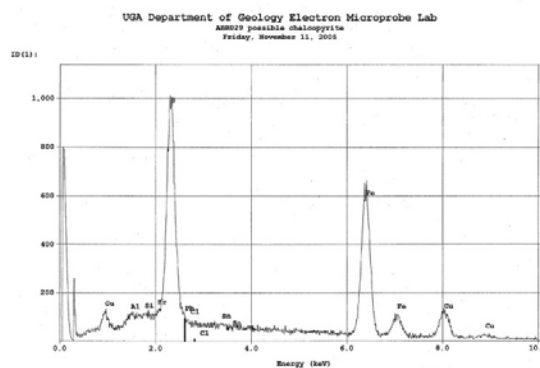
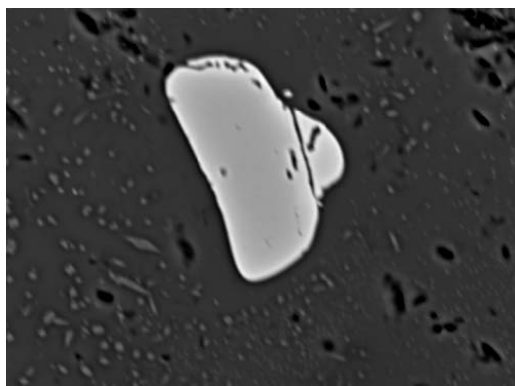


Figure 92: ABR029 chalcopyrite



BEI SEI combo ABR024 chromite - chrome spinel

Figure 93: ABR024 chrome spinel

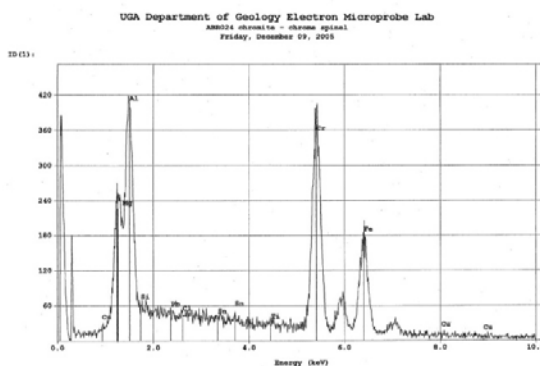
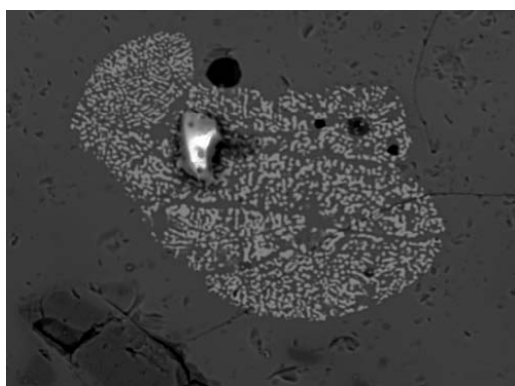


Figure 94: ABR024 chrome spinel



SEI BEI Combo ABR014 Cr spinel nucleation in glass

Figure 95: ABR014 Chrome spinel – like area

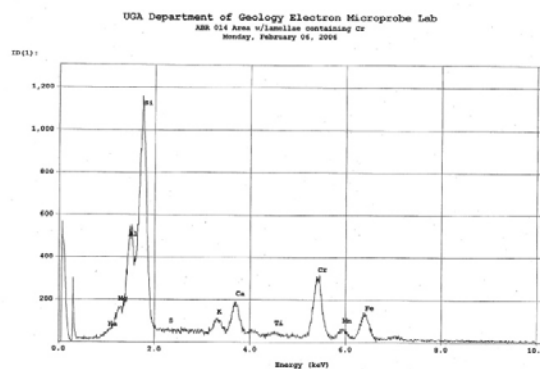
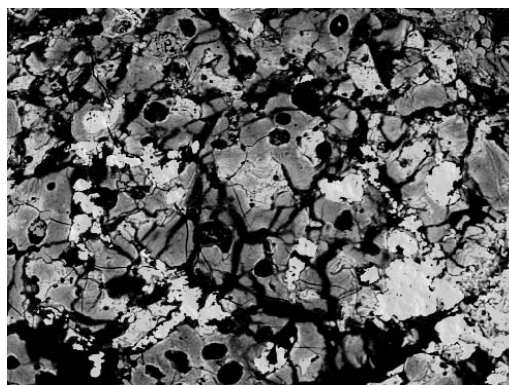


Figure 96: ABR014 Cr phase with anomalous nucleation

**Metal**

BEI Area1 in ABR002 at 400 mag

Figure 97: Cu prills in ABR002



SEI ABR025 leaded bronze and silicate area

Figure 98: ABR025 leaded bronze silicate



## APPENDIX D

## WDS Data

Table 16: Non-normalized data for ceramic portion of AVS722

Pt#	SiO <sub>2</sub>	Al <sub>2</sub> O <sub>3</sub>	FeO	CaO	K <sub>2</sub> O	PbO	SnO <sub>2</sub>	CuO	Na <sub>2</sub> O	Total
16	56.41	21.24	5.4	8.38	2.4531	0.2443	0	0	2.2887	96.4161
20	61.03	19.35	5.36	5.34	2.8922	0.0578	0.012	0	1.6098	95.6518
AVG	58.72	20.295	5.38	6.86	2.6726	0.151	0.006	0	1.94925	
STD	3.266	1.336	0.02	2.149	0.310	0.131	0.008	0	0.480055	
MDL	0.051	0.05	0.173	0.066	0.036	0.243	0.156	0.202	0.051	

Table 17 : Normalized data for ceramic portion of AVS722, minus fayalite analysis

Pt#	SiO <sub>2</sub>	Al <sub>2</sub> O <sub>3</sub>	FeO	CaO	K <sub>2</sub> O	PbO	SnO <sub>2</sub>	CuO	Na <sub>2</sub> O	Total
16	58.51%	22.03%	5.60%	8.69%	2.54%	0.25%	0.00%	0.00%	2.37%	100.00%
20	63.80%	20.23%	5.60%	5.58%	3.02%	0.06%	0.01%	0.00%	1.68%	100.00%
AVG	61.16%	21.13%	5.60%	7.14%	2.78%	0.16%	0.01%	0.00%	2.03%	100.00%
STD	3.75%	1.27%	0.00%	2.20%	0.34%	0.14%	0.01%	0.00%	0.49%	
MDL	0.051	0.05	0.173	0.066	0.036	0.243	0.156	0.202	0.051	

Table 18: Non-normalized data for metals

Label	Pt#	Cu	Sn	Pb	Fe	As	Sb	Total
ABR001	1	81.53	9.93	6.95	0.0122	0	0	98.42
	1	83.47	9.66	5.17	0.0892	0	0	98.39
	2	82.12	10.29	5.12	0.0569	0	0	97.58
	3	2.9337	53.32	13.66	2.4035	0	0	72.32
	4	2.9036	33.2	26.63	6.9	0	0	69.63
	5	0.0117	77.76	0	0.1517	0	0	77.92
	6	0.0194	79.92	0.0478	0.117	0	0	80.1
	7	0.109	76.6	0.0159	0.2038	0	0	76.93
	8	0.1284	80.14	0.1274	0.0823	0	0	80.48
	9	77.84	15.3	2.1352	0.0616	0	0	95.34
	10	23.73	32.33	10.97	0.8726	0	0	67.91
	11	3.54	57.76	6.48	3.55	0	0	71.33
	12	6.31	51.52	17.11	0.322	0	0	75.27
	1	81.17	9.94	5.74	0	0	0	96.84
	2	82.98	9.75	5.83	0	0	0	98.55
	3	2.6773	49.88	14.91	2.7033	0	0	70.17
	4	1.3271	48.98	16.17	3.92	0	0	70.4
	5	0	77.11	0.0478	0.1907	0	0	77.35

Label	Pt#	Cu	Sn	Pb	Fe	As	Sb	Total
	6	0.1205	78.69	0.9075	0.2512	0	0	79.97
	7	0.0662	77.37	0	0.1517	0	0	77.59
	8	0.1595	80.15	0	0.0347	0	0	80.35
	9	81	14.75	1.6907	0.0982	0	0	97.54
	10	84.58	0.0774	0.1163	0.0226	0	0	84.8
	11	1.8754	55.74	11.2	3.42	0	0	72.25
	19	0.3136	6.34	24.67	4.51	0	0.0025	35.84
	20	77.94	10.05	7.56	0.0083	0.1049	0.139	95.8
	21	3.21	58.27	13.25	2.0403	0.0055	0	76.77
	22	59.48	38.37	0	0.087	0.0547	0	98
	23	0.0261	18.45	18.15	2.8529	0.0275	0	39.51
	24	1.493	62.74	6.1	0.0568	0	0	70.39
	12	0.0868	15.94	10.29	2.4932	0	0	28.81
<b>ABR002</b>	14	88.2	0.4645	0.5028	0.606	0	0	89.77
<b>ABR003</b>	16	98.82	1.4286	0.3092	0	0	0	100.56
<b>ABR028</b>	1	90.99	0	0	0.05	0.0909	0	91.15
	2	74.83	6.94	5.65	0.0169	0.0891	0	87.52
	3	37.23	1.6981	10.98	0	0.0431	0	50.02
<b>AVS901</b>	4	82.32	0.0143	0	0.0948	0.1285	0	82.64
	5	84.61	11.31	3.29	0	0.1361	0.041	99.51
	6	87.27	2.784	8.25	0.0886	0.0072	0.0219	98.51
	7	87.62	7.09	1.6784	0.0692	0.0439	0	96.5
	8	81.32	6.79	7.51	0.0477	0.0779	0	95.88
	9	90.88	9.03	0.8737	0.0528	0	0	100.88
	10	79.87	9.86	1.2359	0.0477	0.0725	0.0151	91.25
	11	38.87	2.5153	42.3	0	0.0365	0	83.72
	12	64.72	2.342	23.2	0	0.0228	0.0134	90.38
	13	67.71	1.7812	20.7	0.0339	0	0	90.37
	53	77.39	2.1665	16.47	0.0601	0.0284	0.0961	103.03
	54	84.41	9.83	7.68	0.0478	0.0883	0.0296	106.74
	55	75.82	4.31	17.8	0.0971	0	0	105.91
	56	63.74	3.31	28.21	0.0337	0.0261	0	103.51
	57	93.73	7.2	0.4334	0.0747	0.0274	0	103.55
	58	94.17	8.32	0.4136	0.0403	0	0	104.02
<b>AVS 902</b>	22	96.22	0.0072	0.1947	0.0131	0.0189	0	96.45
	23	96.13	0	0.2655	0	0.0189	0	96.42
	24	72.95	0.0621	0.3717	0	0.0226	0	73.42
	25	98.74	0.0239	0.1947	0.0868	0	0.0391	99.14
	26	95.92	0.0167	0.2655	0	0.0226	0	96.25
	27	97.87	0.0286	0.2301	0.0184	0	0.0391	98.22
<b>AVS903</b>	38	97.7	4.64	0.4571	0.1903	0.02	0	103.03



Label	Pt#	Cu	Sn	Pb	Fe	As	Sb	Total
AVS903	39	90.77	6.66	0.9847	0.1094	0.1107	0	98.68
	40	94.95	5.84	1.1563	0.1031	0.0793	0.0136	102.14
	41	95.67	6.84	1.0786	0.1208	0.0514	0	103.8
	42	99.02	2.6686	1.1208	0.1993	0.06	0	103.15
	43	75.67	3.47	18.55	0.1097	0.0143	0	97.82
	44	88	5.67	5.89	0.1365	0.0614	0.025	99.79
	45	68.36	5.5	21.54	0.1046	0.1139	0	95.69
	46	85.15	7.84	3.31	0.1869	0.0902	0.057	103.49
	47	96.84	4.67	0.9648	0.2415	0	0.0474	103.78
	48	12.12	0.713	79.97	0.0216	0.0069	0.0721	108.24
	49	89.55	5.96	2.7999	0.1692	0.046	0.0887	103.37
	50	88.77	4.77	5.23	0.2091	0.0554	0	112.16
	51	89.72	11.67	0.5984	0.0029	0.1689	0.0872	104.31
	52	89.49	6.7	3.3	0.1366	0.0231	0.0023	102.09
AVS905	14	86.28	5.58	0.6668	0.1426	0.0554	0.0151	92.9
	15	83.58	4.93	0.5269	0.2132	0	0	89.34
	16	73.99	4.23	1.14	0.1232	0.0958	0.0433	79.65
	17	61.44	14.18	5.47	0.0979	0	0.0708	81.27
	18	88.9	6.03	0.4386	0.1426	0.0554	0.0518	95.62
	19	58.8	3.81	0.4387	0.1645	0	0	63.31
	20	72.41	4.51	0.2108	0.0738	0	0.0994	77.35
	21	65.06	6.28	4.86	0.1517	0.0071	0.0976	76.51
	28	90.21	275.95	25.16	0.2281	2.0976	3.09	399.07
	29	89.97	6.94	0.3811	0.1244	0.1274	0	97.66
	30	90.16	6	0.1525	0.2328	0.02	0.0045	96.57
	31	86.42	5.16	0.1718	0.1375	0.084	0.0748	92.2
	32	93.66	5.47	0.1717	0.1946	0	0.0317	99.58
	33	94.3	5.41	0.1907	0.1972	0	0	100.11
	34	83.7	5.78	0.4374	0.1842	0.0636	0.1085	90.3
	35	91.77	7.39	0.3037	0.127	0.0754	0.0474	99.81
	36	46.53	23.49	9.28	0.4388	0.081	0.049	79.88
	37	91.08	5.69	0.1332	0.2203	0	0.0836	97.25

Table 19: Normalized data for metals

Label	Pt#	Cu	Sn	Pb	Fe	As	Sb	Total
ABR001	1	82.84%	10.09%	7.06%	0.01%	0.00%	0.00%	100.00%
	1	84.84%	9.82%	5.25%	0.09%	0.00%	0.00%	100.00%
	2	84.15%	10.54%	5.25%	0.06%	0.00%	0.00%	100.00%
	9	81.65%	16.05%	2.24%	0.06%	0.00%	0.00%	100.00%
	1	83.81%	10.26%	5.93%	0.00%	0.00%	0.00%	100.00%
	2	84.19%	9.89%	5.92%	0.00%	0.00%	0.00%	100.00%
	9	83.04%	15.12%	1.73%	0.10%	0.00%	0.00%	100.00%
	20	81.56%	10.52%	7.91%	0.01%	0.00%	0.00%	100.00%

Label	Pt#	Cu	Sn	Pb	Fe	As	Sb	Total
ABR001	22	60.73%	39.18%	0.00%	0.09%	0.00%	0.00%	100.00%
	AVG	80.76%	14.61%	4.59%	0.05%	0.00%	0.00%	
	SD	7.59%	9.51%	2.65%	0.04%	0.00%	0.00%	
ABR003	16	98.27%	1.42%	0.31%	0.00%	0.00%	0.00%	
	AVG	n/a	n/a	n/a	n/a	n/a	n/a	
	SD	n/a	n/a	n/a	n/a	n/a	n/a	
ABR028	1	99.95%	0.00%	0.00%	0.05%	0.00%	0.00%	100.00%
	AVG	n/a	n/a	n/a	n/a	n/a	n/a	
	SD	n/a	n/a	n/a	n/a	n/a	n/a	
AVS901	5	85.28%	11.40%	3.32%	0.00%	0.00%	0.00%	100.00%
	6	88.70%	2.83%	8.38%	0.09%	0.00%	0.00%	100.00%
	7	90.84%	7.35%	1.74%	0.07%	0.00%	0.00%	100.00%
	8	85.00%	7.10%	7.85%	0.05%	0.00%	0.00%	100.00%
	9	90.13%	8.96%	0.87%	0.05%	0.00%	0.00%	100.00%
	10	87.76%	10.83%	1.36%	0.05%	0.00%	0.00%	100.00%
	12	71.70%	2.59%	25.70%	0.00%	0.00%	0.00%	100.00%
	13	75.05%	1.97%	22.94%	0.04%	0.00%	0.00%	100.00%
	53	80.54%	2.25%	17.14%	0.06%	0.00%	0.00%	100.00%
	54	82.78%	9.64%	7.53%	0.05%	0.00%	0.00%	100.00%
	55	77.35%	4.40%	18.16%	0.10%	0.00%	0.00%	100.00%
	56	66.89%	3.47%	29.60%	0.04%	0.00%	0.00%	100.00%
	57	92.40%	7.10%	0.43%	0.07%	0.00%	0.00%	100.00%
	58	91.48%	8.08%	0.40%	0.04%	0.16%	0.00%	100.00%
AVS902	AVG	83.28%	6.28%	10.39%	0.05%	0.01%	0.00%	
	SD	7.96%	3.32%	10.31%	0.03%	0.04%	0.00%	
	22	99.78%	0.01%	0.20%	0.01%	0.00%	0.00%	100.00%
	23	99.72%	0.00%	0.28%	0.00%	0.00%	0.00%	100.00%
	25	99.69%	0.02%	0.20%	0.09%	0.00%	0.00%	100.00%
	26	99.71%	0.02%	0.28%	0.00%	0.02%	0.00%	100.00%
AVS903	27	99.72%	0.03%	0.23%	0.02%	0.05%	0.00%	100.00%
	AVG	99.72%	0.02%	0.24%	0.02%	0.01%	0.00%	
	SD	0.03%	0.01%	0.04%	0.04%	0.02%	0.00%	
	38	94.87%	4.51%	0.44%	0.18%	0.00%	0.00%	100.00%
	39	92.13%	6.76%	1.00%	0.11%	0.00%	0.00%	100.00%
	40	93.04%	5.72%	1.13%	0.10%	0.12%	0.00%	100.00%
	41	92.25%	6.60%	1.04%	0.12%	0.00%	0.00%	100.00%
	42	96.13%	2.59%	1.09%	0.19%	0.00%	0.00%	100.00%
	43	77.37%	3.55%	18.97%	0.11%	0.00%	0.00%	100.00%
	44	88.86%	5.69%	5.91%	0.14%	0.53%	0.77%	100.00%
	45	71.58%	5.76%	22.55%	0.11%	0.13%	0.00%	100.00%
	46	88.25%	8.13%	3.43%	0.19%	0.00%	0.00%	100.00%
	47	94.28%	4.55%	0.94%	0.24%	0.00%	0.00%	100.00%
	48	13.06%	0.77%	86.15%	0.02%	0.00%	0.00%	100.00%
	49	90.93%	6.05%	2.84%	0.17%	0.00%	0.00%	100.00%
	50	89.69%	4.82%	5.28%	0.21%	0.00%	0.00%	100.00%
	51	87.97%	11.44%	0.59%	0.00%	0.00%	0.00%	100.00%
	52	89.83%	6.73%	3.31%	0.14%	0.00%	0.00%	100.00%
	AVG	84.02%	5.58%	10.31%	0.14%	0.05%	0.05%	
	SD	20.68%	2.45%	22.03%	0.07%	0.14%	0.20%	

Label	Pt#	Cu	Sn	Pb	Fe	As	Sb	Total
AVS905	14	93.11%	6.02%	0.72%	0.15%	0.00%	0.00%	100.00%
	18	93.08%	6.31%	0.46%	0.15%	0.00%	0.00%	100.00%
	29	92.36%	7.12%	0.39%	0.13%	0.00%	0.00%	100.00%
	30	93.39%	6.21%	0.16%	0.24%	0.10%	0.00%	100.00%
	31	94.05%	5.62%	0.19%	0.15%	0.00%	0.00%	100.00%
	32	94.13%	5.50%	0.17%	0.20%	0.00%	0.00%	100.00%
	33	94.21%	5.40%	0.19%	0.20%	0.00%	0.00%	100.00%
	34	92.90%	6.41%	0.49%	0.20%	0.00%	0.00%	100.00%
	35	92.15%	7.42%	0.30%	0.13%	0.00%	0.00%	100.00%
	37	93.78%	5.86%	0.14%	0.23%	0.00%	0.00%	100.00%
AVG		93.32%	6.19%	0.32%	0.18%	0.01%	0.00%	
SD		0.73%	0.67%	0.19%	0.04%	0.03%	0.00%	
MDL		0.15	0.10	0.32	0.11	0.09	0.11	

Table 20: Non-normalized data for groundmass

	Pt#	SiO <sub>2</sub>	Al <sub>2</sub> O <sub>3</sub>	FeO	CaO	K <sub>2</sub> O	PbO	SnO <sub>2</sub>	CuO	Total
ABR001	25	36.31	9.92	4.39	3.81	3.18	16.83	23.8	0.006	99.58
	27	38.59	8.18	6.87	13.14	1.8968	19.5	5.74	0.1482	95.03
	28	37.82	8.52	5.59	7.04	2.2834	25.33	6.82	0.0841	94.62
	28	37.82	8.52	5.59	7.04	2.2834	25.33	6.82	0.0841	94.62
ABR002	13	40.36	7.14	9.63	9.91	1.8067	20.51	2.7151	0.209	92.28
	25	36.31	9.92	4.39	3.81	3.18	16.83	23.8	0.006	99.58
	27	38.59	8.18	6.87	13.14	1.8968	19.5	5.74	0.1482	95.03
	28	37.82	8.52	5.59	7.04	2.2834	25.33	6.82	0.0841	94.62
	1	49.19	10.1	4.85	9.24	3.93	11.13	4.64	1.2757	95.99
	2	43.38	8.77	6.73	9.89	2.8028	17.21	4.7	0.4509	95.08
	3	39.85	8.48	6.84	9.17	2.9991	21.21	5.62	0.276	95.61
	4	44.82	8.97	6.74	9.29	3.37	16.55	4.33	0.4216	95.85
	5	45.63	8.46	5.41	8.99	3.28	16.21	5.44	0.2829	95.17
ABR003	1	67.15	19.42	0	0.7808	8.15	0.1103	0	1.099	99.76
	2	53.9	12.02	4.96	6.58	4.92	3.94	1.4236	6.65	96.12
	3	54.44	7.5	6.34	11.75	3.14	4.24	3.47	5.9	98.39
	1	68.28	19.02	0	12.07	6.38	0.1551	0	1.6773	110.08
	5	52.06	7.14	12.99	18.83	2.7734	0.1812	0.4252	0.0134	95.8
	6	66.64	18.86	0.0815	0.3104	9.89	0.1254	0	1.7742	101.13
	7	54.45	9.89	5.89	11.03	3.6	3.52	2.073	2.6963	95.29
	8	66.22	19.55	1.1365	1.4387	7.1	0.2671	0	0.6806	99.81
	9	60.52	7.5	4.23	4.55	2.4436	10.96	4.82	0.1473	96.24
	10	64.49	9.66	2.6271	2.4322	3.13	11.15	4.32	0.456	99.4
	11	59.41	5.53	5.88	6.06	1.911	11.25	4.71	0.6063	96.6
	8	80.14	3.29	3.08	3.11	1.5142	2.9805	0.6513	1.8665	97.22
	11	51.87	7.01	12.67	16.7	3.37	1.6494	1.171	0.7404	96.83

	Pt#	SiO <sub>2</sub>	Al <sub>2</sub> O <sub>3</sub>	FeO	CaO	K <sub>2</sub> O	PbO	SnO <sub>2</sub>	CuO	Total
<b>ABR003</b>	17	53.85	7.24	11.66	14.71	2.3655	2.3119	0.7853	0	92.92
<b>ABR004</b>	56	48.61	9.45	10.62	11.72	2.535	8.66	3	0.0835	97.93
	57	48.39	9.81	7.88	10.99	2.5171	11.24	3.6	0.3291	97.94
	58	45.04	8.59	13.18	10.17	2.2071	12.72	3.9	0	98.71
	59	44.67	8.5	15.04	10.72	2.2615	11.08	2.8704	0.2247	98.37
	60	46.79	8.73	12.82	10.05	2.4745	12.02	3.57	0.1751	99.44
	61	44.22	8.12	14.73	9.76	2.2056	13.94	4.41	0.1593	100.35
	62	45.22	8.59	13.97	10.39	2.2443	11.68	4.54	0.3915	99.72
	63	46.33	8.69	14.83	11.16	2.3976	10.23	2.8396	0.0495	99.71
<b>ABR005</b>	42	51.8	9.46	9.71	17.24	2.1016	3.66	1.9226	0.2197	99.65
	44	54.4	10.51	8.77	14.87	2.3464	2.6347	1.4561	0.2928	98.9
	45	52.21	8.51	8.08	20.11	2.6611	3.03	2.3528	0.2345	100.5
	46	44.57	8.15	14.52	20.07	1.6209	6	1.9493	0.1327	100.17
	47	52.02	9.55	8.82	18.92	2.6543	2.2616	1.603	0.0357	99.41
	48	59.3	10.2	6.4	11.28	3.68	3.82	2.5367	0	100.55
	49	50.65	9.17	14.66	11.09	2.6955	7.27	1.9028	0.0764	100.75
	50	62.93	12.24	4.57	8.13	3.25	4.31	1.477	0.2916	100.36
	51	63.3	11.95	4.62	7.91	3.18	3.89	1.6506	0.2076	100.27
	52	65.35	8.93	5.24	9.36	3.27	3.33	1.6346	0.2626	100.22
	54	41.54	9.36	6.34	11.62	2.0757	3.54	1.5767	0.3642	79.96
	55	54.29	10.84	7.33	13.66	2.6062	4.47	1.6812	0.2367	98.82
<b>ABR006</b>	30	53.4	8.76	12.9	10.92	2.3606	5.75	1.905	0.65	99.67
	31	66.84	8.5	5.82	4.81	3.9	3.93	2.888	0.3327	99.38
	32	64.38	21.16	1.329	4.03	7.61	0.2014	0.0126	0.2417	103.26
	33	64.5	14.63	2.7777	10.23	4.26	0.0143	0	0	100.64
	34	61.7	10.52	5.93	6.28	3.89	6.64	1.7692	0.2873	100.34
	35	60.47	13.41	4.29	4.89	4.71	4.49	0.9722	0.7018	98.48
	36	55.91	9.14	14.47	11.2	2.3974	2.3791	0.9154	0.1938	100.04
	37	56.76	10.16	10.24	11.43	2.7957	2.4008	1.1275	0.1701	98.7
<b>ABR007</b>	14	49.09	9.49	11.83	17.25	1.9382	2.7381	1.2614	0.217	97.49
	15	48.44	9.63	10.19	9.54	2.6625	7.37	4.17	2.1386	97.49
<b>ABR008</b>	22	50.76	10.86	8.7	12.8	2.8829	2.0714	5.36	0.7813	98.07
	23	54.32	11.34	7.36	12.01	3.24	2.0994	5.31	0.5648	100.23
	24	57.13	13.57	4.96	10.57	3.74	2.3945	4.67	0.1443	100.49
	26	74.61	16.97	0.5499	0.9002	2.3955	0	0	0.1142	98.94
	27	69.82	20.13	0.565	1.2052	2.3405	0	0.0095	0	98.02
	1	47.48	10.64	5.94	14.52	3.3	8.82	1.7247	1.4085	98.05
	2	55.29	13.93	7.74	8.93	1.79	2.4599	4.11	0.0776	98.71
	3	55.67	14.01	5.7	8.71	2.7511	2.3385	3.81	0.9502	98.4

	Pt#	SiO <sub>2</sub>	Al <sub>2</sub> O <sub>3</sub>	FeO	CaO	K <sub>2</sub> O	PbO	SnO <sub>2</sub>	CuO	Total
<b>ABR008</b>	4	98.41	1.2859	0.0074	0.0644	0.0965	0	0.0678	0.0248	100.09
	5	46.03	9.28	7.44	17.98	3.71	6.71	2.6648	0.1347	98.26
	6	43.6	7.98	6.98	13.48	2.1004	11.4	6.81	0.2664	95.98
	7	32.49	7.3	3.54	5.8	1.9029	7.15	4.11	41.38	106.22
	8	12.61	1.6848	0.9759	0.4422	0.1445	2.1588	5.34	88.63	112.8
	9	41.06	8.87	6.61	9.8	2.4557	12.73	5.54	0.5293	90.94
<b>ABR009</b>	21	35.17	6.24	25.04	22.02	0.0388	1.9865	3.21	0.1377	97.29
	22	60.92	17.59	4.75	7.1	4.76	0.0578	0.0308	0.0934	100.47
	23	61.06	17.92	4.52	7.23	4.37	0	0.0893	0.0561	99.74
	25	60.66	16.29	4.95	7.01	5.33	0.1153	0.1413	0.1553	99.47
<b>ABR010</b>	29	48.72	10.04	6.35	8.11	2.7632	11.63	5.61	2.4886	99.19
	30	47.69	9.56	6.11	8.97	2.2507	13.79	6.46	0.3469	98.93
	31	49.08	9.99	5.99	8.84	2.7857	13.31	6.09	0.3744	99.99
	32	49.41	10.09	5.75	8.32	2.6661	12.44	5.79	0.1978	98.07
	33	62.35	17.42	0.555	3.31	4.74	3.01	1.3739	0.6911	95.94
	34	52.54	10.7	4.95	8.97	3.22	8.35	4.98	0.3833	97.52
	35	52.47	12.34	4.68	3.87	2.9427	14.62	3.24	0.5133	98.29
	33	56.77	16.36	5.68	5.56	3.14	0.24	0	0.1504	94.44
	16	59.29	15.75	5.27	4.96	5.15	0.0323	0.0126	0.1159	97.71
	17	63.74	15.59	5.12	5	3.74	0.0486	0.1012	0.0362	99.31
	19	46.77	8.39	7.37	32.27	2.0706	0.263	0.3588	0	100.72
<b>ABR011</b>										
<b>ABR012</b>	14	51.4	10.44	7.04	12.37	3.64	7.3	2.5702	0.1464	98.84
	15	47.87	8.75	9.49	10.46	2.5176	11.21	5.07	0.2659	99.13
	16	45.21	8.05	7.38	7.18	2.6294	18.3	5.83	0.5232	97.57
	17	43.93	8	5.33	7.2	2.6872	17.84	2.0294	6.92	96.89
	18	58.67	11.38	5.22	10.01	3.87	4.6	2.309	0.2123	99.34
	56	46.06	9.33	8.94	10.87	2.4908	13.31	3.79	0.8162	99.09
	58	50.31	10.13	8.45	13.25	2.9526	7.19	2.7963	0.2985	99.13
	60	61.8	9.73	5.24	10.58	3.44	3.85	2.4168	0.3166	100.25
	61	47.02	8.87	3.79	7.8	2.9116	19.41	1.3191	5.19	99.43
	62	49.73	10.43	7.81	13.04	3.42	6.93	2.9028	0.1434	98
	63	49.1	10.74	7.4	13.19	3.24	7.53	3.23	0.4642	98.45
	64	49.06	10.16	7.1	12.1	3.17	7.38	2.7842	3.53	99.19
	65	59.57	10.68	4.79	9.76	4.28	4.23	1.7831	0.2493	98.8
	66	42.95	9.71	7.03	10.41	2.4531	20.16	3.58	0.8901	100.03
	67	59.29	12.91	5	7.85	4.12	4.91	1.9777	0.4728	100.34
	69	44.24	9.74	12.29	11.99	2.5063	11.98	3.13	0.1687	99.24
	70	44.78	9.44	12.02	12.55	2.5871	11.54	2.945	0.2741	99.59
	71	43.92	9.7	13.21	13.02	2.7532	10.31	2.3588	0.1642	99.16

	Pt#	SiO <sub>2</sub>	Al <sub>2</sub> O <sub>3</sub>	FeO	CaO	K <sub>2</sub> O	PbO	SnO <sub>2</sub>	CuO	Total
<b>ABR012</b>	72	44	8.36	8.58	8.68	2.1451	19.25	5.01	0.4279	99.29
<b>ABR013</b>	16	45.17	7.68	5.9	6.44	2.1297	24.83	5.31	2.4855	102.28
	17	47.16	10.22	11.76	12.43	2.9736	8.49	2.4096	0.315	99.66
	18	51.64	9.78	9.42	13.14	3.25	6.49	2.1107	0.3512	100.17
	19	43.18	9.24	10.47	10	2.399	17.07	4.44	0.2224	100.18
	20	41.96	9.17	5.6	7.31	1.3368	29.65	1.8781	0.5686	100.43
<b>ABR014</b>	50	63.6	19	4.38	3.52	3.98	0.0159	0.0471	0.0818	99.47
	52	60.57	19.12	5.93	5.28	3.72	0.0159	0.0125	0.2641	100.31
	53	63.25	14.57	4.98	7.86	4.07	0.0316	0.1629	0.2077	99.63
	54	66.82	16.15	4.31	3.27	4.15	0.1276	0	0.0504	99.49
	55	63.84	18.2	5.41	4.02	3.52	0.1432	0	0.1825	100.29
	1	57.42	14.8	6.5	12.68	2.2703	0.0565	0.0965	0.1345	99.25
	2	63.68	17.91	4.58	5.03	3.45	0.1294	0.0031	0.1909	99.24
	3	56.57	13.6	5.76	13.64	2.7647	0.3533	0.1815	1.0597	99.43
	4	65.74	16.68	4.74	3.65	3.81	0.0144	0	0.1913	99.09
	5	62.64	15.4	4.81	7.59	3.98	0.0726	0.1422	0.1436	99.75
<b>ABR016</b>	6	44.49	11.33	7.6	2.4672	2.0378	9.47	2.3833	16.68	100.01
	7	51.78	17.52	9.39	2.1944	2.7774	4.1	1.1089	3.55	96.81
	8	54.3	17.53	8.25	2.2002	2.6777	3.74	0.8633	3.93	97.59
	9	53.84	10.33	4.64	1.7445	2.3395	14.9	6.97	2.0338	99.13
	14	51.16	10.22	4.39	1.8314	2.2684	17.89	6.88	0.9085	98.06
	16	38.13	23.26	12.43	24.11	0	0	0	0.0555	98.06
<b>ABR017</b>	12	43.31	8.31	19.63	14.35	2.6575	3.83	2.7162	0.026	98.84
	13	39.31	7.74	20.57	13.28	2.4931	7.32	4.55	0.2611	99.27
	14	62.55	17.44	5.02	5.84	3.57	0.0323	0	0	99.35
	15	62.68	16.65	3.27	7.9	5.11	0.3052	0.0714	0.4124	100.64
<b>ABR018</b>	25	62.37	20.93	5.74	1.6815	4.09	0.0727	0.0159	0.0187	100.71
	26	50.61	16.09	4.91	18.55	1.8743	0.0566	0.0031	0.124	98.77
	27	55.06	22.07	6.11	2.0775	3.64	0	0.0158	0.118	94.26
	28	56.87	18.34	5.18	2.7582	4.04	0.1159	0	0	92.06
	29	54.95	27.78	1.7497	7.74	2.0457	0.0578	0	0.0685	99.02
<b>ABR019</b>	36	57	19.53	6.64	5.84	2.7853	0.1686	0	0.829	98.08
	37	59.53	14.66	4.58	12.66	1.8841	0.1981	0	0.8512	98.24
	38	54.85	19.21	6.75	6.52	2.3945	0	0.0216	2.5317	97.48
	39	65.98	14.51	3.9	4.54	2.864	0.1393	0.0062	0.6425	96.66
	40	57.63	18.38	6.77	6.16	2.5687	0	0.0185	0.4083	97.25
	41	59.2	18.42	6.65	5.17	2.7833	0	0	0.0634	97.66
	42	57.45	17.8	6.69	6.26	2.2883	0.2149	0	0	95.93
	18	57.77	11.27	4.39	19.86	1.6597	0	0	0	98.84

	Pt#	SiO <sub>2</sub>	Al <sub>2</sub> O <sub>3</sub>	FeO	CaO	K <sub>2</sub> O	PbO	SnO <sub>2</sub>	CuO	Total
<b>ABR019</b>	19	42.1	6.34	3.82	10.54	1.0079	26	1.0041	0.6514	94.02
	20	66.33	16.62	5.77	4.96	3.1	0.0162	0.0442	0.0722	102.54
	21	61.95	12.9	3.73	7.06	3.46	0.0805	0.0221	0	95.87
<b>ABR020</b>	8	60.56	19.22	7	2.6986	3.49	1.3862	0.2754	0.7656	100.22
	9	51.73	9.91	10.67	8.32	3.24	10.27	1.2404	0.9494	99.7
	10	44.99	9.04	9.81	9.43	3.14	13.64	3.58	1.6369	98.97
	11	49.6	9.47	11.63	8.22	2.3462	9.59	3.41	1.1436	99.06
<b>ABR021</b>	10	56.82	13.88	5.4	12.58	2.9853	0.6213	0.9591	1.0833	99.51
	11	58.12	14.83	5.18	11.94	2.8397	0.343	0.4182	1.2986	100
	12	62.99	18.69	4.38	5.12	3.7	0.0948	0	0.2319	100.01
	14	61.5	17.33	4.87	5.47	4.08	0.3148	0.163	0.6445	99.4
	15	58.69	18.17	6.88	5.54	2.8408	0	0	0.058	97.63
<b>ABR022</b>	9	53.13	13.82	5.25	9.25	3.19	5.24	1.4124	3.37	98.65
<b>ABR022</b>	10	49.25	12.63	5.19	7.81	2.7039	8.6	2.2004	5.13	97.11
	11	50.53	9.72	5.7	8.22	2.5654	9.4	6.94	1.5789	97.64
	13	45.26	8.69	4.82	6.01	2.0151	17.48	0.4927	9.22	97
<b>ABR023</b>	22	56.36	14.7	6.6	8.5	3.39	3.9	2.4229	0.3093	100.57
	23	56.27	15.65	7.2	8.97	3.32	2.2342	0.9702	0.0924	99.31
	24	43.93	10.87	14.89	11.41	2.5895	5.49	4.02	0.3714	97.23
	25	52.16	13.14	11.14	9.14	2.9924	4.75	1.1855	0.2238	98.84
	26	36.92	4.26	7.31	7.07	8.23	1.8322	1.0677	1.1665	95.59
	27	50.45	9.78	15.7	12.68	2.2941	4.08	2.0261	0.2157	101.03
	28	42.03	11.33	17.52	11.4	1.9453	5.99	1.8089	0.2748	95.71
	29	50.76	12.32	12.83	11.34	3.24	4.33	1.0794	0.1186	99.94
	30	57.5	10.88	9.9	8.78	3.78	4.42	1.9958	0.0628	100.55
<b>ABR024</b>	31	55.02	13.68	9.77	9.9	3.38	0.4273	0.0528	0.0071	98.09
	32	50.1	12.58	18.11	8.21	2.6866	0.4709	0.0583	0.0142	96.2
	43	53.07	23.2	3.62	12.87	0.7506	0.1374	0.0525	0.0775	98.33
	44	58.92	19.07	6.03	3.49	3.46	0.1233	0	0.2255	96.33
	45	62.94	17.9	5.5	2.7761	3.15	0.0774	0	0.0353	96.87
	46	69.08	14.76	3.49	2.0209	3.44	0.0934	0.0655	0.2052	96.82
	47	64.59	18.44	3.97	2.8396	3.67	0.1237	0.0155	0.0564	98.25
	48	54.11	14.8	9.51	10.49	3.47	0.2116	0.1958	0.0979	96.64
<b>ABR025</b>	1	50.21	9.84	14.45	14.66	2.3997	1.7217	1.3844	0.1294	98.87
	2	61.83	12.21	5.25	11.92	2.8099	0.3947	1.8411	0.1132	100.27
	3	58.12	12.09	6.5	13.05	2.8199	0.7574	1.4955	0.4469	99.66
	4	42.7	7.44	8.59	18.22	1.7876	10.87	2.421	1.2238	97.19
	5	64.9	14.41	3.64	10.32	3.58	0.1282	0.0543	0	101.23
<b>ABR028</b>	24	56.25	9.75	7.51	7.68	4.77	0.0622	0.0092	0	90.67

	Pt#	SiO <sub>2</sub>	Al <sub>2</sub> O <sub>3</sub>	FeO	CaO	K <sub>2</sub> O	PbO	SnO <sub>2</sub>	CuO	Total
<b>ABR028</b>	25	59.96	15.79	5.23	8.65	3.04	0.0939	0.031	0	98.18
	26	60.22	17.89	4.56	10.69	2.7983	0.0781	0.0124	0	100.67
	27	51.99	29.76	1.4252	16.21	1.0162	0.0467	0	0	103.34
	28	61.59	15.09	5.54	8.06	4.14	0.1095	0.0186	0	99.2
<b>ABR029</b>	20	68.82	19.25	0.0805	0.043	12.67	0.0434	0	0.0499	103.38
	21	69.77	20.73	0.0367	1.7185	1.2232	0	0	0	102.95
	22	65.95	18.71	0.2263	0.0352	16.62	0.043	0.0221	0	102.88
	23	66.92	21.19	0.3002	2.4737	3.82	0	0.0639	0	101.53
	2	67.45	20.24	1.6463	3.62	3.41	0	0	0.05	100.4
	3	63.9	17.99	6.81	2.286	4.06	0.0146	0	0.1308	99.61
	4	65.38	18.69	3.59	1.5637	4.56	0.0587	0	0	97.41
	5	30.47	38.51	13	0.8135	1.2597	0.1443	0	0.2092	93.45
	6	60.57	12.97	5.61	6.28	3.67	0.058	0.0481	0	94.36
<b>ABR029</b>	7	51.55	14.66	7.26	7	2.8822	0	0.006	0.167	89.07
<b>ABS905</b>	37	47.43	17.67	15.18	3.73	2.9907	0.5064	0.0333	0	98.49
	38	64.35	19.1	0.1869	0.5988	12.76	0	0	0	99.25
	39	50.42	20.5	6.73	7.39	1.8038	0.4482	0	0	96.71
	40	86.4	15.49	0.4123	0.3419	0.2853	0.1442	0.0188	0.2069	103.55

Table 21: Normalized data for slag minus null oxides

Label	Pt#	SiO <sub>2</sub>	Al <sub>2</sub> O <sub>3</sub>	Fe <sub>2</sub> O <sub>3</sub>	CaO	K <sub>2</sub> O	PbO	SnO <sub>2</sub>	CuO	Total
<b>ABR001</b>	25	36.96%	10.10%	4.47%	3.88%	3.24%	17.13%	24.22%	0.01%	100.00%
	27	41.02%	8.70%	7.30%	13.97%	2.02%	20.73%	6.10%	0.16%	100.00%
	28	40.45%	9.11%	5.98%	7.53%	2.44%	27.09%	7.30%	0.09%	100.00%
	<b>Avg.</b>	<b>39.48%</b>	<b>9.30%</b>	<b>5.92%</b>	<b>8.46%</b>	<b>2.57%</b>	<b>21.65%</b>	<b>12.54%</b>	<b>0.08%</b>	
	<b>S.D.</b>	<b>2.20%</b>	<b>0.72%</b>	<b>1.42%</b>	<b>5.11%</b>	<b>0.62%</b>	<b>5.05%</b>	<b>10.14%</b>	<b>0.08%</b>	
<b>ABR002</b>	13	43.74%	7.74%	10.44%	10.74%	1.96%	22.23%	2.94%	0.23%	100.00%
	25	36.96%	10.10%	4.47%	3.88%	3.24%	17.13%	24.22%	0.01%	100.00%
	27	41.02%	8.70%	7.30%	13.97%	2.02%	20.73%	6.10%	0.16%	100.00%
	28	40.45%	9.11%	5.98%	7.53%	2.44%	27.09%	7.30%	0.09%	100.00%
	1	52.13%	10.70%	5.14%	9.79%	4.17%	11.80%	4.92%	1.35%	100.00%
	2	46.18%	9.34%	7.16%	10.53%	2.98%	18.32%	5.00%	0.48%	100.00%
	3	42.19%	8.98%	7.24%	9.71%	3.18%	22.46%	5.95%	0.29%	100.00%
<b>ABR002</b>	4	47.43%	9.49%	7.13%	9.83%	3.57%	17.51%	4.58%	0.45%	100.00%
	5	48.70%	9.03%	5.77%	9.59%	3.50%	17.30%	5.81%	0.30%	100.00%
	<b>Avg.</b>	<b>44.31%</b>	<b>9.24%</b>	<b>6.74%</b>	<b>9.51%</b>	<b>3.00%</b>	<b>19.40%</b>	<b>7.42%</b>	<b>0.37%</b>	
	<b>S.D.</b>	<b>4.72%</b>	<b>0.84%</b>	<b>1.72%</b>	<b>2.70%</b>	<b>0.74%</b>	<b>4.34%</b>	<b>6.41%</b>	<b>0.40%</b>	
<b>ABR003</b>	1	69.43%	20.08%	0.00%	0.81%	8.43%	0.11%	0.00%	1.14%	100.00%
	2	57.10%	12.73%	5.25%	6.97%	5.21%	4.17%	1.51%	7.04%	100.00%



Label	Pt#	SiO <sub>2</sub>	Al <sub>2</sub> O <sub>3</sub>	Fe <sub>2</sub> O <sub>3</sub>	CaO	K <sub>2</sub> O	PbO	SnO <sub>2</sub>	CuO	Total
ABR003	3	56.25%	7.75%	6.55%	12.14%	3.24%	4.38%	3.59%	6.10%	100.00%
	1	63.47%	17.68%	0.00%	11.22%	5.93%	0.14%	0.00%	1.56%	100.00%
	5	55.14%	7.56%	13.76%	19.94%	2.94%	0.19%	0.45%	0.01%	100.00%
	6	68.22%	19.31%	0.08%	0.32%	10.12%	0.13%	0.00%	1.82%	100.00%
	7	58.45%	10.62%	6.32%	11.84%	3.86%	3.78%	2.23%	2.89%	100.00%
	8	68.70%	20.28%	1.18%	1.49%	7.37%	0.28%	0.00%	0.71%	100.00%
	9	63.59%	7.88%	4.44%	4.78%	2.57%	11.52%	5.06%	0.15%	100.00%
	10	65.63%	9.83%	2.67%	2.48%	3.19%	11.35%	4.40%	0.46%	100.00%
	11	62.30%	5.80%	6.17%	6.36%	2.00%	11.80%	4.94%	0.64%	100.00%
	8	82.93%	3.40%	3.19%	3.22%	1.57%	3.08%	0.67%	1.93%	100.00%
	11	54.50%	7.36%	13.31%	17.55%	3.54%	1.73%	1.23%	0.78%	100.00%
	17	57.95%	7.79%	12.55%	15.83%	2.55%	2.49%	0.85%	0.00%	100.00%
	<b>Avg.</b>	<b>63.12%</b>	<b>11.29%</b>	<b>5.39%</b>	<b>8.21%</b>	<b>4.47%</b>	<b>3.94%</b>	<b>1.78%</b>	<b>1.80%</b>	
	<b>S.D.</b>	<b>7.68%</b>	<b>5.72%</b>	<b>4.84%</b>	<b>6.55%</b>	<b>2.59%</b>	<b>4.41%</b>	<b>1.92%</b>	<b>2.19%</b>	
ABR004	56	51.34%	9.98%	11.22%	12.38%	2.68%	9.15%	3.17%	0.09%	100.00%
	57	51.07%	10.35%	8.32%	11.60%	2.66%	11.86%	3.80%	0.35%	100.00%
	58	47.01%	8.97%	13.76%	10.62%	2.30%	13.28%	4.07%	0.00%	100.00%
	59	46.84%	8.91%	15.77%	11.24%	2.37%	11.62%	3.01%	0.24%	100.00%
	60	48.42%	9.03%	13.27%	10.40%	2.56%	12.44%	3.69%	0.18%	100.00%
	61	45.33%	8.32%	15.10%	10.01%	2.26%	14.29%	4.52%	0.16%	100.00%
	62	46.61%	8.85%	14.40%	10.71%	2.31%	12.04%	4.68%	0.40%	100.00%
	63	48.00%	9.00%	15.36%	11.56%	2.48%	10.60%	2.94%	0.05%	100.00%
	<b>Avg.</b>	<b>48.08%</b>	<b>9.18%</b>	<b>13.40%</b>	<b>11.06%</b>	<b>2.45%</b>	<b>11.91%</b>	<b>3.74%</b>	<b>0.18%</b>	
	<b>S.D.</b>	<b>2.14%</b>	<b>0.66%</b>	<b>2.51%</b>	<b>0.77%</b>	<b>0.16%</b>	<b>1.57%</b>	<b>0.67%</b>	<b>0.14%</b>	
ABR005	42	53.89%	9.84%	10.10%	17.94%	2.19%	3.81%	2.00%	0.23%	100.00%
	44	57.09%	11.03%	9.20%	15.61%	2.46%	2.77%	1.53%	0.31%	100.00%
	45	53.72%	8.76%	8.31%	20.69%	2.74%	3.12%	2.42%	0.24%	100.00%
	46	45.94%	8.40%	14.97%	20.69%	1.67%	6.18%	2.01%	0.14%	100.00%
	47	54.26%	9.96%	9.20%	19.74%	2.77%	2.36%	1.67%	0.04%	100.00%
	48	61.00%	10.49%	6.58%	11.60%	3.79%	3.93%	2.61%	0.00%	100.00%
	49	51.94%	9.40%	15.03%	11.37%	2.76%	7.46%	1.95%	0.08%	100.00%
	50	64.74%	12.59%	4.70%	8.36%	3.34%	4.43%	1.52%	0.30%	100.00%
	51	65.45%	12.36%	4.78%	8.18%	3.29%	4.02%	1.71%	0.21%	100.00%
	52	67.11%	9.17%	5.38%	9.61%	3.36%	3.42%	1.68%	0.27%	100.00%
	54	54.36%	12.25%	8.30%	15.21%	2.72%	4.63%	2.06%	0.48%	100.00%
	55	57.08%	11.40%	7.71%	14.36%	2.74%	4.70%	1.77%	0.25%	100.00%
	<b>Avg.</b>	<b>57.22%</b>	<b>10.47%</b>	<b>8.69%</b>	<b>14.45%</b>	<b>2.82%</b>	<b>4.24%</b>	<b>1.91%</b>	<b>0.21%</b>	
	<b>S.D.</b>	<b>6.27%</b>	<b>1.45%</b>	<b>3.44%</b>	<b>4.64%</b>	<b>0.57%</b>	<b>1.43%</b>	<b>0.34%</b>	<b>0.13%</b>	
ABR006	30	55.25%	9.06%	13.35%	11.30%	2.44%	5.95%	1.97%	0.67%	100.00%

Label	Pt#	SiO <sub>2</sub>	Al <sub>2</sub> O <sub>3</sub>	Fe <sub>2</sub> O <sub>3</sub>	CaO	K <sub>2</sub> O	PbO	SnO <sub>2</sub>	CuO	Total
ABR006	31	68.89%	8.76%	6.00%	4.96%	4.02%	4.05%	2.98%	0.34%	100.00%
	32	65.05%	21.38%	1.34%	4.07%	7.69%	0.20%	0.01%	0.24%	100.00%
	33	66.90%	15.17%	2.88%	10.61%	4.42%	0.01%	0.00%	0.00%	100.00%
	34	63.60%	10.84%	6.11%	6.47%	4.01%	6.84%	1.82%	0.30%	100.00%
	35	64.37%	14.28%	4.57%	5.21%	5.01%	4.78%	1.03%	0.75%	100.00%
	36	57.87%	9.46%	14.98%	11.59%	2.48%	2.46%	0.95%	0.20%	100.00%
	37	59.69%	10.69%	10.77%	12.02%	2.94%	2.52%	1.19%	0.18%	100.00%
	Avg.	62.71%	12.46%	7.50%	8.28%	4.13%	3.35%	1.24%	0.34%	
	S.D.	4.67%	4.31%	4.97%	3.40%	1.71%	2.51%	1.00%	0.25%	
ABR007	14	52.33%	10.12%	12.61%	18.39%	2.07%	2.92%	1.34%	0.23%	100.00%
	15	51.45%	10.23%	10.82%	10.13%	2.83%	7.83%	4.43%	2.27%	100.00%
	Avg.	51.89%	10.17%	11.72%	14.26%	2.45%	5.37%	2.89%	1.25%	
	S.D.	0.62%	0.08%	1.26%	5.84%	0.54%	3.47%	2.18%	1.44%	
ABR008	22	53.88%	11.53%	9.23%	13.59%	3.06%	2.20%	5.69%	0.83%	100.00%
	23	56.44%	11.78%	7.65%	12.48%	3.37%	2.18%	5.52%	0.59%	100.00%
	24	58.79%	13.96%	5.10%	10.88%	3.85%	2.46%	4.81%	0.15%	100.00%
	26	78.09%	17.76%	0.58%	0.94%	2.51%	0.00%	0.00%	0.12%	100.00%
	27	74.22%	21.40%	0.60%	1.28%	2.49%	0.00%	0.01%	0.00%	100.00%
	1	50.60%	11.34%	6.33%	15.47%	3.52%	9.40%	1.84%	1.50%	100.00%
	2	58.61%	14.77%	8.21%	9.47%	1.90%	2.61%	4.36%	0.08%	100.00%
	3	59.26%	14.91%	6.07%	9.27%	2.93%	2.49%	4.06%	1.01%	100.00%
	5	48.99%	9.88%	7.92%	19.14%	3.95%	7.14%	2.84%	0.14%	100.00%
	6	47.08%	8.62%	7.54%	14.55%	2.27%	12.31%	7.35%	0.29%	100.00%
	7	31.34%	7.04%	3.41%	5.59%	1.84%	6.90%	3.96%	39.91%	100.00%
	9	46.87%	10.13%	7.55%	11.19%	2.80%	14.53%	6.32%	0.60%	100.00%
	Avg.	55.35%	12.76%	5.85%	10.32%	2.87%	5.19%	3.90%	3.77%	
	S.D.	12.41%	4.04%	2.90%	5.50%	0.71%	4.82%	2.34%	11.39%	
ABR009	21	37.48%	6.65%	26.68%	23.46%	0.04%	2.12%	3.42%	0.15%	100.00%
	22	63.92%	18.46%	4.98%	7.45%	4.99%	0.06%	0.03%	0.10%	100.00%
	23	64.11%	18.81%	4.75%	7.59%	4.59%	0.00%	0.09%	0.06%	100.00%
	25	64.09%	17.21%	5.23%	7.41%	5.63%	0.12%	0.15%	0.16%	100.00%
	Avg.	57.40%	15.28%	10.41%	11.48%	3.81%	0.57%	0.92%	0.12%	
ABR010	29	50.90%	10.49%	6.63%	8.47%	2.89%	12.15%	5.86%	2.60%	100.00%
	30	50.11%	10.04%	6.42%	9.42%	2.36%	14.49%	6.79%	0.36%	100.00%
	31	50.88%	10.36%	6.21%	9.16%	2.89%	13.80%	6.31%	0.39%	100.00%
	32	52.20%	10.66%	6.07%	8.79%	2.82%	13.14%	6.12%	0.21%	100.00%
	33	66.72%	18.64%	0.59%	3.54%	5.07%	3.22%	1.47%	0.74%	100.00%
	34	55.84%	11.37%	5.26%	9.53%	3.42%	8.87%	5.29%	0.41%	100.00%

Label	Pt#	SiO <sub>2</sub>	Al <sub>2</sub> O <sub>3</sub>	Fe <sub>2</sub> O <sub>3</sub>	CaO	K <sub>2</sub> O	PbO	SnO <sub>2</sub>	CuO	Total
	35	55.42%	13.03%	4.94%	4.09%	3.11%	15.44%	3.42%	0.54%	100.00%
	33	64.58%	18.61%	6.46%	6.33%	3.57%	0.27%	0.00%	0.17%	100.00%
	16	65.46%	17.39%	5.82%	5.48%	5.69%	0.04%	0.01%	0.13%	100.00%
	17	68.26%	16.70%	5.48%	5.35%	4.01%	0.05%	0.11%	0.04%	100.00%
	<b>Avg.</b>	<b>58.04%</b>	<b>13.73%</b>	<b>5.39%</b>	<b>7.02%</b>	<b>3.58%</b>	<b>8.15%</b>	<b>3.54%</b>	<b>0.56%</b>	
	<b>S.D.</b>	<b>7.37%</b>	<b>3.67%</b>	<b>1.77%</b>	<b>2.32%</b>	<b>1.06%</b>	<b>6.54%</b>	<b>2.87%</b>	<b>0.75%</b>	
<b>ABR011</b>	19	47.97%	8.61%	7.56%	33.10%	2.12%	0.27%	0.37%	0.00%	100.00%
	<b>Avg.</b>	<b>n/a</b>	<b>n/a</b>	<b>n/a</b>	<b>n/a</b>	<b>n/a</b>	<b>n/a</b>	<b>n/a</b>	<b>n/a</b>	
	<b>S.D.</b>	<b>n/a</b>	<b>n/a</b>	<b>n/a</b>	<b>n/a</b>	<b>n/a</b>	<b>n/a</b>	<b>n/a</b>	<b>n/a</b>	
<b>ABR012</b>	14	54.16%	11.00%	7.42%	13.03%	3.84%	7.69%	2.71%	0.15%	100.00%
	15	50.06%	9.15%	9.92%	10.94%	2.63%	11.72%	5.30%	0.28%	100.00%
	16	47.54%	8.46%	7.76%	7.55%	2.76%	19.24%	6.13%	0.55%	100.00%
	17	46.77%	8.52%	5.67%	7.66%	2.86%	18.99%	2.16%	7.37%	100.00%
	18	60.94%	11.82%	5.42%	10.40%	4.02%	4.78%	2.40%	0.22%	100.00%
	56	48.18%	9.76%	9.35%	11.37%	2.61%	13.92%	3.96%	0.85%	100.00%
	58	52.75%	10.62%	8.86%	13.89%	3.10%	7.54%	2.93%	0.31%	100.00%
	60	63.47%	9.99%	5.38%	10.87%	3.53%	3.95%	2.48%	0.33%	100.00%
	61	48.82%	9.21%	3.94%	8.10%	3.02%	20.15%	1.37%	5.39%	100.00%
	62	52.68%	11.05%	8.27%	13.81%	3.62%	7.34%	3.07%	0.15%	100.00%
	63	51.74%	11.32%	7.80%	13.90%	3.41%	7.94%	3.40%	0.49%	100.00%
	64	51.49%	10.66%	7.45%	12.70%	3.33%	7.75%	2.92%	3.70%	100.00%
	65	62.48%	11.20%	5.02%	10.24%	4.49%	4.44%	1.87%	0.26%	100.00%
	66	44.19%	9.99%	7.23%	10.71%	2.52%	20.74%	3.68%	0.92%	100.00%
	67	61.42%	13.37%	5.18%	8.13%	4.27%	5.09%	2.05%	0.49%	100.00%
	69	46.06%	10.14%	12.80%	12.48%	2.61%	12.47%	3.26%	0.18%	100.00%
	70	46.58%	9.82%	12.50%	13.05%	2.69%	12.00%	3.06%	0.29%	100.00%
	71	46.02%	10.16%	13.84%	13.64%	2.88%	10.80%	2.47%	0.17%	100.00%
	72	45.62%	8.67%	8.90%	9.00%	2.22%	19.96%	5.19%	0.44%	100.00%
	<b>Avg.</b>	<b>51.63%</b>	<b>10.26%</b>	<b>8.04%</b>	<b>11.13%</b>	<b>3.18%</b>	<b>11.40%</b>	<b>3.18%</b>	<b>1.19%</b>	
	<b>S.D.</b>	<b>6.20%</b>	<b>1.23%</b>	<b>2.77%</b>	<b>2.23%</b>	<b>0.64%</b>	<b>5.88%</b>	<b>1.24%</b>	<b>2.02%</b>	
<b>ABR013</b>	16	45.19%	7.68%	5.90%	6.44%	2.13%	24.84%	5.31%	2.49%	100.00%
	17	49.25%	10.67%	12.28%	12.98%	3.11%	8.87%	2.52%	0.33%	100.00%
	18	53.69%	10.17%	9.79%	13.66%	3.38%	6.75%	2.19%	0.37%	100.00%
	19	44.51%	9.52%	10.79%	10.31%	2.47%	17.59%	4.58%	0.23%	100.00%
	20	43.05%	9.41%	5.75%	7.50%	1.37%	30.42%	1.93%	0.58%	100.00%
	<b>Avg.</b>	<b>47.14%</b>	<b>9.49%</b>	<b>8.90%</b>	<b>10.18%</b>	<b>2.49%</b>	<b>17.69%</b>	<b>3.31%</b>	<b>0.80%</b>	
	<b>S.D.</b>	<b>4.32%</b>	<b>1.13%</b>	<b>2.95%</b>	<b>3.21%</b>	<b>0.80%</b>	<b>10.13%</b>	<b>1.53%</b>	<b>0.95%</b>	
<b>ABR014</b>	50	67.21%	20.08%	4.63%	3.72%	4.21%	0.02%	0.05%	0.09%	100.00%
	52	63.82%	20.14%	6.25%	5.56%	3.92%	0.02%	0.01%	0.28%	100.00%

Label	Pt#	SiO <sub>2</sub>	Al <sub>2</sub> O <sub>3</sub>	Fe <sub>2</sub> O <sub>3</sub>	CaO	K <sub>2</sub> O	PbO	SnO <sub>2</sub>	CuO	Total
	53	66.49%	15.32%	5.23%	8.26%	4.28%	0.03%	0.17%	0.22%	100.00%
	54	70.43%	17.02%	4.54%	3.45%	4.37%	0.13%	0.00%	0.05%	100.00%
	55	66.98%	19.09%	5.68%	4.22%	3.69%	0.15%	0.00%	0.19%	100.00%
	1	61.11%	15.75%	6.92%	13.50%	2.42%	0.06%	0.10%	0.14%	100.00%
	2	67.05%	18.86%	4.82%	5.30%	3.63%	0.14%	0.00%	0.20%	100.00%
	3	60.23%	14.48%	6.13%	14.52%	2.94%	0.38%	0.19%	1.13%	100.00%
	4	69.33%	17.59%	5.00%	3.85%	4.02%	0.02%	0.00%	0.20%	100.00%
	5	66.09%	16.25%	5.07%	8.01%	4.20%	0.08%	0.15%	0.15%	100.00%
	<b>Avg.</b>	<b>65.87%</b>	<b>17.46%</b>	<b>5.43%</b>	<b>7.04%</b>	<b>3.77%</b>	<b>0.10%</b>	<b>0.07%</b>	<b>0.27%</b>	
	<b>S.D.</b>	<b>3.27%</b>	<b>2.02%</b>	<b>0.79%</b>	<b>4.05%</b>	<b>0.63%</b>	<b>0.11%</b>	<b>0.08%</b>	<b>0.31%</b>	
<b>ABR016</b>	6	46.12%	11.75%	7.88%	2.56%	2.11%	9.82%	2.47%	17.29%	100.00%
	7	56.03%	18.96%	10.16%	2.37%	3.01%	4.44%	1.20%	3.84%	100.00%
	8	58.08%	18.75%	8.82%	2.35%	2.86%	4.00%	0.92%	4.20%	100.00%
	9	55.62%	10.67%	4.79%	1.80%	2.42%	15.39%	7.20%	2.10%	100.00%
	14	53.54%	10.70%	4.59%	1.92%	2.37%	18.72%	7.20%	0.95%	100.00%
	16	38.91%	23.74%	12.69%	24.61%	0.00%	0.00%	0.00%	0.06%	100.00%
	<b>Avg.</b>	<b>51.38%</b>	<b>15.76%</b>	<b>8.16%</b>	<b>5.94%</b>	<b>2.13%</b>	<b>8.73%</b>	<b>3.17%</b>	<b>4.74%</b>	
	<b>S.D.</b>	<b>7.38%</b>	<b>5.49%</b>	<b>3.13%</b>	<b>9.15%</b>	<b>1.09%</b>	<b>7.25%</b>	<b>3.22%</b>	<b>6.35%</b>	
<b>ABR017</b>	12	45.67%	8.76%	20.70%	15.13%	2.80%	4.04%	2.86%	0.03%	100.00%
	13	41.15%	8.10%	21.53%	13.90%	2.61%	7.66%	4.76%	0.27%	100.00%
	14	66.22%	18.46%	5.31%	6.18%	3.78%	0.03%	0.00%	0.00%	100.00%
	15	65.02%	17.27%	3.39%	8.20%	5.30%	0.32%	0.07%	0.43%	100.00%
	<b>Avg.</b>	<b>54.52%</b>	<b>13.15%</b>	<b>12.74%</b>	<b>10.85%</b>	<b>3.62%</b>	<b>3.01%</b>	<b>1.93%</b>	<b>0.18%</b>	
	<b>S.D.</b>	<b>12.96%</b>	<b>5.48%</b>	<b>9.72%</b>	<b>4.34%</b>	<b>1.23%</b>	<b>3.60%</b>	<b>2.31%</b>	<b>0.20%</b>	
<b>ABR018</b>	25	65.71%	22.05%	6.05%	1.77%	4.31%	0.08%	0.02%	0.02%	100.00%
	26	54.88%	17.45%	5.32%	20.12%	2.03%	0.06%	0.00%	0.13%	100.00%
	27	61.80%	24.77%	6.86%	2.33%	4.09%	0.00%	0.02%	0.13%	100.00%
	28	65.14%	21.01%	5.93%	3.16%	4.63%	0.13%	0.00%	0.00%	100.00%
	29	58.21%	29.43%	1.85%	8.20%	2.17%	0.06%	0.00%	0.07%	100.00%
	<b>Avg.</b>	<b>61.15%</b>	<b>22.94%</b>	<b>5.20%</b>	<b>7.12%</b>	<b>3.44%</b>	<b>0.07%</b>	<b>0.01%</b>	<b>0.07%</b>	
	<b>S.D.</b>	<b>4.61%</b>	<b>4.48%</b>	<b>1.95%</b>	<b>7.70%</b>	<b>1.24%</b>	<b>0.05%</b>	<b>0.01%</b>	<b>0.06%</b>	
<b>ABR019</b>	36	61.43%	21.05%	7.16%	6.29%	3.00%	0.18%	0.00%	0.89%	100.00%
	37	63.09%	15.54%	4.85%	13.42%	2.00%	0.21%	0.00%	0.90%	100.00%
	38	59.44%	20.82%	7.31%	7.07%	2.59%	0.00%	0.02%	2.74%	100.00%
	39	71.27%	15.67%	4.21%	4.90%	3.09%	0.15%	0.01%	0.69%	100.00%
	40	62.69%	19.99%	7.36%	6.70%	2.79%	0.00%	0.02%	0.44%	100.00%
	41	64.15%	19.96%	7.21%	5.60%	3.02%	0.00%	0.00%	0.07%	100.00%
	42	63.34%	19.62%	7.38%	6.90%	2.52%	0.24%	0.00%	0.00%	100.00%
	18	60.84%	11.87%	4.62%	20.92%	1.75%	0.00%	0.00%	0.00%	100.00%

Label	Pt#	SiO <sub>2</sub>	Al <sub>2</sub> O <sub>3</sub>	Fe <sub>2</sub> O <sub>3</sub>	CaO	K <sub>2</sub> O	PbO	SnO <sub>2</sub>	CuO	Total
ABR019	19	46.03%	6.93%	4.18%	11.52%	1.10%	28.43%	1.10%	0.71%	100.00%
	20	68.44%	17.15%	5.95%	5.12%	3.20%	0.02%	0.05%	0.07%	100.00%
	21	69.45%	14.46%	4.18%	7.91%	3.88%	0.09%	0.02%	0.00%	100.00%
	Avg.	62.74%	16.64%	5.86%	8.76%	2.63%	2.66%	0.11%	0.59%	
	S.D.	6.69%	4.38%	1.45%	4.82%	0.77%	8.54%	0.33%	0.80%	
ABR020	8	63.48%	20.15%	7.34%	2.83%	3.66%	1.45%	0.29%	0.80%	100.00%
	9	53.70%	10.29%	11.08%	8.64%	3.36%	10.66%	1.29%	0.99%	100.00%
	10	47.23%	9.49%	10.30%	9.90%	3.30%	14.32%	3.76%	1.72%	100.00%
	11	51.99%	9.93%	12.19%	8.62%	2.46%	10.05%	3.57%	1.20%	100.00%
	Avg.	54.10%	12.46%	10.23%	7.49%	3.19%	9.12%	2.23%	1.18%	
	S.D.	6.83%	5.13%	2.08%	3.17%	0.51%	5.45%	1.71%	0.40%	
ABR021	10	60.24%	14.71%	5.72%	13.34%	3.16%	0.66%	1.02%	1.15%	100.00%
	11	61.20%	15.62%	5.45%	12.57%	2.99%	0.36%	0.44%	1.37%	100.00%
	12	66.16%	19.63%	4.60%	5.38%	3.89%	0.10%	0.00%	0.24%	100.00%
	14	65.17%	18.36%	5.16%	5.80%	4.32%	0.33%	0.17%	0.68%	100.00%
	15	63.67%	19.71%	7.46%	6.01%	3.08%	0.00%	0.00%	0.06%	100.00%
	Avg.	63.29%	17.61%	5.68%	8.62%	3.49%	0.29%	0.33%	0.70%	
	S.D.	2.53%	2.31%	1.08%	3.97%	0.59%	0.26%	0.43%	0.56%	
ABR022	9	56.13%	14.60%	5.55%	9.77%	3.37%	5.54%	1.49%	3.56%	100.00%
	10	52.67%	13.51%	5.55%	8.35%	2.89%	9.20%	2.35%	5.49%	100.00%
	11	53.38%	10.27%	6.02%	8.68%	2.71%	9.93%	7.33%	1.67%	100.00%
	13	48.16%	9.25%	5.13%	6.39%	2.14%	18.60%	0.52%	9.81%	100.00%
	Avg.	52.58%	11.91%	5.56%	8.30%	2.78%	10.82%	2.93%	5.13%	
	S.D.	3.31%	2.55%	0.37%	1.41%	0.51%	5.53%	3.03%	3.49%	
ABR023	22	58.60%	15.28%	6.86%	8.84%	3.52%	4.05%	2.52%	0.32%	100.00%
	23	59.41%	16.52%	7.60%	9.47%	3.51%	2.36%	1.02%	0.10%	100.00%
	24	46.95%	11.62%	15.91%	12.19%	2.77%	5.87%	4.30%	0.40%	100.00%
	25	55.06%	13.87%	11.76%	9.65%	3.16%	5.01%	1.25%	0.24%	100.00%
	26	54.41%	6.28%	10.77%	10.42%	12.13%	2.70%	1.57%	1.72%	100.00%
	27	51.89%	10.06%	16.15%	13.04%	2.36%	4.20%	2.08%	0.22%	100.00%
	28	45.54%	12.28%	18.98%	12.35%	2.11%	6.49%	1.96%	0.30%	100.00%
	29	52.87%	12.83%	13.36%	11.81%	3.37%	4.51%	1.12%	0.12%	100.00%
	30	59.08%	11.18%	10.17%	9.02%	3.88%	4.54%	2.05%	0.06%	100.00%
	Avg.	53.76%	12.21%	12.40%	10.76%	4.09%	4.41%	1.99%	0.39%	
	S.D.	5.05%	3.01%	4.07%	1.61%	3.07%	1.33%	1.00%	0.51%	
ABR024	31	59.65%	14.83%	10.59%	10.73%	3.66%	0.46%	0.06%	0.01%	100.00%
	32	54.32%	13.64%	19.64%	8.90%	2.91%	0.51%	0.06%	0.02%	100.00%
	43	56.59%	24.74%	3.86%	13.72%	0.80%	0.15%	0.06%	0.08%	100.00%
	44	64.52%	20.88%	6.60%	3.82%	3.79%	0.14%	0.00%	0.25%	100.00%

Label	Pt#	SiO <sub>2</sub>	Al <sub>2</sub> O <sub>3</sub>	Fe <sub>2</sub> O <sub>3</sub>	CaO	K <sub>2</sub> O	PbO	SnO <sub>2</sub>	CuO	Total
ABR024	45	68.13%	19.38%	5.95%	3.01%	3.41%	0.08%	0.00%	0.04%	100.00%
	46	74.16%	15.84%	3.75%	2.17%	3.69%	0.10%	0.07%	0.22%	100.00%
	47	68.93%	19.68%	4.24%	3.03%	3.92%	0.13%	0.02%	0.06%	100.00%
	48	58.25%	15.93%	10.24%	11.29%	3.74%	0.23%	0.21%	0.11%	100.00%
	Avg.	63.07%	18.12%	8.11%	7.08%	3.24%	0.22%	0.06%	0.10%	
	S.D.	6.95%	3.71%	5.38%	4.57%	1.03%	0.17%	0.07%	0.09%	
ABR025	1	52.97%	10.38%	15.24%	15.46%	2.53%	1.82%	1.46%	0.14%	100.00%
	2	64.16%	12.67%	5.45%	12.37%	2.92%	0.41%	1.91%	0.12%	100.00%
	3	61.00%	12.69%	6.82%	13.70%	2.96%	0.79%	1.57%	0.47%	100.00%
	4	45.79%	7.98%	9.21%	19.54%	1.92%	11.66%	2.60%	1.31%	100.00%
	5	66.88%	14.85%	3.75%	10.64%	3.69%	0.13%	0.06%	0.00%	100.00%
	Avg.	58.16%	11.71%	8.10%	14.34%	2.80%	2.96%	1.52%	0.41%	
ABR028	24	65.38%	11.33%	8.73%	8.93%	5.54%	0.07%	0.01%	0.00%	100.00%
	25	64.62%	17.02%	5.64%	9.32%	3.28%	0.10%	0.03%	0.00%	100.00%
	26	62.57%	18.59%	4.74%	11.11%	2.91%	0.08%	0.01%	0.00%	100.00%
	27	51.76%	29.63%	1.42%	16.14%	1.01%	0.05%	0.00%	0.00%	100.00%
	28	65.14%	15.96%	5.86%	8.52%	4.38%	0.12%	0.02%	0.00%	100.00%
	Avg.	61.89%	18.50%	5.28%	10.80%	3.42%	0.08%	0.02%	0.00%	
ABR029	S.D.	5.77%	6.78%	2.63%	3.14%	1.70%	0.03%	0.01%	0.00%	
	20	68.17%	19.07%	0.08%	0.04%	12.55%	0.04%	0.00%	0.05%	100.00%
	21	74.64%	22.18%	0.04%	1.84%	1.31%	0.00%	0.00%	0.00%	100.00%
	22	64.91%	18.41%	0.22%	0.03%	16.36%	0.04%	0.02%	0.00%	100.00%
	23	70.61%	22.36%	0.32%	2.61%	4.03%	0.00%	0.07%	0.00%	100.00%
	2	69.96%	20.99%	1.71%	3.75%	3.54%	0.00%	0.00%	0.05%	100.00%
	3	67.13%	18.90%	7.15%	2.40%	4.27%	0.02%	0.00%	0.14%	100.00%
	4	69.67%	19.92%	3.83%	1.67%	4.86%	0.06%	0.00%	0.00%	100.00%
	5	36.10%	45.62%	15.40%	0.96%	1.49%	0.17%	0.00%	0.25%	100.00%
	6	67.90%	14.54%	6.29%	7.04%	4.11%	0.07%	0.05%	0.00%	100.00%
	7	61.72%	17.55%	8.69%	8.38%	3.45%	0.00%	0.01%	0.20%	100.00%
AVS 905	Avg.	65.08%	21.95%	4.37%	2.87%	5.60%	0.04%	0.02%	0.07%	
	S.D.	10.75%	8.63%	5.06%	2.81%	4.89%	0.05%	0.03%	0.09%	
	37	54.18%	20.18%	17.34%	4.26%	3.42%	0.58%	0.04%	0.00%	100.00%
	38	66.34%	19.69%	0.19%	0.62%	13.16%	0.00%	0.00%	0.00%	100.00%
	39	57.76%	23.48%	7.71%	8.47%	2.07%	0.51%	0.00%	0.00%	100.00%
	40	83.64%	15.00%	0.40%	0.33%	0.28%	0.14%	0.02%	0.20%	100.00%
	Avg.	65.48%	19.59%	6.41%	3.42%	4.73%	0.31%	0.01%	0.05%	
	S.D.	13.14%	3.49%	8.08%	3.81%	5.76%	0.28%	0.02%	0.10%	
MDL		0.051	0.05	0.173	0.066	0.036	0.243	0.156	0.202	

APPENDIX E

Statistical analyses

Table 22: Correlation results

	SiO <sub>2</sub>	Al <sub>2</sub> O <sub>3</sub>	FeO	CaO	K <sub>2</sub> O	PbO	SnO <sub>2</sub>
SiO <sub>2</sub>	1						
Al <sub>2</sub> O <sub>3</sub>	0.383107	1					
FeO	-0.52688	-0.34583	1				
CaO	-0.41416	-0.3748	0.512594	1			
K <sub>2</sub> O	0.335284	0.269588	-0.35888	-0.35766	1		
PbO	-0.59042	-0.56738	0.153509	0.0826	-0.26346	1	
SnO <sub>2</sub>	-0.50677	-0.45866	0.109143	0.049262	-0.18114	0.619848	1

Cluster Analysis

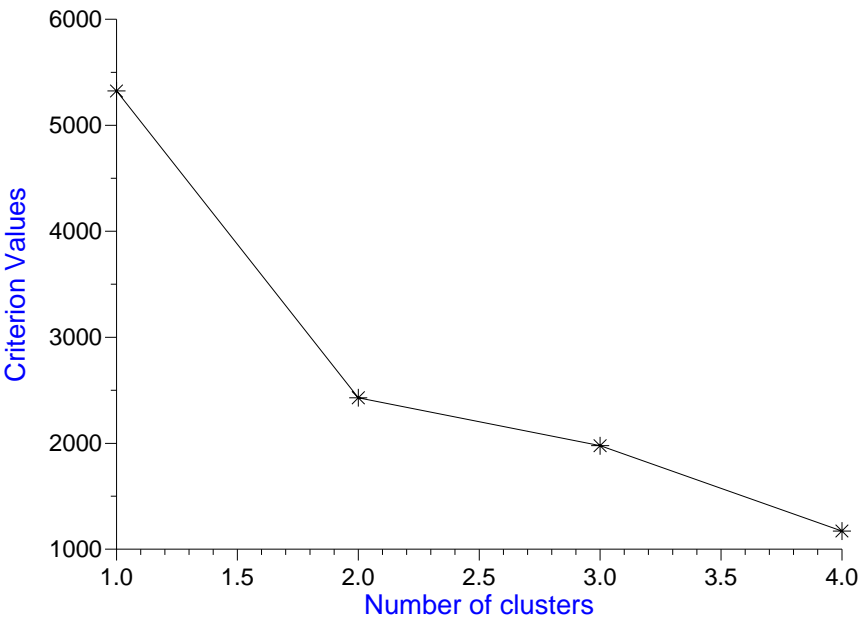


Figure 99: Criterion values in cluster analysis plotted against potential number of clusters

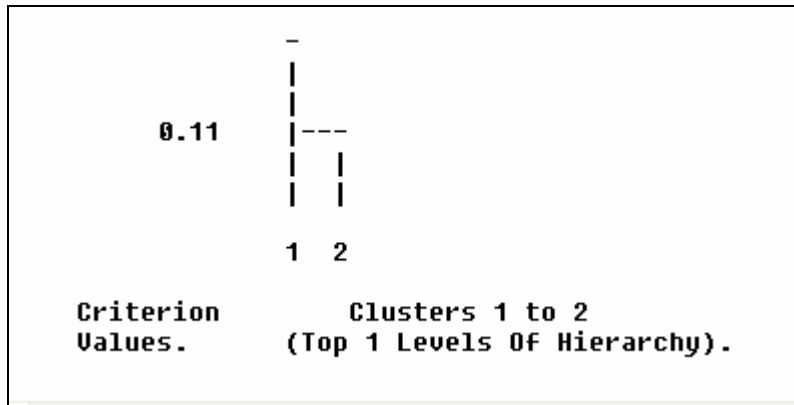


Figure 100: Cluster analysis dendrogram of all WDS analyses of the groundmass